

**THERMODYNAMIC MODEL AND DATA ON THE PARTITIONING OF NON-
PROCESS ELEMENTS BETWEEN KRAFT FIBRES AND WATER IN A PULP
SUSPENSION**

by

GEOFFREY SCOTT BYGRAVE

B.Sc. (Chemical Engineering) University of Calgary, 1995

**A THESIS SUBMITTED IN PARTIAL FULFILLMENT OF THE
REQUIREMENTS FOR THE DEGREE OF
MASTER OF APPLIED SCIENCE**

in

**THE FACULTY OF GRADUATE STUDIES
DEPARTMENT OF BIORESOURCE AND CHEMICAL ENGINEERING**

We accept this thesis as conforming
to the required standard

THE UNIVERSITY OF BRITISH COLUMBIA

NOVEMBER 1997

© Geoffrey Scott Bygrave, 1997

In presenting this thesis in partial fulfilment of the requirements for an advanced degree at the University of British Columbia, I agree that the Library shall make it freely available for reference and study. I further agree that permission for extensive copying of this thesis for scholarly purposes may be granted by the head of my department or by his or her representatives. It is understood that copying or publication of this thesis for financial gain shall not be allowed without my written permission.

Department of Chemical Engineering

The University of British Columbia
Vancouver, Canada

Date December 5, 1997

Abstract

The partitioning of non-process elements in kraft fibre suspensions has been modeled using the Donnan equilibrium framework with activity coefficients introduced to account for the non-ideal nature of the electrolyte solutions. Activity coefficients have been obtained using Pitzer's model. Total anionic charge, dissociation constants, and mass of water within the fibres are used as input to the model and were determined by independent experiments. Partitioning data were also obtained for a post brown stock washer kraft pulp, from an interior BC mill, for the metal ions of Na^+ , Ca^{+2} , and Mg^{+2} over the pH range 2-13. Such data above a pH of 11 were not previously available in the literature.

Two models were used to obtain the charge on the fibres at any pH; a two dissociation constant model (corresponding roughly to the carboxyl and phenolic hydroxyl) and an "exact" charge model. Results indicate that below a pH of 7 both models do a good job of representing the experimental data obtained in this work and data available in the literature. Above a pH of 7 the two dissociation constant model under-predicts the partitioning data while the exact charge model follows the experimental data over the entire pH range. This indicates Donnan equilibrium is an excellent framework for non-process element partitioning prediction as long as the fibre charge is known accurately. Experiments with elevated Mg and Ca contents were also performed, resulting in precipitation within the fibres at pHs above 10. The model does not account for precipitation phenomena that may occur when concentrations of Ca and Mg are increased above those naturally occurring in post brown stock pulps.

Table of Contents

Abstract	ii
List of Tables	vii
List of Figures	x
List of Symbols	xiii
Acknowledgments	xv
1. Introduction	1
1.1 Chemical Pulping Technologies and the Environment.....	1
1.2 Closed Cycle Operation	2
1.3 Importance of Non-Process Elements	3
1.4 Scope of thesis and thesis contents.....	4
2. Background and Research Objectives.....	6
2.1 Non-Process Elements in Kraft Mills.....	6
2.2 Wood Fibres, Pulping, and Bleaching.....	8
2.2.1 Fibre Chemistry	8
2.2.2 Pulping and Bleaching Reactions.....	10
2.3 Metal Ion Partitioning in Pulp Suspensions	12
2.3.1 Modeling Based on Ion Exchange.....	12
2.3.2 Modeling Based on Donnan Equilibrium	14
2.4 Mixture Thermodynamics	16
2.5 Electrolyte Solution Thermodynamics.....	20
2.6 Research Objectives.....	23

3. Partitioning of Non-Process Elements: Theory	25
3.1 Donnan Equilibrium.....	25
3.2 Mass Balances and Dissociation Relationships	27
3.3 Model Summary	31
3.4 Model Assumptions and Computational Algorithm	34
4. Partitioning of Non-Process Elements: Experimental.....	37
4.1 Materials	37
4.2 Metal Ion Partitioning with Pulp As-Received.....	38
4.2.1 General 1L Vessel Equilibrium Procedure	39
4.2.2 Data Analysis for 1L Mixing Vessel Experiments	41
4.3 Metal Ion Partitioning with Acid-Washed Pulp	44
4.3.1 Acid Washing Procedure.....	45
4.3.2 150 mL Vessel Equilibrium Procedure	46
4.3.3 Data Analysis for 150 mL Mixing Vessel Experiments	49
4.4 Sample Preparation and Metal Ion Analysis	50
4.4.1 Ashing Procedure	50
4.4.2 Atomic Absorption Preparation Procedure	51
4.4.3 Metal Ion Analysis	51
4.5 Model Parameter Determination	53
4.5.1 Conductometric Titrations	53
4.5.1.1 Required Equipment.....	53
4.5.1.2 Procedure for a kraft pulp	53
4.5.2 Potentiometric Titrations	54
4.5.3 Water Retention Value and Fibre Saturation Point	59

5. Results and Discussion	61
5.1 Determining Model Parameters.....	61
5.1.1 Potentiometric Titration to Determine Fibre Properties	62
5.1.2 Conductometric Titration.....	68
5.1.3 Fibre Saturation Point	71
5.2 Comparison of Partitioning Model with Ideal Donnan Model and Published Data	75
5.2.1 Explanation of Partitioning Curves.....	76
5.3 Metal Ion Partitioning with Post Brown Stock Pulp.....	82
5.3.1 1% Consistency Equilibrium and Metal Profile of Original Pulp.....	83
5.3.2 Acidified 1% Consistency Equilibrium.....	86
5.3.3 Elevated Calcium 1% Consistency Equilibrium.....	86
5.3.4 0.46% and 1.95% Consistency Equilibriums.....	87
5.4 Metal Ion Partitioning with Acid Washed Pulp.....	88
5.4.1 Brown Stock Pulp Ion Contents in 150 mL Vessels.....	88
5.4.2 Elevated Magnesium Content in 150 mL Vessels	102
5.4.3 Elevated Magnesium Content in 1L Vessel: AA analysis	105
5.4.4 Elevated Magnesium Content Experiments in 1L Vessel: EDTA / EGTA analysis.....	114
5.5 Sensitivity to Model Parameters.....	116
6. Summary, Conclusions, and Recommendations	120
6.1 Conclusions	123
6.2 Recommendations	124
7. References.....	125

Appendix A: Titration data for kraft pulp fibres	130
Appendix B: Pitzer's Equations	132
Appendix C: Unknowns and Equations of Gibbs-Donnan Equilibrium	135
Appendix D: Errors propagation in calculations.....	138
Appendix E: Difference between K_a' and K_a	144
Appendix F: FORTRAN code for NPE partitioning predictions	147
Appendix G: FORTRAN code for potentiometric titration interpretation	154

List of Tables

Table 3.3.1: Equations describing ion partitioning on fibres within the Donnan framework.....	33
Table 5.1.1: Fibre saturation point dependence on pH.....	73
Table 5.3.1: Partitioning of ions in post brown stock pulp under various conditions. Standard deviations were obtained only for the first two experiments. Other experiments were not duplicated.....	84
Table 5.3.2: Measured NPE contents in post brown stock pulp (as-received).....	85
Table 5.3.3: Donnan distribution coefficients (λ') at various consistencies.....	87
Table 5.4.1: Calcium partitioning in 150 mL equilibrium vessels. Concentration in the external solution determined by EGTA titration. Negative values result from back calculation with the known total calcium content in the system. Standard errors are given in brackets. Data determined in triplicate.....	92
Table 5.4.2: Magnesium partitioning in 150 mL equilibrium vessels. Concentration in the external solution determined by EDTA and EGTA titration. Negative values result from back calculation with the known total magnesium content in the system. Standard errors are given in brackets. Data determined in triplicate.....	93
Table 5.4.3: Sodium partitioning in 150 mL equilibrium vessels. Concentrations determined by AA. All back calculated fibre values were negative and have not been tabulated. Standard errors are given in brackets. Data determined in triplicate.....	94
Table 5.4.4: Calcium partitioning in 150 mL vessels with elevated Mg contents. Concentration in the external solution determined by EGTA titration. Negative values result from back calculation with the known total calcium content in the system. Standard errors are given in brackets. Data determined in triplicate.....	103
Table 5.4.5: Magnesium partitioning in 150 mL vessels with elevated Mg contents. Concentration in the external solution determined by EDTA and EGTA titration. Standard errors are given in brackets. Data determined in triplicate.....	104
Table 5.4.6: Sodium external solution concentrations in 150 mL vessels with elevated Mg contents. Concentrations determined by AA. Standard errors are given in brackets. Data determined in triplicate.....	104

Table 5.4.7: Calcium partitioning in 1L vessel with high Mg. AA used to analyze filtrate and ash NPE contents. Values use both filtrate and ash concentrations to calculate contents on fibres. Standard errors are given in brackets. Data determined in triplicate.	106
Table 5.4.8: Magnesium partitioning in 1L vessel with high Mg. AA used to analyze filtrate and ash NPE contents. Values use both filtrate and ash concentrations to calculate contents on fibres. Standard errors are given in brackets. Data determined in triplicate.	106
Table 5.4.9: Sodium partitioning in 1L vessel with high Mg. AA used to analyze filtrate and ash NPE contents. Values use both filtrate and ash concentrations to calculate contents on fibres. Standard errors are given in brackets. Data determined in triplicate.	107
Table 5.4.10: Calcium partitioning in 1L vessel with high Mg. AA used to analyze filtrate and only the filtrate concentration and the known total salts added are used to calculate NPE contents on fibres. Standard errors are given in brackets. Data determined in triplicate.	107
Table 5.4.11: Magnesium partitioning in 1L vessel with high Mg. AA used to analyze filtrate and only the filtrate concentration and the known total salts added are used to calculate NPE contents on fibres. Standard errors are given in brackets. Data determined in triplicate.	107
Table 5.4.12: Common precipitates of calcium and magnesium. The concentration of anion necessary to cause precipitation is calculated assuming ideal solution behaviour.....	113
Table 5.4.13: Calcium Partitioning in 1L vessel with high Mg. EDTA and EGTA used to analyze external solution concentration. Standard errors are given in brackets. Data determined in triplicate.	114
Table 5.4.14: Magnesium Partitioning in 1L vessel with high Mg. EDTA and EGTA used to analyze external solution concentrations. Standard errors are given in brackets. Data determined in triplicate.	116

Table A 1: Conductometric titration results for kraft pulp fibres without the addition of a strong acid.....	130
Table A.2: Potentiometric titration results for the two sets of data representing the extremes of the experimental data recovered.....	131

List of Figures

Figure 2.2.1: Wood fibres and their constituents. Fibres are held together in wood by the middle lamella and are composed of tiny strands, each composed of cellulose, hemicellulose, and lignin. Adapted from Scallan and Tigerstrom (1992).	9
Figure 2.2.2: A typical lignin reaction in the pulping process. Ester bonds are attacked. Adapted from Smook (1992).	11
Figure 3.1.1: The Donnan equilibrium for a pulp fibre suspension	26
Figure 3.3.1: Model predictions of calcium (Ca^{+2}) activity coefficients over a range of pHs. The activity coefficients deviate a great deal from one, indicating the system is not ideal.	32
Figure 3.4.1: Block diagram of computer algorithm.....	36
Figure 4.2.1: Experimental procedure for determining the metal ion contents in ash and external solution. Procedure uses a 1L vessel.....	42
Figure 4.3.1: Experimental procedure for determining the metal ion contents in external solution for 150mL vessel experiments	48
Figure 5.1.1: Potentiometric titration of kraft pulp fibres. Two curves are shown, representing the titration of a blank solution containing only the background of NaCl and HCl, and the titration of kraft fibres within the same background of NaCl and HCl.	63
Figure 5.1.2: Comparison of theoretical curve for two calculated dissociation constants with experimental potentiometric titration data.	65
Figure 5.1.3: Fibre charge as a function of pH within the fibres. Two methods of modeling the fibre charge give very different curves. The exact charge model gives a cubic approximation to the dissociating behaviour of the fibres.	66
Figure 5.1.4: Comparison of alkalimetric titration of an equimolar (10^{-4} M) acetic acid ($\text{pK}_a=4.8$) and phenol ($\text{pK}_a=10$) with titration of humic acid containing $\sim 10^{-4}$ mol carboxylic groups (Stumm and Morgan, 1996).	69
Figure 5.1.5: Specific conductance during the titration of kraft pulp with NaOH. The intersection of the lines indicates the point at which all charged groups on the fibres have been titrated and free hydroxyl ions begin increasing solution conductance.	70

Figure 5.1.6: Fibre saturation point (FSP) over the relevant pH range. Quadratic interpolation through the data gives an approximate relation between the FSP and pH for acid washed fibres.	72
Figure 5.2.1: Fibre concentration of calcium (Ca^{+2}) over a range of pHs. The fibre saturation point (FSP) is assumed constant at 1.4, for comparison to the experimental data of Towers and Scallan (1996).	77
Figure 5.2.2: Fibre concentration of calcium (Ca^{+2}) over a range of pHs. The fibre saturation point (FSP) is assumed constant at 1.4. Data obtained from Bryant and Edwards (1996).	78
Figure 5.4.1: External solution concentration of calcium (Ca^{+2}) over a range of pHs. Dissociated groups on the fibres draw the cations into the fibres, causing the concentration to decrease in the external solution.	89
Figure 5.4.2: External solution concentration of magnesium (Mg^{+2}) over a range of pHs. Dissociated groups on the fibres draw the cations into the fibres, causing the concentration to decrease in the external solution.	90
Figure 5.4.3: External solution concentration of sodium (Na^{+}) over a range of pHs. Sodium hydroxide is used to increase the pH of the fibre suspension, so the amount of sodium is constantly increasing.	91
Figure 5.4.4: Fibre phase concentration of calcium over the pH range 1-13.	99
Figure 5.4.5: Fibre phase concentration of magnesium over the pH range 3-13.	100
Figure 5.4.6: External solution concentration of calcium with 1L and 150mL vessels.	108
Figure 5.4.7: Fibre phase concentration of calcium with 1L and 150mL vessels.	109
Figure 5.4.8: External solution concentration of magnesium with 1L and 150mL vessels.	110
Figure 5.4.9: Fibre phase concentration of magnesium with 1L and 150mL vessels.	111
Figure 5.4.10: Comparison of calcium contents within the fibres for elevated magnesium equilibrium experiments. Data plotted for different vessel volumes and metal ion analysis methods.	115
Figure 5.5.1: Dissociation constant effect on partitioning predictions.	117
Figure 5.5.2: Non-ideal and ideal predictions by the exact charge model.	119

Figure E - 1: Partitioning predictions for two dissociation constants including and ignoring the activity coefficient of hydrogen	145
Figure E - 2: Partitioning predictions for two dissociation constants at various ratios of the fibre phase activity coefficients	146

List of Symbols

A_j	total moles of anion j in the system
C_j	total moles of cation j in the system
E_j	electrochemical potential of species j
F	mass of solvent in the β (fibre) phase
G	Gibbs free energy
K_a	dissociation constant (based on activities)
K_a'	ideal dissociation constant (based on molalities)
K_w	dissociation constant of water, 10^{-14}
M^T	total quantity of metal ions in fibre suspension
M^F	quantity of metal ions in the fibres
M^S	quantity of metal ions in the external solution
M^{FM}	quantity of metal ions in the fibre mat
M^{TS}	quantity of metal ions in the trapped external solution
N	number of species j
P	pressure of the system
P°	reference pressure
Q	charge
Q_x	moles of fixed charged groups on the fibre
R	ideal gas constant
S	entropy
T	absolute temperature
U	internal energy
V	total mass of solvent in the system
\bar{V}_j	partial molar volume of component j
X	bound charged group on the non-diffusing species
a_j	activity of component j .
m_{X-}^β	molality of charged groups in the β phase in the dissociated state
m_{XH}^β	molality of charged groups in the β phase with hydrogen bound to them
m_i	molality of component i

m_j^0	reference molality
n_j	moles of species j
r	radius
z^+, z^-	valences of the cation and anion
\mathfrak{F}	Faraday's constant
λ	accumulation ratio of the system (activity basis)
λ'	accumulation ratio of the system (molality basis)
λ_j	absolute activity of component j
ψ^α	electric potential of phase α
ν_C, ν_A	stoichiometric numbers of the cation and anion
μ_j	chemical potential of component j
μ_j^0	reference chemical potential of component j
γ_j	molal activity coefficient of component j
ϵ_0	permittivity of a vacuum.

Acknowledgements

I would like to thank Dr. Peter Englezos for his constructive input and patience. Also thanks to Dr. Haynes and Dr. Bennington for fruitful discussions. Thank you Hyeon for helping me learn by answering and asking many questions. The financial support of NSERC through the Strategic Grants Program and Postgraduate Research Scholarship is greatly appreciated.

The technical support of PAPRICAN is also appreciated. In addition, I would like to thank Mike Towers, Brian Richardson, Jim Wearing, and Vic Uloth for their insight and useful discussion.

Chapter 1

1. Introduction

1.1 Chemical Pulping Technologies and the Environment

The liquid effluents of kraft pulp mills have been an environmental concern for many years. The public and government demand that mills operate with as little effect on the environment as possible (Bihani, 1996), including minimizing and ultimately eliminating liquid effluents. Liquid effluents in kraft pulp mills originate mainly from wood debarking and chip washing, digester and evaporator condensates, screening and cleaning white water, and the bleach plant washer filtrates (Smook, 1994). Many companies, as well as government research organizations, are supporting research into reducing liquid effluents to satisfy consumer concerns, reduce product cost, and stay within regulated effluent levels.

Wood can be pulped in several ways, the most common chemical means being the kraft process. In the kraft pulping process, wood chips are cooked in an aqueous solution of sodium hydroxide (NaOH) and sodium sulfide (Na₂S). The cooking process occurs at an elevated temperature and pressure, and chemically dissolves lignin between fibres. The kraft process is the most popular chemical pulping method because the pulp produced is strong, pulping chemicals can be easily recovered and reused, and a wide variety of wood species can be effectively pulped. After kraft pulping, the fibre is washed to remove pulping liquor. Washing is followed by bleaching of the pulp to increase the brightness. The majority of the effluent from bleached kraft pulp mills originates from the washing and bleaching processes.

A closed mill is one which produces only the desired product, pulp (Reeve et. al., 1979). For a kraft pulp mill to be considered truly “closed cycle” it would generate no gaseous, liquid or solid wastes in the production of the pulp. This is quite impossible at present. It is accepted that pulp mills will produce gaseous and solid emissions during operation but it should be possible to eliminate liquid effluents. Closed cycle in the context here means closed with respect to liquid effluents, particularly those of the bleach plant. This has never been achieved in a kraft mill, but closed cycle sulphite and chemithermomechanical pulp (CTMP) mills exist (Galloway, 1994; Barnes and Reid, 1995; Ricketts, 1994). A mill with no liquid discharges would have larger solid and gaseous emissions, since dissolved or suspended compounds that used to be purged in the liquid effluent would need to find new outlets to prevent build up.

1.2 Closed Cycle Operation

A major concern in the development of closed cycle technology is the build up of non-process elements. Non-process elements are ions such as aluminum (Al^{+3}), calcium (Ca^{+2}), magnesium, (Mg^{+2}) manganese (Mn^{+2}), and potassium (K^{+}). These ions enter the system as part of the wood, water, and chemicals. They are called non-process elements (NPEs) because they are not required by the chemical processes used to manufacture pulp (Galloway, 1994). The accumulation of NPEs can cause a variety of operational problems including corrosion, scale and deposit formation, and reduced bleaching effectiveness.

Models that predict the behaviour of NPEs in the fibreline and chemical recovery system will be very valuable in the design, optimization, and implementation of closed cycle operational strategies in kraft mills. In chemical recovery systems, the NPEs cause corrosion and deposit problems that must be addressed. Cations in the washing and bleaching stages of the fibreline

partition between fibres and water in the pulp suspension as a function of pH, temperature, ionic strength, metal precipitation, and chelating agent concentration. Understanding this partitioning is important and is the focus of this work.

1.3 Importance of Non-Process Elements

Successful implementation of closed cycle technology requires a thorough understanding of NPEs. Unfortunately, basic chemistry knowledge of some NPEs has yet to be determined (Ulmgren, 1996). NPEs are generally put into two categories: those which are soluble in alkaline solution (aluminum, chlorine, and potassium), and those which form insoluble hydroxides and carbonates (calcium, magnesium, and manganese) (Ulmgren, 1982). Insoluble NPE compounds can be removed from the alkali cycle in the green liquor clarifier or slaker, but then build up in the lime cycle. The major outlet from the lime cycle for calcium, magnesium and manganese is in the dregs, grits, and lime losses (Keitaanniemi and Virkola, 1982; Magnusson et. al., 1979; Gleadow et. al., 1997).

Accumulation of NPEs occurs when purge points are eliminated by system closure. One example is the build up of ions like calcium or magnesium in the bleach plant while using counter-current washing. Generally these divalent NPEs are solublized in the first acidic stage, washed from the pulp, and purged with the bleach plant effluents (Towers, 1997). When bleach plant effluents are recycled within the mill, a purge is lost. Other purges include washing losses, liquor spills, flue gas particulates, dust, grit, dregs, precipitated inorganic salts and scales, and deposits (Frederick, 1984).

Recycling bleach plant effluents is a critical step in achieving closed cycle operation. In totally chlorine free (TCF) bleach plants all effluent can be recycled to the chemical recovery system, while in elementally chlorine free (ECF) processes the acidic effluent must be treated (to remove metals) before recycle, or concentrated and disposed of (Ricketts, 1994). ECF mills will also need a means of chlorine removal in the liquor loop. Mills that have eliminated chlorine use in the bleach plant are thus the best candidates for closed cycle operation.

1.4 Scope of thesis and thesis contents

Two basic methods of modeling ion partitioning between fibres and water in a pulp suspension have been employed. Bryant and Edwards (1996) used ion exchange to predict the distribution of NPEs in a fibre suspension. Towers and Scallan (1996) use Donnan equilibrium to make similar predictions. In this work the approach of Towers and Scallan has been adopted. In their work, they ignored the non-ideality of the electrolyte solution. In this work, activity coefficients are introduced to account for the non-ideal nature of the solution of ions being considered.

The experimental data obtained by Bryant and Edwards agrees well with their model. At pHs above 10, the quantity of divalent cations attached to the fibres decreases. The data of Towers and Scallan indicates no such decrease as the pH rises to 10. This could be due to the precipitation of calcium or magnesium within the fibres as carbonates or hydroxides. Obtaining more experimental data at pHs above 10 will be valuable in elucidating the behaviour of NPEs at these higher pHs. In this work, partitioning data in this pH range were obtained.

This thesis includes a review of the importance of NPEs, the interaction of NPEs with pulp fibres, fibre chemistry, and a thermodynamics based model that will predict the partitioning of

NPEs between fibres and the external solution of a pulp suspension under a variety of process conditions. The partitioning model is compared to experimental data to verify the accuracy of the predictions. Model parameters describing the fibre properties are obtained by independent experiments.

Chapter 2

2. Background and Research Objectives

2.1 Non-Process Elements in Kraft Mills

Chemicals present in pulping, washing or bleaching that are not desired or required for the process are called non-process elements (NPEs). In general, the effect of non-process elements is detrimental to bleaching and recovery operations in a mill. Some elements, such as calcium, are process elements in parts of the mill (lime cycle) and non-process elements in other areas (bleach plant). The important NPEs are ions of aluminum (Al^{+3}), barium (Ba^{+2}), calcium (Ca^{+2}), iron (Fe^{+2} , Fe^{+3}), magnesium (Mg^{+2}), manganese (Mn^{+2}), phosphorus (PO_4^{-3} , as the phosphate ion), potassium (K^{+}), silicon (Si^{+3}), sodium (Na^{+}) and chlorine (Cl^{-}) (Galloway, 1994). Elements present in small amounts can be easily dealt with or ignored in modern open mills, but closure may cause these same species to build up to levels which cause precipitation or promote corrosion of process equipment.

Some of the effects of NPEs are recovery boiler corrosion, deposit formation, scale formation on hot surfaces, filter blinding, lime kiln operation problems, and hydrogen peroxide and ozone decomposition and free radical formation (Galloway, 1994). The elements, manganese and copper, catalyze the decomposition of the bleaching chemicals ozone and hydrogen peroxide and are presently removed by an acidic stage before pulp bleaching (Ulmgren, 1996). In acidic conditions, the carboxyl and phenolic groups on the fibres are fully protonated. Cations (like the transition metal ions of Mn^{+2} and Cu^{+2}) are present in very similar concentrations in the external solution and the solution within the fibres (internal solution). The mass of solution within the fibres is relatively small compared to the solution outside the fibres, so the majority of cations

are present outside the fibres and can be easily washed away. This means acidic washing can remove a great deal of the cationic NPEs from the fibre line. Of course, something must still be done with the acidic filtrates rich in NPEs.

The ions of potassium, magnesium, chlorine, and several reduced sulphur species participate most noticeably in process equipment corrosion. Potassium and chlorine cause the corrosion and plugging problems common to recovery boilers. One method of removing these two ions from the system is to discharge recovery boiler dust. The dust has about twice the concentration of potassium and chlorine as the smelt bed (Ulmgren, 1996). Unfortunately, but predictably, the problem of NPEs would again be simply transferred to another form of effluent, in this case solid. Magnesium is also involved in the corrosion of black liquor evaporators (Bihani, 1996) but the largest problem due to elevated magnesium levels is the formation of magnesium hydroxide ($\text{Mg}(\text{OH})_2$) which plugs white liquor and lime mud filters (Galloway, 1994).

Deposits are commonly formed by carry over of partially burned black liquor or the condensation of recovery boiler gases. These deposits contain ions of sodium, sulphate, carbonate, chloride, potassium, and reduced sulphurs (Tran, 1986). Deposits of calcium oxalate and calcium carbonate are major concerns during mill closure (Bihani, 1996). These calcium deposits can plug washer shower nozzles, filtrate lines, and washer fabrics and wires. Potassium carried into the calcium cycle causes ring formation and slabbing in the lime kiln by an adhesive effect due to the low melting point of potassium carbonate (Galloway, 1994; Gilbert and Rapson, 1980).

Most NPEs enter the pulping process with the wood, but many also enter in the process water and chemicals. They are most concentrated in the green parts of the tree, such as branches, roots, and bark (Smook, 1992). The elements enter the tree in the soil and water, but their concentration also depends on the age, species, and location in the tree. Calcium has the highest concentration, with potassium, chlorine, magnesium and manganese following. Entering the fibreline, calcium concentrations are typically 1000 - 3000 mg/kg of fibre (Bryant, 1996).

2.2 Wood Fibres, Pulping, and Bleaching

2.2.1 Fibre Chemistry

Understanding the physical and chemical properties of fibres is crucial to the modeling of NPE partitioning. Papermaking fibres are produced by the chemical or mechanical pulping of wood. Wood is a complex substance consisting of four main parts; cellulose, hemicellulose, lignin, and extractives. Cellulose is a polysaccharide of glucose molecules, between 600 and 1500 units in length for good papermaking fibres (Smook, 1992). In native wood the degree of polymerization is above 10000, but pulping and bleaching decrease this significantly (Biermann, 1996). Many long parallel strands of cellulose form the wall of the fibre and give it strength. These strands are wrapped in the fibre wall at various angles to make up three distinct fibre wall layers. Figure 2.2.1 shows a schematic of a fibre as it appears in wood, the strands (microfibrils) that make up the wall of the fibre, and the three complex chemicals that compose each strand. The schematic is adapted from Scallan and Tigerstrom (1992).

Lignin, a highly polymerized 3D structure of phenyl propane units, bonds the fibres of wood together. Although there is lignin in the fibres, it is most concentrated in the middle lamella,

where it encrusts individual fibres in the matrix of wood. During kraft pulping most of the lignin is broken apart and dissolved into the pulping liquor, freeing the fibres.

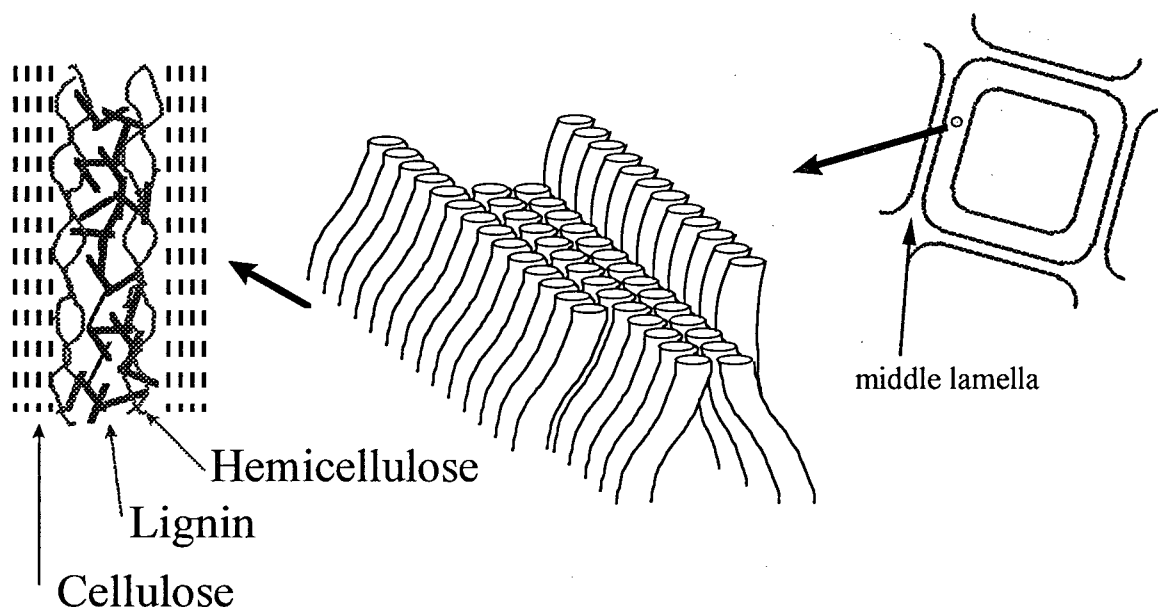


Figure 2.2.1: Wood fibres and their constituents. Fibres are held together in wood by the middle lamella and are composed of tiny strands, each composed of cellulose, hemicellulose, and lignin. Adapted from Scallan and Tigerstrom (1992).

Hemicellulose is a polymer of six-carbon sugars (glucose, mannose, galactose, 4-O-methyl-D-glucuronic acid) and five-carbon sugars (xylose and arabinose). Physically, it is a white solid material that is the transition substance between cellulose and lignin. Hemicellulose is more easily dissolved and degraded than cellulose but less easily than lignin. Ideally, papermaking fibres should have all lignin removed and all hemicellulose retained. This provides fibres that are both flexible and strongly bonding. In industrial pulping processes, it is not possible to remove only the lignin; hemicellulose is also dissolved due to the non-specific nature of the pulping chemicals.

In kraft pulp fibres, the residual hemicellulose and lignin after pulping have a large effect on the quantity and type of ionizable groups remaining on the fibre. The two important ionizing groups in kraft fibres are the carboxylic group (-COOH) and the hydroxyl group (-OH). Hydroxyl groups will be found in two main forms, phenolic hydroxyls attached mostly to lignin and somewhat to hemicellulose and cellulose hydroxyls (Scallan, 1989). The carboxylic groups are present in the lignin and hemicellulose and are ionized in weak acidic and neutral solutions. The pK_a is often approximated as 4-5 for carboxylic groups. Cellulose, hemicellulose, and lignin all contain hydroxyl groups, which are ionized only in strong alkali solutions ($pK_a = 10 - 14$).

When ionized, the negatively charged groups on pulp fibres form an equilibrium system with the positive ions in the surrounding water of the pulp suspension (assuming sufficient time is given for equilibrium to be attained). The concentration of counterions in the fibre or in the solution are controlled by phenomena such as electroneutrality, Donnan equilibrium, possible chemical reactions, and precipitation. The concentration of fixed charged groups on the fibre is decreased during pulping and bleaching as lignin and hemicellulose are removed and changed in chemical form.

2.2.2 Pulping and Bleaching Reactions

Kraft pulping uses an alkaline liquor of sodium sulfide (Na_2S) and sodium hydroxide ($NaOH$) at a temperature of 150 to 180°C for 1 - 2 hours to create free fibres from wood chips. The active ions are OH^- and HS^- . In the digester, lignin is typically attacked as shown in Figure 2.2.2. Typically, softwood pulps are 4 - 5% lignin after kraft pulping, compared to 26 - 32% lignin in the wood chips. Breaking the ether linkages that bond the phenyl propane units together leads to the fragmentation of the lignin polymer (Minor, 1996).

The purpose of bleaching is to increase brightness of fibres, with the secondary objectives of high brightness stability, pulp cleanliness, and cellulose content. While pure cellulose is white, lignin is responsible for the colour of pulp. During bleaching, lignin is removed and decolourized by more selective chemicals than are used in the pulping process. Oxidants (chlorine, chlorine dioxide, oxygen, ozone, hydrogen peroxide) and alkali (sodium hydroxide) are used to brighten the pulp.

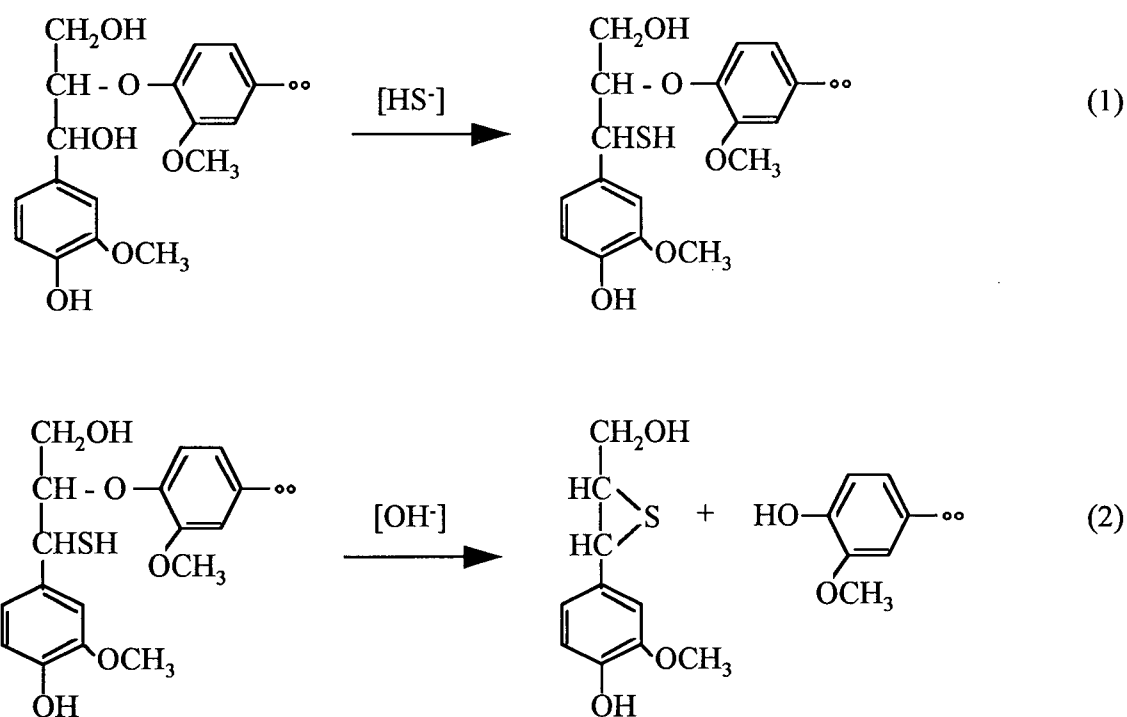


Figure 2.2.2: A typical lignin reaction in the pulping process. Ester bonds are attacked. Adapted from Smook (1992).

Oxidants degrade the lignin, which decreases its molecular size. The alkali degrades the oxidized lignin by hydrolysis and ionizes the acidic groups on the lignin fragments. This ionization increases the solubility of the lignin fragments in water and alkaline solutions so they

can be washed from the pulp. The important acidic groups that improve lignin solubility are the carboxylic, phenolic, and enolic. "Carboxylic acid groups arise mainly from the oxidative rupture and later fragmentation of aromatic rings in the initial bleaching stage..." (Dence, 1996). Carboxyl in the lignin of wood is 0%, after kraft pulping, 2.1%, after oxygen delignification, 3.5%, and after an OD(EOP) sequence, 10%. These same acidic groups attract NPEs in solution when they are ionized.

2.3 Metal Ion Partitioning in Pulp Suspensions

Two basic approaches to modeling ion partitioning between fibres and water in a pulp suspension have been proposed in the literature; one based on Donnan equilibrium, the other on ion exchange and chemical equilibrium. Ion exchange assumes that cations are bound chemically to the acidic groups within the pulp. Thus, there is competition between cations for the fixed negative charges on the fibres and cations are distributed accordingly between the solution and fibres. Modeling based on Donnan equilibrium assumes that no binding occurs between the free cations and fixed anionic groups but they are drawn to each other because of their opposite charges. The final concentration is determined by the quantities of fixed and free charge, and the volumes of the phases.

2.3.1 Modeling Based on Ion Exchange

Rosen (1975) studied the adsorption of sodium ions on kraft pulp fibres during washing. Effects of pulp type, Kappa number, pH, sodium concentration, and temperature on sodium adsorption were investigated. Pulps of slash pine and white oak were prepared in a laboratory. One major conclusion was that at least two ionizing groups on the kraft fibres are important, one important group in the pH range 3 - 6, the other above pH 10. Thus, the kraft fibres act as bifunctional

cation exchangers. Temperature and sodium concentration did not have a significant effect on the sorption of sodium.

Ampulski (1989) modeled the exchange of sodium for calcium on kraft fibres of bleached northern softwood. The objective of the work was to determine the equilibrium constant (K_a) for the $2\text{Na}^+ \leftrightarrow \text{Ca}^{+2}$ exchange. Experiments were performed at 0.1% consistency for an equilibrium period of 60 minutes. He found the thermodynamic equilibrium value of this exchange to change (decrease as solution concentration increases) over the range of calcium fraction bound to the pulp at pH 8. This implies that more than one ion exchange site exists on the pulp fibres. Calcium replaced sodium on the fibres in all cases.

Ions do not necessarily remain soluble as the pH changes and can precipitate on the fibres. Such a case was studied by Arnson and Stratton (1983) with aluminum ions. Cotton linters pulp at 0.3% consistency was used for experiments over the pH range 4 - 5.5 with aluminum concentrations from 2.5×10^{-4} M to 1.0×10^{-3} M. Results show that while the increase in ionized carboxyl groups over the pH range was 10%, the aluminum on fibres increased 300 - 400%. This behaviour is attributed to the formation of polynuclear aluminum species which precipitate due to the aluminum concentration and pH. Thus, aluminum under papermaking conditions does not follow the ion exchange of metal ions with carboxyl groups on fibres. Arnson and Stratton also evaluated the effect of time on aluminum adsorption and found that when aluminum is present primarily as Al^{+3} (at a pH of 4.2) there is no time dependence on adsorption. At higher pHs adsorption depends on time, but seems to approach equilibrium by 60 minutes.

Recently, a model using ion exchange and chelation was presented (Bryant and Edwards, 1996). The model predicts the distribution of Ca, Mn, Mg, and Na over the pH range 1.5 to 11.5 for a kraft pulp obtained after the last oxygen stage washer. They found that the concentrations of Fe and Al had little dependence on pH. The model provides good predictions over the pH range, with the largest differences in predicted and measured ion concentrations between the pHs of 2.5 to 5.5. The inhomogeneity of pulp makes it difficult to determine a good or poor fit, as the scatter in the data is fairly large. The ion exchange constants of Ca^{+2} , Mg^{+2} , Na^+ , Mn^{+2} , and MnOH^+ were adjusted to give a best fit from the experimental data. The ion exchange is predicted using ligands interacting with monovalent and divalent cations.



Each metal ion (M^+ or M^{+2}) has its own equilibrium constant with the fixed groups on the pulp fibres (L^-). The equilibrium constants were fitted to the experimental data which is a disadvantage because extensive experiments are first needed to obtain equilibrium constants before the model can be used as a predictive tool. Chelant addition was incorporated into the model. Chelants bind to metal ions forming soluble complexes that can be washed from the pulp. They are commonly added prior to bleaching stages to prevent ions from catalyzing the decomposition of bleaching chemicals (Lapierre et. al., 1995).

2.3.2 Modeling Based on Donnan Equilibrium

Application of Donnan equilibrium in the pulp and paper industry has concentrated on its influence on fibre swelling (Katz et. al., 1981). It has also found uses in describing the electrical conductivity of wet fibres (Been and Oloman, 1995) and the conductometric titration of fibres

(Scallan et. al., 1989). Recently, Donnan equilibrium has been the successful foundation for models predicting ion distributions between fibres and external solution.

Towers and Scallan (1996) used Donnan equilibrium theory to predict the distribution of cations in a pulp suspension. Donnan equilibrium uses chemical thermodynamics to show that, in the absence of an osmotic pressure difference, the ratio of the activity (or in the ideal case, concentration) of an ion in the fibre and solution is constant, regardless of the ion. The ratio deviates from unity if charge is restricted to one phase, as is the case with the anionic groups in fibre walls. This allows the concentration of any ion, in either the fibre solution or external solution, to be predicted if the distribution of a single ion is known. The other requirement to solve the equations is that both phases, fibre and solution, are electroneutral. Their model assumes only the carboxyl groups ($pK = 4$) on the fibres are important over the pH range considered. Experiments were performed with two softwood pulps from interior British Columbia mills at 0.74% and 1.1% consistency. Comparison to experimental data shows Donnan equilibrium is effective in predicting the distribution of Ca, Mn, Mg, and Na over the pH range 2 - 10. The use of Donnan equilibrium also allows for the concentration of the soluble ions to be predicted within the fibres, which means potential in-fibre precipitation can be predicted as cation concentrations increase.

Diniz (1996) compared ion exchange and Donnan equilibrium models through the partitioning of sodium and calcium cations. Experiments were performed under acidic conditions with a 30 minute equilibrium period. Two major conclusions are drawn from the results of potentiometric pulp titrations. First, calcium is present at half the concentration of sodium in the solution within the fibres (as opposed to Ca^{+2} being at the same concentration as Na^{+} , bringing with it a Cl^{-} to

maintain electroneutrality). Second, the ion exchange model agrees well with the experimental data, while the Donnan framework is not supported by the experimental data.

Others have followed the work of Towers and Scallan using Donnan equilibrium to predict sorption onto laboratory made kraft fibres (Rasanen and Stenius, 1997). An electrostatic double layer was added to the Donnan framework and the acidic groups on the fibres were characterized using potentiometric titration. Two dissociation constants are used to characterize the charged groups over the pH range 2 - 8. All ions, except the protons, are found to distribute themselves according to Donnan equilibrium. Hydrogen ions are considered specifically bound to the charge bearing groups.

Donnan equilibrium has also been used to theoretically evaluate the delignification of pulp (Haglund et. al., 1989). Theoretical predictions of anion partitioning at 10% consistency were performed and included fixed anionic groups corresponding to the sulphonic, carboxylic, and phenolic groups. Results indicate that including these three groups changes only the concentration of anions in the fibres; decreasing the anion concentration by approximately half due to the increased repulsive charge present. Since the concentrations in the fibre are quite low already, this change causes little difference in the partitioning predictions. The significance of this is that acceptable partitioning predictions are obtained simply by considering the carboxyl groups on the pulp fibres.

2.4 Mixture Thermodynamics

This section is concerned with the fundamental thermodynamic relations that govern the behaviour of electrolyte and non-electrolyte solutions. Some systems lend themselves easily to

the Gibbs definition of chemical potential, while others are more easily explained using the Helmholtz definition of chemical potential (Eisenberg, 1976; Guggenheim, 1977; Pitzer, 1991; Tanford, 1961; Tombs and Peacocke, 1974). In this work the Gibbs definition is used.

The definition of Gibbs free energy for a single phase is:

$$G = U + PV - TS \quad (3)$$

where: G is the Gibbs free energy

U is the internal energy

S is the entropy of the system

T is the absolute temperature

V is the volume of the system

P is the pressure of the system

The partial molar derivatives of each of the quantities in equation (3) can be taken to give:

$$\left(\frac{\partial G}{\partial n_j} \right)_{T,P,n_{i \neq j}} = \left(\frac{\partial U}{\partial n_j} \right)_{T,P,n_{i \neq j}} + P \left(\frac{\partial V}{\partial n_j} \right)_{T,P,n_{i \neq j}} - T \left(\frac{\partial S}{\partial n_j} \right)_{T,P,n_{i \neq j}} = \mu_j \quad (4)$$

$j=1,2,\dots,N$

where: μ_j is the chemical potential of neutral species j

n_j is the moles of species j

N is the number of species j

The subscript indicates that the variables of temperature, pressure, and the species other than j are to remain constant in the differentiation. Taking the partial derivative of equation (4) with respect to pressure, P , gives the important relation describing the effect of pressure on the chemical potential.

$$\left(\frac{\partial \mu_j}{\partial P} \right)_{T, n_j} = \left(\frac{\partial V}{\partial n_j} \right)_{T, P, n_{i \neq j}} = \bar{V}_j \quad (5)$$

where \bar{V}_j is the partial molar volume of component j at T and P

What makes this equation valuable is that it can be integrated from an initial chemical potential and pressure, μ° and P° , to a final chemical potential and pressure, μ and P . The result of the integration is shown in equation (6).

$$\mu_j - \mu_j^\circ = \int_{P^\circ}^P \left(\frac{\partial \mu_j}{\partial P} \right)_{T, n_j} dP = \int_{P^\circ}^P \bar{V}_j dP \quad (6)$$

The significance of this relation is that the chemical potential can be split into two terms; one (μ_j°) at a reference pressure, P° , and dependent on composition and temperature (because these were held constant in the integration). The second term depends on pressure, temperature, and composition (through \bar{V}_j). This is summarized in the equation below.

$$\mu_j(P, T, m) = \mu_j^\circ(P^\circ, T, m) + \int_{P^\circ}^P \bar{V}_j dP \quad (7)$$

where m is the molality. Molality is a measure of composition, and is defined as the mass of solute in moles per 1000 g of pure solvent. In this case, m represents the molality of all neutral species in the solution because the chemical potential is affected by all species present.

The activity is another way to represent the chemical potential. From statistical mechanics, the absolute activity can be defined in exponential relation to the chemical potential. The RT portion of the equation comes from the ideal gas origin of the relation where pressure (or fugacity) was used instead of activity.

$$\lambda_j = \exp\left(\frac{\mu_j}{RT}\right)$$

$$\mu_j = RT \ln \lambda_j \quad (8)$$

where: λ_j is the absolute activity of component j

μ_j is the chemical potential of component j

R is the ideal gas constant

T is the absolute temperature

Equation (8) can also be written for a reference chemical potential defined at a proper reference state, usually infinite dilution of solute component j or unit molality of j at the system temperature and pressure (Zemaitis et. al., 1986). The reference chemical potential is given by μ_j^0 . Defining the relative activity (activity) as $a_j = \lambda_j/\lambda_j^0$ and substituting into equation (8) gives the relation between activity and chemical potential.

$$\mu_j = \mu_j^0 + RT \ln a_j \quad (9)$$

where a_j is the activity of component j. Activity measures the difference between the components' chemical potential at the state of interest and the reference state. The activity is often written as a function of composition through the use of the activity coefficient. In terms of molality, the activity is:

$$a_j = \frac{\gamma_j m_j}{m_j^0} \quad (10)$$

where: a_j is the activity of neutral component j

γ_j is the molal activity coefficient of neutral component j

m_j is the molality of neutral component j

m_j^0 is the reference molality, set to one, but included so activity is dimensionless. This reference molality will not be included in the relations that follow.

The condition of equilibrium for any system of neutral components is equality of chemical potential of any component j in each phase involved. For the phases α , β , and χ , equilibrium is then written as:

$$\mu_j^\alpha = \mu_j^\beta = \mu_j^\chi = \dots \quad (11)$$

It should be pointed out that this is only true for neutral components. In the case of ions in solution a somewhat different relation from equation (11) is obtained or an additional relationship is required. Solutions with ions can be treated as ones containing only electrically neutral molecules by imposing the condition of electroneutrality (Guggenheim, 1977):

$$\sum_i m_i z_i = 0 \quad (12)$$

where: m_i is the molality of component i

z_i is the valence of component i

If there is no electric current and the electric potential is not considered, solutions of electrolytes can be described in the same manner as non-electrolytes as long as the electroneutral criteria is obeyed. The general relationships for electrolyte solutions that account for currents and potentials are discussed next.

2.5 Electrolyte Solution Thermodynamics

Cations and anions of a salt contribute to its chemical potential. Consider the dissociation of a typical salt:



where: C is the cation of the salt

A is the anion of the salt

v_C , v_A are the stoichiometric numbers of the cation and anion

$z+$, $z-$ are the valences of the cation and anion

The chemical potential is then defined by:

$$\mu_{CA} = \nu_C \mu_C + \nu_A \mu_A \quad (14)$$

where: μ_{CA} is the chemical potential of the whole salt CA

μ_C is the chemical potential of the cation

μ_A is the chemical potential of the anion

Substituting equation (9) into equation (14) and simplifying gives the following series of equations:

$$\mu_{CA} = \nu_C (\mu_C^O + RT \ln a_C) + \nu_A (\mu_A^O + RT \ln a_A) \quad (15)$$

$$\mu_{CA} = \mu_{CA}^O + RT (\ln a_C^{\nu_C} + \ln a_A^{\nu_A}) \quad (16)$$

$$\mu_{CA} = \mu_{CA}^O + RT \ln (\gamma_C^{\nu_C} m_C^{\nu_C} \gamma_A^{\nu_A} m_A^{\nu_A}) \quad (17)$$

$$\mu_{CA} = \mu_{CA}^O + RT \ln (\bar{\gamma}_{CA}^{\nu} m_C^{\nu_C} m_A^{\nu_A}) \quad (18)$$

where: $\bar{\gamma}_{CA}^{\nu}$ is the mean molal activity coefficient

$$\bar{\gamma}_{CA}^{\nu} = \gamma_C^{\nu_C} \gamma_A^{\nu_A}$$

$$\nu = \nu_C + \nu_A$$

m is the molality of the cation or anion

μ_{CA}^O is the reference chemical potential of the salt

$$\mu_{CA}^O = \nu_C \mu_C^O + \nu_A \mu_A^O$$

R is the ideal gas constant

T is the absolute temperature

The mean molal activity coefficient gives the activity of the whole salt. Relating the whole salt activity coefficient to its individual ions is very important because only the whole salt activity

can be measured. Many activity coefficient models do not give the activity coefficient of ions that make up the salt. However, Pitzer's model is one activity coefficient model that provides individual ion activity coefficients (Pitzer, 1973). Pitzer's activity coefficient model is presented in Appendix B and has been used to calculate all ion activity coefficients in this work (Pitzer, 1991).

Electrically charged species have a different measure of free energy, which is called the electrochemical potential (Guggenheim, 1929). It includes both a chemical and an electrical part, although splitting into these parts has no physical meaning (Guggenheim, 1977).

$$E_j^\alpha = \mu_j^\alpha + z_j \mathfrak{F} \psi^\alpha \quad (19)$$

where: E_j^α is the electrochemical potential of species j in phase α

μ_j^α is the chemical potential of species j in phase α

z_j is the valence of species j

\mathfrak{F} is Faraday's constant

ψ^α is the electric potential of phase α

Departures from electroneutrality (due to the electric potential) cause huge changes in the equilibrium state of the system. Considering an example of the electric potential is worthwhile to understand its importance (Guggenheim, 1977; Hatsopoulos and Keenan, 1965). Consider a conducting sphere in a vacuum with a charge Q on its surface and radius r . The electrical potential is given by:

$$\psi = \frac{Q}{4\pi\epsilon_0 r} \quad (20)$$

where ϵ_0 is the permittivity of a vacuum. Substituting a charge of 1×10^{-10} C, due to an excess of 10^{-10} moles of a material with charge $+1$, and a radius of 1 cm gives an electric potential of $0.86 \times$

10^7 V. This very high potential is due to an excess of material which is too small to measure chemically, thus, the electric potential is a very important parameter. Physically, liquids and solids are very, very close to electrically neutral under most circumstances.

The condition of equilibrium is then adjusted appropriately for the charged species in the phases α , β , and χ , becoming:

$$E_j^\alpha = E_j^\beta = E_j^\chi = \dots \quad (21)$$

Equilibrium requires the electrochemical potential in each phase to be the same. The second major statement in equilibrium electrolyte thermodynamics is that of electroneutrality, which simply means the total charge in each phase must equal zero. For a two phase system, α and β , the requirement of electroneutrality in terms of molality is:

$$\begin{aligned} \sum_j z_j m_j^\alpha &= 0 \\ \sum_k z_k m_k^\beta &= 0 \end{aligned} \quad (22)$$

where different indices have been used to account for the fact that some species may be confined to one phase, resulting in a different number of species in each phase, as will be discussed in Chapter 3.

2.6 Research Objectives

The purpose of this work is to describe, theoretically and experimentally, the partitioning behaviour of NPEs between kraft pulp fibres and solution. The specific research objectives are as follows:

1. Develop a thermodynamic based partitioning model which predicts the concentrations of soluble ions in fibres and external solution over the range of pHs important in pulping and

bleaching processes. The model will include activity coefficients (γ) since these deviate significantly from unity, even in ionic solutions of low concentration.

2. Obtain experimental data of important non-process element (those in the highest concentrations) partitioning behaviour to compare with the model predictions. Obtaining data at pHs above 10 will be important because limited published data are available. Furthermore, the existing published data do not agree with each other.
3. Determine important fibre properties by independent experiments. These parameter are needed in the partitioning model to adequately describe the system. The specific parameters needed are the total quantity of charge on the fibres, dissociation constants of charged groups on the fibres, and the quantity of water within the fibres.

Chapter 3

3. Partitioning of Non-Process Elements: Theory

3.1 Donnan Equilibrium

Donnan theory was developed to describe the distribution of ions between phases when some ions are not free to travel between the phases (Donnan and Harris, 1911). It was originally derived for ideal systems, where all the activity coefficients are considered to equal unity. The fundamental result of Donnan equilibrium is the “accumulation ratio” which gives the ratio of molality (really activity) of any species in each phase. The accumulation ratio is the same for each species, as will be shown in the following.

A pulp suspension can be considered a two phase system, a fibre phase and external solution phase. The fibre phase consists of the solution in intimate contact with the fibres (the solution within the walls of the fibre). The much larger second phase is the external solution to the fibres, which is the majority of the systems volume. This physical model was conceptualized by Towers and Scallan (1996). Consider two phases as shown in Figure 3.1.1. A non-diffusing species is present in the β phase, and is given the name species X. An osmotic pressure difference may develop between the phases, and this is given by $(P - P^o)$.

Starting with equation (21) and substituting equation (19) gives:

$$E_j^\alpha - E_j^\beta = 0 = \mu_j^\alpha - \mu_j^\beta + z_j \mathfrak{I}(\psi^\alpha - \psi^\beta) \quad (23)$$

Equation (6) can be substituted above. If the reference pressure is taken as P^0 , then only phase β needs to be adjusted for the pressure difference. Equations (9) and (10) give the chemical potential in terms of molalities and activity coefficients in both phases. Substituting gives:

$$E_j^\alpha - E_j^\beta = 0 = RT \ln \left(\frac{\gamma_j^\alpha m_j^\alpha}{\gamma_j^\beta m_j^\beta} \right) - \int_{P^0}^P \bar{V}_j^\beta dP + z_j \mathfrak{F}(\psi^\alpha - \psi^\beta) \quad (24)$$

where the reference state for chemical potential was taken to be the same for species j regardless of which phase is considered.

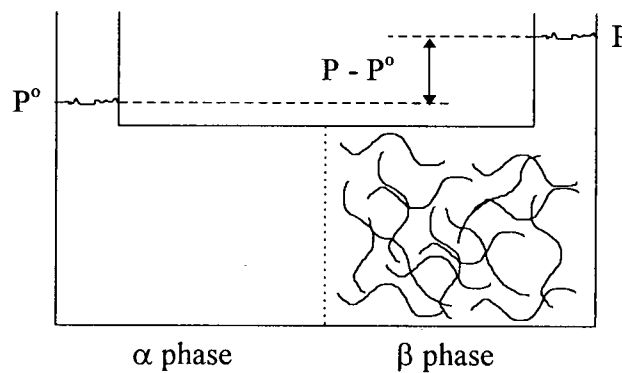


Figure 3.1.1: The Donnan equilibrium for a pulp fibre suspension

For a set of equations similar to Donnan's (these ones using activities rather than concentrations), the integral of the partial molar volume of component j is removed because its effect is generally small. Rearranging equation (24) to show all the ion dependent parameters on the left side gives:

$$\frac{1}{z_j} \ln \left(\frac{\gamma_j^\alpha m_j^\alpha}{\gamma_j^\beta m_j^\beta} \right) = - \frac{\mathfrak{F}}{RT} (\psi^\alpha - \psi^\beta) \quad (25)$$

Donnan's realization was that this relation holds for any mobile ion in solution. The valence of ion j can be drawn into the logarithm and the accumulation ratio defined to give the final relation

of Donnan equilibrium (which should be called Gibbs-Donnan equilibrium because activities are used), written here for ions j , k , and l :

$$\left(\frac{\gamma_j^\alpha m_j^\alpha}{\gamma_j^\beta m_j^\beta} \right)^{\frac{1}{z_j}} = \left(\frac{\gamma_k^\alpha m_k^\alpha}{\gamma_k^\beta m_k^\beta} \right)^{\frac{1}{z_k}} = \left(\frac{\gamma_l^\alpha m_l^\alpha}{\gamma_l^\beta m_l^\beta} \right)^{\frac{1}{z_l}} = \dots = \lambda \quad (26)$$

where λ is the accumulation ratio of the system. This relation shows that, when the pressure difference between phases is not significant, ions of the same valence are present in the same proportion in each phase. Counterions to the non-diffusing species will accumulate in the β phase to maintain electroneutrality and the final composition will be determined by the accumulation ratio λ .

Ideal Donnan equilibrium is applicable if the activities ($a = \gamma m$) of the free species are approximately equal to the molalities (m) of those species. This simpler form of equilibrium was used by Towers and Scallan (1996) to predict the distribution of ions between fibres and external solution. The equilibrium relationship is very similar to equation (26) but without the activity coefficients.

$$\left(\frac{m_j^\alpha}{m_j^\beta} \right)^{\frac{1}{z_j}} = \left(\frac{m_k^\alpha}{m_k^\beta} \right)^{\frac{1}{z_k}} = \left(\frac{m_l^\alpha}{m_l^\beta} \right)^{\frac{1}{z_l}} = \dots = \lambda' \quad (27)$$

3.2 Mass Balances and Dissociation Relationships

To calculate results (that is the molalities of all species in the α and β phases) from the data available about a system of fibres in solution, some additional relations are needed. The first of these is the mass balance. Knowing the total moles of some cation j , the moles of j in phase α can be related to the moles of j in phase β .

Total moles cations j = Moles Cations j in α + Moles Cations j in β

$$C_j = (\text{mass solvent}^\alpha)(m_{C_j}^\alpha) + (\text{mass solvent}^\beta)(m_{C_j}^\beta)$$

$$C_j = (V-F)(m_{C_j}^\alpha) + F(m_{C_j}^\beta)$$

$$m_{C_j}^\alpha = \frac{C_j - F(m_{C_j}^\beta)}{V - F} \quad (28)$$

The same relationship holds for all anions in the system, and gives:

$$m_{A_j}^\alpha = \frac{A_j - F(m_{A_j}^\beta)}{V - F} \quad (29)$$

where: C_j is the total moles of cation j in the system

A_j is the total moles of anion j in the system

F is the mass of solvent in the β phase

V is the total mass of solvent in the system

m_j is the molality in a phase of cation or anion j

The second important relation is the dissociation of the acidic charged groups on the non-diffusing species. The general reaction for the dissociation is:



where: X^- is the bound charged group on the non-diffusing species

H^+ is the dissociating group (assumed hydrogen)

If K_a is the dissociation constant, then the activities of the species present can be used to represent the equilibrium that is attained.

$$K_a = \frac{(a_{X^-}^\beta)(a_{H^+}^\beta)}{(a_{XH}^\beta)} \quad (31)$$

Experimental data used to obtain K_a are rarely good enough to warrant using activity coefficients. Here, the kraft fibres make for a very difficult titration system, so the ideal

dissociation constant, K_a' , will be used. The result of making this approximation within the fibres is explored in Appendix E. The dissociation relationship becomes,

$$K_a' = \frac{(m_{X^-}^\beta)(m_{H^+}^\beta)}{(m_{XH}^\beta)} \quad (32)$$

Now let Q_X be the moles of fixed charged groups on the fibre. These charged groups can have two forms, bonded to a hydrogen or dissociated. The relationship can then be written:

$$\frac{Q_X}{F} = m_{XH}^\beta + m_{X^-}^\beta \quad (33)$$

where: Q_X is the equivalents of fixed charged groups on the fibres

F is the mass of solvent in the β phase

m_{XH}^β is the molality of charged groups with hydrogen bound to them

$m_{X^-}^\beta$ is the molality of charged groups in the dissociated state

It is worth while to note that because these equations are derived with the idea of a Gibbs-Donnan equilibrium in mind, ions in solution (besides hydrogen) will not bind with the fibre. The theory assumes that ions in solution are partitioned because of the charge on the fibre, but do not form chemical bonds with the charged groups. Thus, the state of fibre charged groups is completely defined by equation (33). Substituting equation (33) into equation (32) and solving for $m_{X^-}^\beta$ gives:

$$m_{X^-}^\beta = \frac{K_a'(Q_X/F)}{m_{H^+}^\beta + K_a'} \quad (34)$$

For multiple dissociating sites on the fibre (K_{a1}' , K_{a2}' , K_{a3}' ,... K_{aj}') the sum of all types of fixed charged groups on the fibres is needed to describe the charge.

$$\begin{aligned}
m_{X^-}^\beta &= m_{X_1^-}^\beta + m_{X_2^-}^\beta + \dots + m_{X_j^-}^\beta \\
Q_X &= Q_{X_1} + Q_{X_2} + \dots + Q_{X_j} \\
m_{X^-}^\beta &= \sum_j \frac{K_{aj}'(Q_{X_j}/F)}{m_{H^+}^\beta + K_{aj}'}
\end{aligned} \tag{35}$$

Specifically for kraft pulp fibres there are two acidic groups responsible for the majority of charge; the carboxyl and phenolic hydroxyl. Written for two dissociating sites, charge on the fibres is modeled as:

$$Q_X = Q_{X_1} + Q_{X_2} \tag{36}$$

$$\begin{aligned}
m_{X^-}^\beta &= m_{X_1^-}^\beta + m_{X_2^-}^\beta \\
m_{X^-}^\beta &= \frac{K_{a_1}'(Q_{X_1}/F)}{m_{H^+}^\beta + K_{a_1}'} + \frac{K_{a_2}'(Q_{X_2}/F)}{m_{H^+}^\beta + K_{a_2}'}
\end{aligned} \tag{37}$$

In Section 5.5.1 it will be shown that grouping the charge on fibres into two forms is still not an adequate modeling method. Charge is best described by an "exact charge" model to reflect the polyfunctionality of the acidic groups within the fibres.

All the relations needed to solve the partitioning problem have now been developed. There are five relations that need to be considered. The first is the condition of electroneutrality (equation 22), next the condition of equilibrium (equation 26), two mass balances on cations and anions (equations 28 and 29), and finally the dissociation relations (equation 37). Activity coefficients are involved in two of these relations. An activity coefficient model is needed to determine these values.

Pitzer's model has been chosen to obtain free ion activity coefficients. The Pitzer model is a semi-empirical expansion of the Debye-Huckel method to account for the kinetic effects of the

hard core of ions and the effect of ionic strength on short range forces (Zemaitis et. al., 1986). The model includes interaction parameters between two and three ions. Model parameters for many ions have been published, and are valid over a specific range of molality (generally less than 6 molal). Figure 3.3.1 shows the variation of the activity coefficient of calcium in the fibre and external solutions for a pulp suspension at 1% consistency as predicted by Pitzer's model. The activity coefficients deviate significantly from unity over the pH range of interest.

3.3 Model Summary

The equations used to predict the partitioning of ions, assuming a Gibbs - Donnan equilibrium is obeyed, are summarized in Table 3.3.1. The notation α and β has been replaced by S and F to indicate the external solution (S) and fibre (F) phases respectively. This is somewhat more intuitive. The corresponding relationships for an ideal Donnan equilibrium are presented for comparison.

Modeling in this work considers four cations; H^+ , Na^+ , Ca^{+2} , and Mg^{+2} . The anions present in the system are OH^- , Cl^- , and X^- (the fixed anionic charge on the fibres). These species are added to the system using $NaCl$, $CaCl_2$, and $MgCl_2 \cdot 6H_2O$. All other mobile ions are assumed to be removed from the fibres during acid washing. These ions yield six unknown molalities in the external solution and seven unknown molalities in the fibre phase. The final unknown in the system is the Donnan partitioning ratio or distribution coefficient, λ . Thus, there are 14 unknowns and it must be possible to write 14 equations to solve the system.

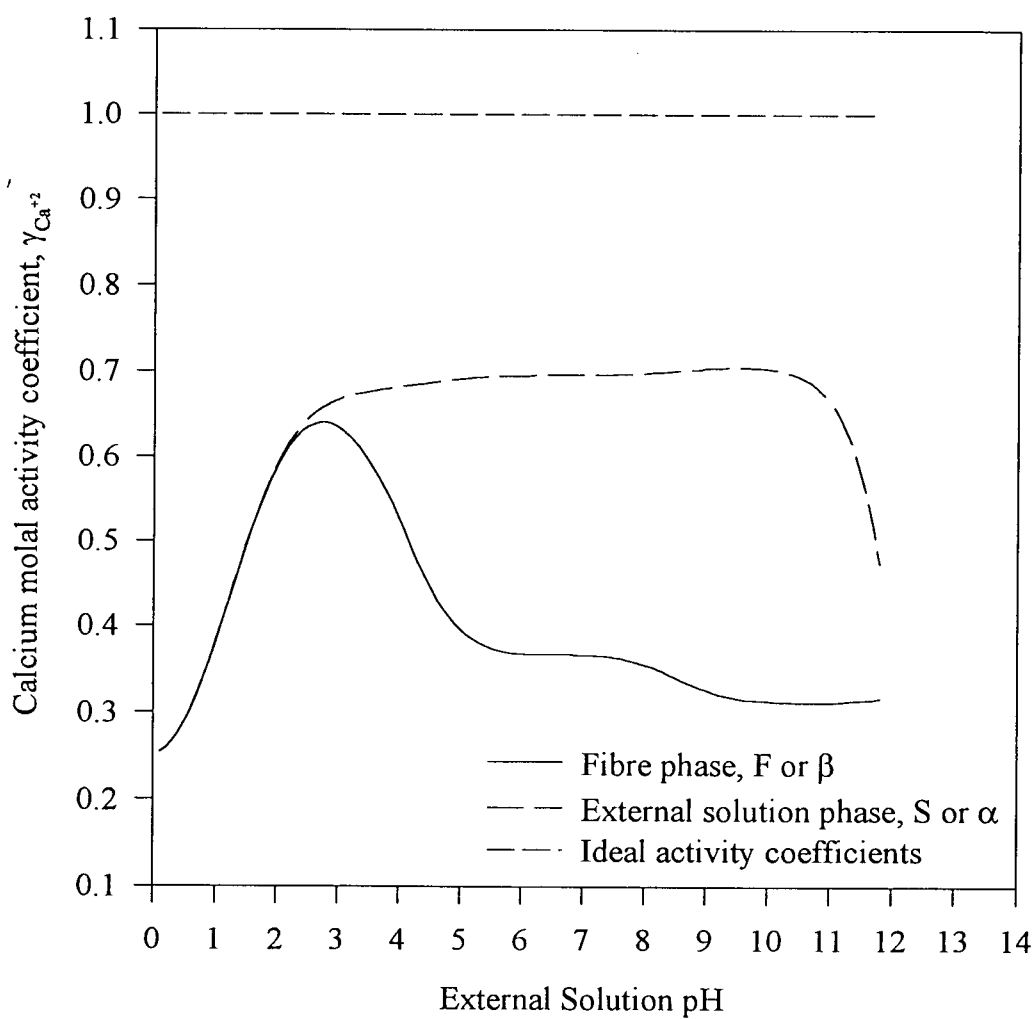


Figure 3.3.1: Model predictions of calcium (Ca^{+2}) activity coefficients over a range of pHs. The activity coefficients deviate a great deal from one, indicating the system is not ideal.

Gibbs - Donnan equilibrium	Ideal Donnan equilibrium
$\sum_j z_j m_j^S = 0$ $\sum_k z_k m_k^F = 0$ $\left(\frac{\gamma_j^S m_j^S}{\gamma_j^F m_j^F} \right)^{\frac{1}{z_j}} = \left(\frac{\gamma_k^S m_k^S}{\gamma_k^F m_k^F} \right)^{\frac{1}{z_k}} = \left(\frac{\gamma_l^S m_l^S}{\gamma_l^F m_l^F} \right)^{\frac{1}{z_l}} = \dots = \lambda$ $m_{C_j}^S = \frac{C_j - F(m_{C_j}^F)}{V - F}$ $m_{A_j}^S = \frac{A_j - F(m_{A_j}^F)}{V - F}$	$\sum_j z_j m_j^S = 0$ $\sum_k z_k m_k^F = 0$ $\left(\frac{m_j^\alpha}{m_j^\beta} \right)^{\frac{1}{z_j}} = \left(\frac{m_k^\alpha}{m_k^\beta} \right)^{\frac{1}{z_k}} = \left(\frac{m_l^\alpha}{m_l^\beta} \right)^{\frac{1}{z_l}} = \dots = \lambda'$ $m_{C_j}^S = \frac{C_j - F(m_{C_j}^F)}{V - F}$ $m_{A_j}^S = \frac{A_j - F(m_{A_j}^F)}{V - F}$
<p>Single Dissociation Constant</p> $m_{X^-}^F = \frac{K_a'(Q_X/F)}{m_{H^+}^F + K_a'}$	<p>Single Dissociation Constant</p> $m_{X^-}^F = \frac{K_a'(Q_X/F)}{m_{H^+}^F + K_a'}$
<p>Two Dissociation Constants</p> $Q_X = Q_{X_1} + Q_{X_2}$ $m_{X^-}^\beta = \frac{K_{a_1}'(Q_{X_1}/F)}{m_{H^+}^\beta + K_{a_1}'} + \frac{K_{a_2}'(Q_{X_2}/F)}{m_{H^+}^\beta + K_{a_2}'}$	<p>Two Dissociation Constants</p> $Q_X = Q_{X_1} + Q_{X_2}$ $m_{X^-}^\beta = \frac{K_{a_1}'(Q_{X_1}/F)}{m_{H^+}^\beta + K_{a_1}'} + \frac{K_{a_2}'(Q_{X_2}/F)}{m_{H^+}^\beta + K_{a_2}'}$

Table 3.3.1: Equations describing ion partitioning on fibres within the Donnan framework

The equations used in the computer algorithm are shown in Appendix C. The Donnan distribution coefficient can be written six times, two electroneutrality relations, one fibre dissociation, three mass balance relations for Na^+ , Ca^{+2} and Mg^{+2} , and the dissociation of water written for the fibre phase. The molality of H^+ in the external solution is set, acting as the last equation required to obtain a solution. The well known relation for the dissociation of water is given below, for completeness.

$$K_w = a_{H^+}^F a_{OH^-}^F = \gamma_{H^+}^F m_{H^+}^F \gamma_{OH^-}^F m_{OH^-}^F \quad (34)$$

where K_w is the dissociation constant of water, 10^{-14} . The fourteen equations are solved through iteration of the Donnan distribution coefficient.

3.4 Model Assumptions and Computational Algorithm

The partitioning model results are presented in Chapter 5. This section deals with the assumptions that are made to solve the equations developed previously and the computer algorithm used to produce results.

There are two assumptions that need to be made to solve the system of equations. First, all ions are considered to be soluble over the entire pH range. The model does not account for the precipitation of any species. Since the components considered in the modeling are Na^+ , H^+ , Ca^{+2} , Mg^{+2} , OH^- and Cl^- , this assumption should not be violated over the pH range 2 - 9. Above a pH of 9 the formation of calcium and magnesium precipitates could become appreciable in the form of carbonates and hydroxides. The solubility products of potential precipitates can be checked at each predicted equilibrium condition in the external solution and within the fibre solution (internal solution).

The second assumption is made to simplify the complex system being considered. It is assumed that only the carboxyl and phenolic hydroxyl are important protonating sites over the pH range 2 - 13. In other words, two dissociation constant, K_{a1}' and K_{a2}' , are used to represent all the anionic groups on the fibres. This assumption is based on an understanding of what the fibres physically contain. The many possible configurations these charged groups may exist in may still not allow two dissociation constants to adequately model the fibres. The validity of this assumption, and the assumptions listed above, will be discussed as the results are presented in Chapter 5.

A FORTRAN computer program has been written to solve the equations that govern Gibbs-Donnan equilibrium presented in Section 3.3 and Appendix C. A block diagram of the computer program is shown in Figure 3.4.1 and the algorithm itself is shown in Appendix F. Fibre properties and total salt contents are the initial input to the program. Fibre properties include the total charge content, Q_{x1} and Q_{x2} , dissociation constants, K_{a1}' and K_{a2}' , mass of water in the fibre phase, F , and mass of oven dry fibre in the system. The quantity of free ions added to the system (Na^+ , Ca^{+2} , and Mg^{+2}) and the total mass of the equilibrium system, V , are also input to the model.

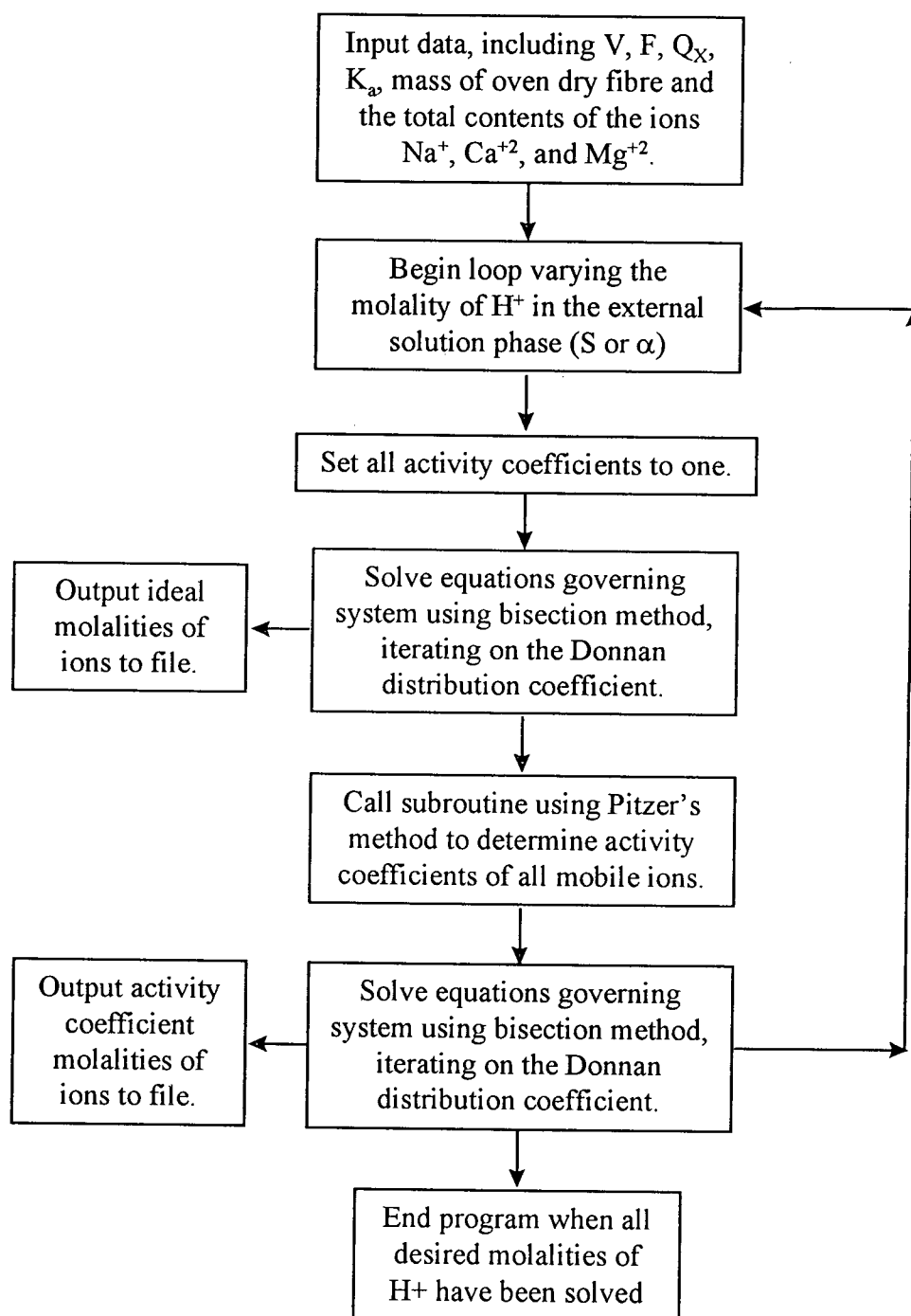


Figure 3.4.1: Block diagram of computer algorithm

Chapter 4

4. Partitioning of Non-Process Elements: Experimental

Ion partitioning experiments determine how a metal ion distributes itself between the fibre and external solution phases in a pulp suspension. Figure 3.1.1 shows the two phases, and since ions can be present in both, the metal contents in both phases need to be determined. Partitioning experiments with pulp as-received from the mill and with acid-washed pulp were conducted, and are compared to the proposed partitioning model. The model contains several parameters such as the total charge content, Q_{X1} and Q_{X2} , dissociation constants, K_{a1} and K_{a2} , and mass of water in the fibre phase, F . These parameters are determined from independent experiments, as explained in Section 4.5.

4.1 Materials

- A pre-oxygen kraft pulp taken after the brown stock washers from an interior British Columbia mill.
- Water is distilled and treated in an Elgastat UHQ unit which purifies water through organic adsorption, ion exchange, and ultra microfiltration.
- NaCl (crystals), CaCl_2 (anhydrous, 20 mesh and finer desiccant grade), and $\text{MgCl}_2 \cdot 6\text{H}_2\text{O}$ (crystals) from Fisher Scientific (USA) for use in re-addition to acid washed pulp and preparation of AA standards.
- KCl (crystals) from Fischer Scientific (USA) and La_2O_3 (99.99%, powder) from Aldrich Chemical Company Inc. (USA) for use in AA.
- NaOH (97.8%, solid, electrolytic pellets) from Fisher Scientific (USA) used for pH adjustment of acid washed pulp experiments.

- Concentrated HCl (trace metal grade) from Fisher Scientific (Napean, ON) used to adjust the pH of the pulp suspensions and for acid washing the as-received pulp.
- EGTA (~97%) from Sigma Chemical Co. (USA) and EDTA (99 +%) from Aldrich Chemical Company Inc. (USA) for use in photometric titrations.

4.2 Metal Ion Partitioning with Pulp As-Received

Pre-oxygen kraft pulp contains many NPEs, dissolved organics, residual pulping chemicals, and possibly dirt or other foreign materials. Of the long list of NPEs, only Na^+ , Ca^{+2} , and Mg^{+2} were examined in detail because these are present in the highest concentrations. Tests were performed on the as-received pulp to determine the total metal content of Na^+ , Ca^{+2} , and Mg^{+2} in the pulp and to examine their partitioning behaviour at a variety of conditions. Since other metal ions on the pulp are also present at unknown quantities it is difficult to compare these results to the partitioning model. Quantities of all mobile ions in the system are needed as input to the partitioning model.

Total metal ion quantities on the post brown stock pulp are determined by performing experiments at 1% consistency in a 1L mixing vessel at the pH that naturally occurs upon dilution of the mill pulp, with water, to the desired consistency. Analyzing the metal quantities in the external solution and in the fibres allows the total metals present on the pulp to be calculated. Ion concentrations, total fixed charge in the system, and varying the pH all affect the equilibrium that is obtained. These effects were explored with the original kraft pulp in the following experiments:

1. Addition of calcium (Ca^{+2}) in quantities of ~50 and ~100% of the total calcium originally present on the pulp. The consistency for these experiments was 1% and the pH was that naturally occurring upon dilution with water.
2. Change the consistencies from 1% (both higher, ~ 2%, and lower, ~0.5%). Changing the consistency changes the total fixed charge and the metal ion concentrations. The pH is again that naturally occurring upon dilution.
3. Reducing the pH of the pulp suspension to decrease the quantity of ionized fixed charged groups. The pH is lowered using dilute HCl, and the consistency is maintained at 1%.

These experiments were performed in a 1L mixing vessel with both the external solution and fibre phases being analyzed by atomic absorption (AA). Following is the detailed experimental procedure and the principles involved in determining the pulp metal profile.

4.2.1 General 1L Vessel Equilibrium Procedure

1. Clean 1 L jacketed glass vessel with HCl solution. Acid washing removes residual ions from previous experiments. Rinse with deionized water and allow to dry. Also clean the platinum crucible in this way, dry, heat in muffle furnace at 575°C for 15 minutes, and cool in a desiccator.
2. Weigh pulp into the vessel and make up the weight with deionized water to give a consistency of 1% (in the 1L vessel this is 10 g of oven dry fibre and 990 g of water for a total mass of 1000g). It's important the values of consistency are quite accurate since this plays a major role in determining charge content and solution phase water content. Record the mass of pulp, consistency of pulp (determined previously), and the mass of water added

to the pulp in the mixing vessel. From these values the consistency of the pulp suspension can be calculated to verify it is 1%.

Experiments performed with elevated calcium contents, different consistencies, and low pH are modified at this step. For elevated calcium experiments, the pulp is weighed into the vessel, then the calcium is added in the form of CaCl_2 before the deionized water is added to the system. For experiments at different consistencies the quantity of pulp added to the mixing vessel is doubled (2% consistency) or halved (0.5% consistency). Finally, experiments with reduced pH are performed by adding enough water to bring the system mass up to about 900g, then slowly adding the dilute HCl to achieve the desired pH. When the desired pH is reached, water can be added to make the system up to 1000g. Adding all the water then adjusting the pH can push the consistency significantly lower than 1%. Subsequent experimental steps are the same for all types of experiments.

3. Begin mixing at 400 rpm with a three bladed, propeller style stainless steel impeller. Insert nitrogen gas line and sweep pulp slurry with N_2 for several minutes. Cover to prevent carbon dioxide absorption and excess evaporation. Equilibrium occurs at room temperature and atmospheric pressure.
4. Allow system to come to equilibrium. This should take at least 15 minutes, but less than two hours based on the work of Park (Park, 1996; Rosen, 1975). The pulp suspension should be swept with nitrogen once or twice to maintain low carbon dioxide levels. Carbon dioxide is soluble in water and forms carbonic acid (Whitten et. al., 1988) which has the tendency to change the pH of the system.

5. At the end of the equilibrium period the fibres must be separated from the bulk solution. A simple way is to use a Buchner funnel without filter paper and a large vacuum flask. Filter paper is not used to prevent potential fibre and filtrate contamination with metal ions. Care should be taken to ensure all the fibre is recovered from the mixing vessel so the oven dry fibre mass can be accurately determined. The fibre mat in the funnel and the external solution must be kept separate after this point. Figure 4.2.1 shows the experimental procedure in diagrammatic form.
6. Remove as much entrained filtrate from the mat of fibres on the vacuum flask as possible. Place the fibre mat in a platinum crucible. Record the mass of the dry crucible and mass of the crucible with the fibre mat. The mass of the moist fibre mat is needed to determine the quantity of external solution trapped among the fibres.
7. Filter the external solution on a membrane filter to remove any fibres that have not been trapped by the fibre mat in the Buchner funnel. Retain the filtrate for analysis by atomic absorption or titration.

4.2.2 Data Analysis for 1L Mixing Vessel Experiments

The fibre mat recovered in the Buchner funnel consists of fibres and external solution. Wet fibres also contain solution within the fibres (an internal solution). The quantity of internal solution can be determined by fibre saturation point (FSP) measurements, as will be discussed later in Chapter 4. Thus, there are two distinct types of solutions in a fibre suspension; the external solution (denoted by α or S) and the internal solution (denoted by β or F). The total metal ions in the system are then given by:

1L mixing vessel procedure

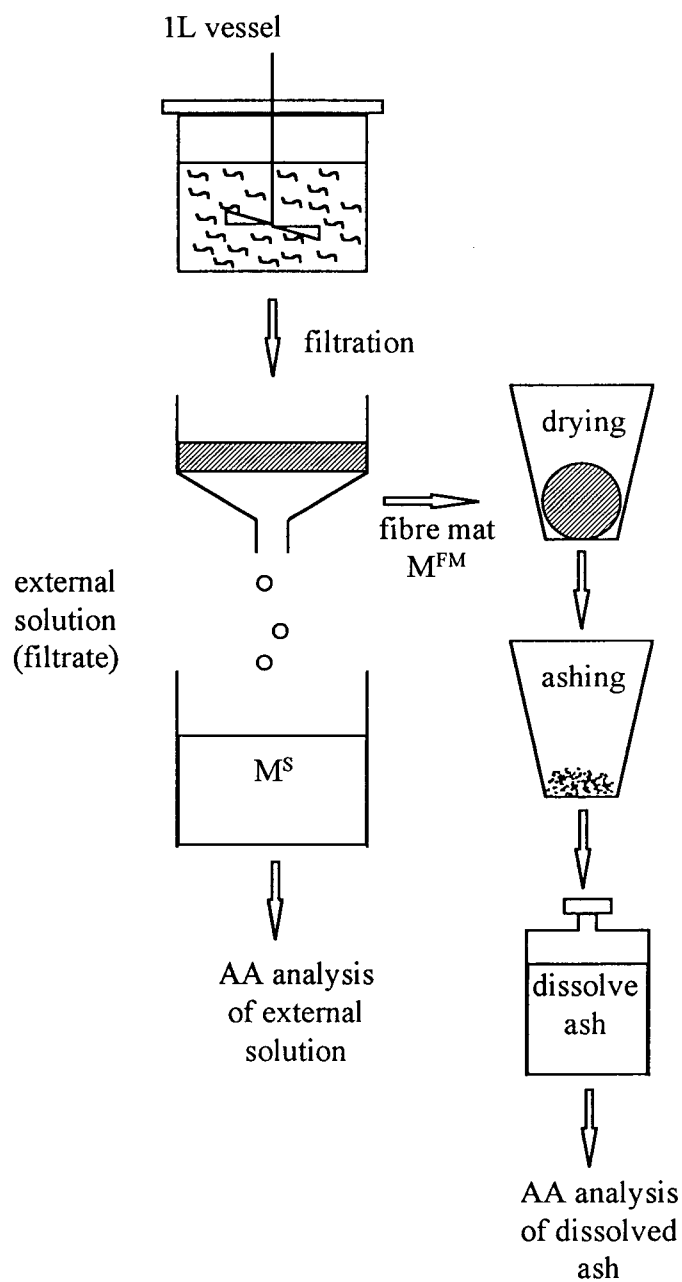


Figure 4.2.1: Experimental procedure for determining the metal ion contents in ash and external solution. Procedure uses a 1L vessel.

$$M^T = M^F + M^S \quad (38)$$

where: M^T is the total quantity of metal ions in the fibre suspension, mg

M^F is the quantity of metal ions in the fibres (internal solution), mg

M^S is the quantity of metal ions in the external solution, mg

Ions within the external solution trapped among the fibres in the fibre mat remain with the fibres during the drying, ashing, and dissolving steps. This quantity of ions must be accounted for in the calculation of M^F . Since the filtration step (see Figure 4.2.1) occurs quickly (less than 1 minute), it is assumed that the trapped external solution is identical in composition to the recovered external solution. Under this assumption, the fibre mat and external solution metal contents allow the metal contents in the fibres to be determined, since:

$$M^{FM} = M^F + M^{TS} \quad (39)$$

where: M^{FM} is the quantity of metal ions in the fibre mat, mg

M^F is the quantity of metal ions in the fibres (internal solution), mg

M^{TS} is the quantity of metal ions in the trapped external solution, mg. The concentration of metals in the M^{TS} solution (trapped external solution) is the same as in the M^S solution (external solution), but only a small fraction of M^S is trapped in the fibre mat.

Determining the quantity of a given metal ion in the fibre mat (M^{FM}) and external solution (M^S) allows the use of equation (39) to determine the quantity in the fibre phase (M^F). Equation (38) can then be used to determine the total metal quantity in the system (M^T). These calculations were performed for all experiments utilizing the 1L mixing vessel.

4.3 Metal Ion Partitioning with Acid-Washed Pulp

Acid-washed pulp is used to simplify the complex fibre system that is being considered. Post brown stock pulp contains many soluble ions and dissolved lignin, which makes determining fibre properties and equilibrium partitioning predictions difficult. Low pHs remove soluble ions from the pulp fibres, allowing pulps with few or no metal ions to be produced. Only the ions of interest are re-added to the acid washed fibres, and the total quantity of the added ions is known exactly. Equilibrium experiments from pHs of 1 to 13 are performed with the acid washed fibres, as well as the conductometric, potentiometric, and FSP experiments.

Two types of equilibrium experiments are performed; 1L vessel experiments and 150 mL vessel experiments. The 1L vessel is used to obtain enough of a fibre mat for ashing, dissolving and atomic absorption analysis (10 g oven dry fibre). The 150 mL vessel experiments are smaller (1 g oven dry fibre) and only the filtrate phase is analyzed for metal content. The 150 mL vessels are used only with acid washed fibre and re-addition of metal ions, since the total quantity of metal ions is known and the metal content in the fibres can be determined by back-calculation. The 1L mixing vessel experiments with acid-washed fibre follow the method of Section 4.2.1, with ion readdition occurring at step 2. Presented below are the methods used for acid washing and 150 mL vessel experiments, as well as a discussion of the calculation procedure used when the total quantity of any given metal ion is known.

Two basic sets of acid-washed data were obtained; low magnesium and elevated magnesium. Low magnesium experiments correspond to the metal contents determined on the post brown stock pulp. Elevated magnesium experiments occur with a much larger amount of magnesium

re-added to the acid washed fibre. The purpose of elevating the magnesium level was to encourage precipitation within the fibres as pH increased.

4.3.1 Acid Washing Procedure

The original pulp is washed three times to remove metal ions. The first washing uses deionized water to remove the majority of the dissolved lignin and ions present in the external solution. HCl reduces the pH of the second washing to 1.5 - 2. Deionized water is again used for the final washing. All washings occur in a batch fashion at 1% consistency, and are similar to the procedure of Section 4.2.1.

1. Clean 1 L jacketed glass vessel with HCl solution. Rinse with deionized water and allow to dry.
2. Weigh pulp into the vessel and make up the weight with deionized water to give a consistency of 1%. Record the mass of pulp, consistency of pulp (determined previously), and the mass of water added to the pulp in the mixing vessel. From these values the consistency of the pulp suspension can be calculated to verify it is 1%.
3. Begin mixing at 400 rpm with a three bladed propeller style stainless steel impeller. Insert nitrogen gas line and sweep pulp slurry with N_2 for several minutes. Cover to prevent carbon dioxide absorption and excess evaporation.
4. Allow system to come to equilibrium for at least one hour. The pulp suspension should be swept with nitrogen once or twice to maintain low dissolved carbon dioxide levels.
5. At the end of the equilibrium period the fibres are separated from the bulk solution on a Buchner funnel. The fibre mat is then placed back into the mixing vessel and deionized water is added to give a consistency above 1% (i.e. add less water).

6. Begin mixing at 400 rpm and insert nitrogen gas line to sweep pulp slurry with N_2 for several minutes. The pulp slurry must now be acidified to attain a pH of 1.5 - 2 using 6M HCl. For 10 g of oven dry fibre at 1% consistency, approximately 7 ml of the 6M HCl is needed to bring the system into the desired pH range. Once the desired pH is obtained deionized water is added to decrease the consistency to the desired 1%. Again the pulp slurry is allowed time to come to equilibrium, sweeping with nitrogen occasionally.
7. At the end of the acidified equilibrium period the fibres are again separated from the bulk solution on a Buchner funnel. The fibre mat is then placed back into the mixing vessel and deionized water is added to give a consistency of 1%.
8. Mix at 400 rpm and sweep for several minutes with nitrogen, as done on previous equilibrium's. The purpose of this washing is to remove the excess acid remaining from the previous acid washing equilibrium. Again the pulp slurry is allowed time to come to equilibrium, sweeping with nitrogen occasionally.
9. Finally, the pulp slurry is filtered on a Buchner funnel and the fibre mat is retained for use in experiments. Fibre treated in this manner is used in large mixing vessel experiments with salt re-addition, 150mL vessel equilibrium's with salt re-addition, FSP measurements, and conductometric and potentiometric titrations.

4.3.2 150 mL Vessel Equilibrium Procedure

The purpose of 1L vessel equilibrium experiments is to obtain both the fibre mat and external solution for analysis of metal contents. The fibre mat is ashed and dissolved as shown in Figure 4.2.1. When the total salt content in the system is known, the external solution can be analyzed for it's metals and quantities of ions in the fibres can be determined by back-calculation. This

eliminates the many steps involved in determining the metal contents in the fibre pad and significantly speeds up the process of obtaining metal ion partitioning data.

PTFE bottles of ~150 mL volume (Nalgene) are used for the experiments. Experiments are performed at 1% consistency, atmospheric pressure, and room temperature with 1g of oven dry fibre used in each bottle. All experiments with 150 mL vessels use acid washed pulp with salts re-added. Thus the total quantity of salt is known for each bottle and only the external solution need be analyzed for metal contents in both the external solution and fibres to be determined. A diagram of the experimental method is shown in Figure 4.3.1.

1. For each 150 mL vessel the following masses are recorded. Mass of 150 mL vessel, acid washed fibre pad, salt solution, NaOH or HCl for pH adjustment, and deionized water to achieve 1% consistency in the pulp suspension. The salt solution used is at a concentration that will match the metal profile on the original pulp.
2. Nitrogen is swept through the pulp suspension in the 150 mL vessel for approximately one minute and the vessel is then capped and shaken to mix contents well.
3. The pulp suspension is given ~12 hours to come to equilibrium. During this time the 150 mL vessels are shaken 3 - 5 times.
4. After the equilibrium period, the pulp suspension in each vessel is filtered on a Teflon membrane filter in a stainless steel column and the external solution is retained for metal analysis. The fibre pad is placed in an oven at 105°C to verify the oven dry mass of fibre. Before metal analysis of the filtrate is carried out, the pH of the recovered solution is determined.

150 ml vessel procedure

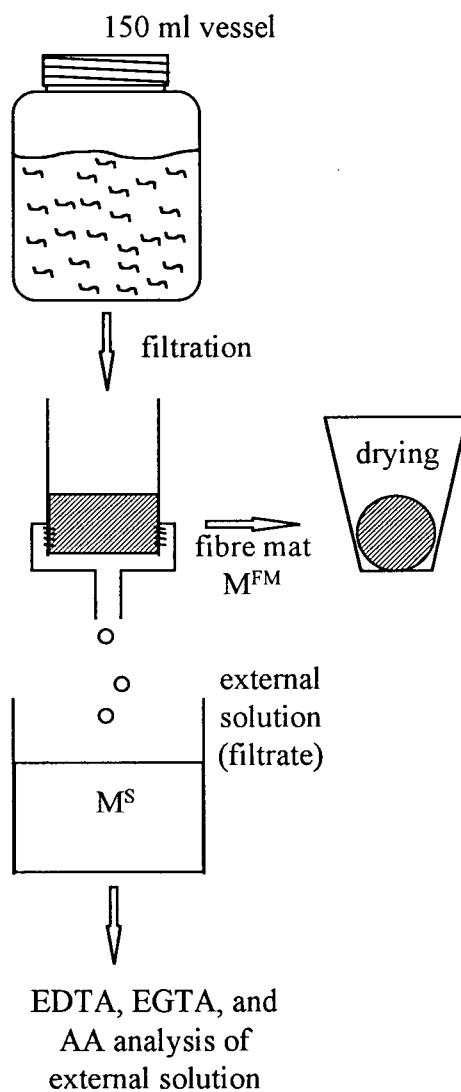


Figure 4.3.1: Experimental procedure for determining the metal ion contents in external solution for 150mL vessel experiments

4.3.3 Data Analysis for 150 mL Mixing Vessel Experiments

In 150 mL vessel equilibrium experiments the quantity of metal ions within the fibre mat is not determined, but the quantity of metals in the fibres can still be determined since the total quantity of metal ions in the system is known. All 150 mL vessel experiments are performed with acid washed pulp and salt solution re-addition, replacing the metal ions washed away during acid treatment. It is assumed that all metals are removed during acid-washing. This is true for most NPEs except Al, Si, and Fe (Park, 1996). Metal ions in the fibres are then determined using a rearrangement of equation (38):

$$M^F = M^T - M^S \quad (40)$$

where: M^F is the quantity of metal ions in the fibres (internal solution), mg

M^T is the total quantity of metal ions in the fibre suspension, mg

M^S is the quantity of metal ions in the external solution, mg

The difference between the 1L and 150 mL experiments is clearly shown by comparing Figures 4.2.1 and 4.3.1. 150 mL experiments are simpler (since they avoid the ashing and digesting steps), but rely entirely on mass balance to determine the quantity of metal ions in the fibres. 1L vessel experiments are more versatile because the total metal ion quantity does not need to be known, the dissolved ash allows for the total metal ions in the suspension to be calculated. The 1L vessel is used to determine the metal quantities in the original pulp for this reason.

4.4 Sample Preparation and Metal Ion Analysis

4.4.1 Ashing Procedure

The purpose of this method is to determine the mineral salts and other inorganic matter in pulp.

1. Place crucible in muffle furnace for 15 minutes at 575°C then cool in a desiccator (approximately 45 minutes) and weigh to the nearest 0.1 mg. It was found that furnace heating had no effect on the mass of the crucible.
2. Place the pulp into the crucible and record the mass. Place in an oven at 105°C until constant weight is obtained (usually it's easiest to leave the pulp in the oven overnight). Determine mass of crucible and dried fibre after cooling in desiccator. This value is critical since a portion of the bulk solution is trapped between the fibres and the ions it contains contribute to the amount measured in the ash by AA or titration. Ash quantities in these experiments were 0.03 - 0.15 g depending on the pH.
3. Place specimen in the muffle furnace at 575°C after preheating in oven at 105°C. Preheating prevents the sample from igniting immediately when it's placed in the furnace. The purpose of furnace heating is to char the specimen and then continue heating until all the carbon is eliminated. Samples used in this work were placed in the furnace with a lid and left for at least 10 hours. A white ash, that contained some black particles, was obtained for all samples.
4. After complete ashing, cool the crucible in a desiccator and weigh immediately to the nearest 0.1 mg. Be sure the lid is in place when transferring between the furnace and desiccator to prevent ash loss.

4.4.2 Atomic Absorption Preparation Procedure

This procedure begins with ash in a crucible that has been removed from the furnace and cooled.

1. Wet the ash with a drop of water, then add 5 mL of 6 M HCl solution. The water prevents the sample from foaming when the HCl is added, which could cause losses. Determine weight of crucible with ash and HCl.
2. After letting the sample dissolve for 5 minutes check for insoluble residue. If some exists there are two ways to help it dissolve. The first is to let the HCl evaporate, added 5 mL of HCl again and let that evaporate, then add 5 mL of HCl and heat the solution for 5 minutes. The second is to simply heat the specimen with the original HCl for 5 minutes, then check for insolubles. If there are few black particles in the original ash, there should not be a problem dissolving the ash. Waiting for HCl to evaporate is time consuming, and the ash did not dissolve further without heating, so the second method was used for all the data presented here.
3. Pour the contents of the crucible (ash dissolved in HCl and H₂O) into a 50 mL beaker and measure the mass exchanged. Rinse the crucible with deionized water and transfer this into the 50 mL beaker. The solution in the beaker is then filtered on a 0.5 mm teflon filter and the filtrate is kept in a vial for analysis of metal ion contents.

4.4.3 Metal Ion Analysis

Concentrations of metal ions in the external solution and dissolved ash are determined by atomic absorption (AA) and photometric titration with EDTA and EGTA. The techniques of analysis using both these methods are well documented (Jeffery, et. al., 1989; Skoog and Leary, 1992; Harris, 1991; Athanasopoulos, 1993) and won't be reviewed in detail here. All analysis are

performed in triplicate for each sample, except where the volume of the sample limited the number of tests that could be performed.

Chemical interferences are prevented in samples of calcium and magnesium by adding lanthanum chloride as a releasing agent. The lanthanum react preferentially with the interfering ions (phosphate or aluminum) to prevent their interaction with the analyte (Skoog and Leary, 1992). 59 g of lanthanum oxide (La_2O_3) is dissolved in 200 mL of 6 M HCl after being wet with deionized water. This LaCl_3 solution is made up to 1 L. Add 5 mL of this to every 50 mL volume of calibration or test solution of calcium or magnesium (there should be 2000-5000 ppm La in the tested solutions). Sodium samples and standards are made with a 1000 ppm potassium background which acts as an ionization suppressor. Potassium has a lower ionization potential than sodium (4.34eV vs. 5.14eV), meaning the potassium provides far more electrons to the flame than sodium, suppressing the ionization of the analyte.

During the atomic absorption testing the calibration solutions and blank are tested every 5 samples to ensure accuracy is being maintained. Generally, the hollow cathode lamps would continue to heat up during testing and the absorbance of a given sample decreases slightly. This was accounted for by testing all the standards every 5 samples (effectively making another standard curve).

Photometric titrations were conducted using Solochrome dark blue indicator and an ammonia - ammonium buffer (pH 10) for all samples. 0.001 M solutions of EDTA and EGTA were used as titrants. A Mettler DL25 titrator was used with the DP550 phototrode to obtain accurate endpoints (indicated by the maximum change in signal per ml titrant added, $\Delta mV / \Delta ml$).

4.5 Model Parameter Determination

Acid-washed pulp is used in all model parameter determinations. There are two reasons; the titrations need simple systems (sodium and hydrogen cations only) and the comparison of model predictions is performed with partitioning data from acid-washed fibre. Thus, the properties of acid-washed fibres are of greatest importance.

4.5.1 Conductometric Titrations

The most important charged group in kraft pulps in the pH range of 2 - 9 is the carboxyl group. The content of these groups in a kraft pulp can be determined by conductometric titration. Large changes in conductance are caused by changes in the concentration of hydrogen and hydroxyl ions in solution (Katz et al., 1984). The ionic hydrogen in solution can be correlated with the dissociation of charged groups on the fibres, and the total of carboxyl charge can be determined.

4.5.1.1 Required Equipment

Beakers (400 mL, 600 mL) and a 1 litre mixing vessel.

Porcelain funnel

Micro-burette (0.1 - 0.5 mL injection range)

Mass balance

4.5.1.2 Procedure for a kraft pulp

1. Acid wash pulp sample. Detailed procedure is found in Section 4.3.1.
2. Titrate pulp sample
 - 2.1. Disperse the washed pulp sample into 0.001 N sodium chloride. For a 2.5 od gram sample, a volume of 450 mL of solution in a 600 mL beaker is good. For kraft pulps 5 mL of

0.1 N HCl should be added to provide strong acid titration behaviour that will give an initial negative slope to the titration curve.

2.2. Tests should be done under a nitrogen atmosphere with the solution being stirred continuously using a magnetic stirring bar. Experiments are conducted at room temperature.

2.3. Prepare a solution of 0.1 N NaOH. This can be added with a micro-burette to the pulp suspension as the experiment progresses.

2.4. Additions of NaOH solution should be between 0.5 and 0.2 mL in volume depending what portion of the titration curve is being determined. Once equilibrium is attained record the conductance of the pulp suspension and the total volume of NaOH added.

3. Determine dry weight of pulp sample

3.1. Determine the mass of a filter paper that will be used to filter the pulp suspension.

3.2. Filter the NaOH - NaCl - pulp suspension in the ceramic funnel, recycling the filtrate once to retain fines on the pulp pad and filter paper.

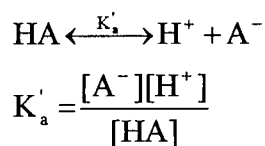
3.3. Wash the pulp pad with deionized water and thoroughly rinse the beaker used for titration.

3.4. Dry pad in oven at 105°C. Place fibre and filter paper in a desiccator while cooling.

3.5. Determine weight of oven dried pad.

4.5.2 Potentiometric Titrations

Potentiometric titrations may be used to determine the equilibrium constant(s) of the charged group(s) in a pulp sample. Dissociation relationships are typically written as:



where: HA is the protonated charged group

A^- is the unprotonated charged group

H^+ is the hydrogen proton

[] indicate concentration units (mol/L)

K_a' is the dissociation constant in the concentration scale for the weak acid A^-

Concentration has been used for dissociation constants rather than activity (K_a' rather than K_a) for simplicity and because the experimental uncertainty, due to the difficult fibre-water system being titrated, is greater than the changes caused by the improved predictions obtained by including activity coefficients.

In this work, two dissociation constants have been chosen to model the fibres. One constant is to correspond roughly to the carboxyl groups (K_{a1}'), the other to the phenolic hydroxyls (K_{a2}') within the fibres. The dissociation occurs within the fibres, so the dissociation relationships (for two charged groups) are written as follows.

$$K_{a1}' = \frac{[A_1^-]^F [H^+]^F}{[HA_1]^F} \quad (41)$$

$$K_{a2}' = \frac{[A_2^-]^F [H^+]^F}{[HA_2]^F} \quad (42)$$

where: F indicates the fibre phase

There is a finite amount of charge on the fibres, so a mass balance on the charged groups can be written.

$$[A_1^-]^F + [HA_1]^F = \frac{Q_{F1}}{V_F} \quad (43)$$

$$[A_2^-]^F + [HA_2]^F = \frac{Q_{F2}}{V_F} \quad (44)$$

where: Q_{F1} is the moles of charge group 1 in the fibres

Q_{F2} is the moles of charge group 2 in the fibres

V_F is the volume of the fibre phase

The values K_{a1}' , K_{a2}' , Q_{F1} , and Q_{F2} can be determined by the potentiometric titration of a solution of fibres. A known quantity of fibre is suspended in water and titrated with a base (in this case sodium hydroxide). A background of ions (sodium chloride and hydrochloric acid) is added to the water-fibre suspension to minimize non-ideal effects. Titration gives the pH of the solution as a function the volume of sodium hydroxide added (V_{NaOH}). Within the fibre phase, F, two other relationships exist. The first is the dissociation of water.

$$K_w = [H^+]^F [OH^-]^F \quad (45)$$

Second is the charge balance (electroneutrality).

$$[Na^+]^F + [H^+]^F = [OH^-]^F + [Cl^-]^F + [A_1^-]^F + [A_2^-]^F \quad (46)$$

where: Na^+ and Cl^- are included to account for the background concentration of NaCl and HCl.

Na^+ , Cl^- , H^+ and OH^- are free to diffuse in and out of the fibres while A_1^- and A_2^- are fixed within the F phase.

In the external solution, S, the dissociation of water and electroneutrality also hold (Butler, 1964).

$$K_w = [H^+]^S [OH^-]^S \quad (47)$$

$$[Na^+]^S + [H^+]^S = [OH^-]^S + [Cl^-]^S \quad (48)$$

The total amount of sodium is known as a function of the volume of base added (V_{NaOH}).

Chloride is present from the background of NaCl and HCl.

$$\text{Na}^+_{\text{Total}} = C_{\text{NaCl}} V_{\text{initial}} + V_{\text{NaOH}} C_{\text{NaOH}} \quad (49)$$

$$\text{Cl}^-_{\text{Total}} = C_{\text{NaCl}} V_{\text{initial}} + C_{\text{HCl}} V_{\text{initial}} \quad (50)$$

where: V_{initial} is the total volume of the system before titrant is added

C_{NaCl} is the concentration of NaCl in solution (initially)

C_{NaOH} is the concentration of NaOH used for titration

C_{HCl} is the concentration of HCl in solution (initially)

Also, mass balances on sodium and chloride give:

$$\text{Na}^+_{\text{Total}} = [\text{Na}^+]^{\text{F}} V_{\text{F}} + [\text{Na}^+]^{\text{S}} V_{\text{S}} \quad (51)$$

$$\text{Cl}^-_{\text{Total}} = [\text{Cl}^-]^{\text{F}} V_{\text{F}} + [\text{Cl}^-]^{\text{S}} V_{\text{S}} \quad (52)$$

where: V_{S} is the volume of the external solution, S

V_{F} is the volume of the internal solution, F

The final relations relate the concentrations in the S and F phases. In the absence of an osmotic gradient between fibres and solution, specific interactions, etc. Donnan equilibrium applies (Helfferich, 1995). The ratio of the concentrations in the external and fibre solutions is a constant for all mobile species. A prime is used (λ') to note that this is the ideal Donnan distribution coefficient, not the activity coefficient based value introduced previously (see equation 26).

$$\lambda' = \frac{[\text{Na}^+]^{\text{F}}}{[\text{Na}^+]^{\text{S}}} \quad (53)$$

$$\lambda' = \frac{[H^+]^F}{[H^+]^S} \quad (54)$$

$$\lambda' = \frac{[Cl^-]^F}{[Cl^-]^M} \quad (55)$$

where: λ' is the Donnan distribution coefficient, a constant for all mobile ions at any equilibrium condition.

Thus, there are 15 equations and 15 unknowns.

- Na^+ , Cl^- , H^+ , and OH^- concentrations in the external solution and fibre phases (8 unknowns)
- A_1^- , HA_1 , A_2^- , and HA_2 concentrations in the fibre phase (4 unknowns)
- Na^+_{Total} and Cl^-_{Total} (2 unknowns)
- λ' (1 unknown)

The potentiometric titrations performed used approximately 60mL ($V_{initial}$) of solution and 0.6g of oven dry fibre to give a consistency of 1%. An initial background concentration of NaCl (C_{NaCl}) and HCl (C_{HCl}) of 90mmol/L and 10mmol/L respectively were used, and titration was performed with 97.6mmol/L NaOH solution (C_{NaOH}). A Mettler DL25 titrator was used with a Mettler Toledo model DG 111-SC glass electrode. The electrode was placed in buffer solutions (Fisher Scientific) of pHs 3, 4, 5, 7, 9, 10, and 11 to determine the electrode calibration curve. During the titrations, a 3-bladed vinyl impeller was used to mix the pulp suspension and water saturated nitrogen was constantly fed into the titration vessel above the solution. Each injection of NaOH was followed by 5 minutes of mixing before the electric potential was read. Minimum and maximum NaOH injections were 0.01mL and 0.2mL respectively.

4.5.3 Water Retention Value and Fibre Saturation Point

The fibre saturation point is the measure of moisture in water saturated cell walls of wood fibres (Tiemann, 1906). It is a critical parameter in the Gibbs - Donnan model developed, since it determines the mass of the water in intimate contact with the fibres. Solute exclusion has been adopted as the method used to measure the fibre saturation point (FSP). In 1972 Scallan and Carles showed that the FSP could be easily obtained from the water retention value (WRV) at the specific centrifuge conditions of 900g for 30 minutes (Scallan and Carles, 1972). The WRV equals the FSP up to a value of 1.8 g water/g of fibre under these centrifuge conditions.

The water retained by a wet pulp sample after centrifuging under standard conditions is defined as the water retention value (TAPPI UM 256, 1991). WRV was determined using an IEC centrifuge with a fixed 45° rotor, and centrifuge tubes with plastic inserts designed to hold a 100 mesh screen half way up the tube (PAPRICAN, 1979). The mesh screen is supported from below by a porous plastic plate for mechanical strength. Triplicate samples were centrifuged for 30 minutes at 900 g (2590 rpm).

1. Disperse acid washed pulp in deionized water at 1% consistency overnight. Filter the pulp on a Buchner funnel and vacuum flask until the fibre pad is at 20% consistency.
2. Place the equivalent of 1 g oven dry fibre from the pad into each centrifuge tube, fit with the inserts and screens. Balance tubes by adding water.
3. Centrifuge the tubes for 30 minutes at 900 g (2590 rpm).
4. After 30 minutes, remove the tubes from the centrifuge, remove the upper inserts and record the mass of the fibre mats.
5. Dry the fibre mats to constant weight in an oven at 105°C. Place the samples in a desiccator for cooling and record the oven dry mass of the fibre mats.

The WRV is calculated from the mass of the wet fibre mat after centrifuging and the mass of the oven dry fibre.

$$\text{WRV} = \frac{\text{Wet Fibre Mat} - \text{OD Fibre Mat}}{\text{OD Fibre Mat}} \quad (56)$$

As well as testing acid washed pulp under acidic conditions, acid washed pulp soaked in alkaline solution (pH = 11) and original pulp soaked in deionized water (pH = 10.3) were tested as examples of the possible conditions fibres may be subject to. The FSP measurements gave results ranging from 1.17 to 1.42 g water/g od fibre, depending on the pH of the pulp suspension. This is well below the maximum value of 1.8 g/g. Thus, the WRV is equivalent to the FSP for the fibres at the test conditions. These test conditions approximately cover the range pH over which partitioning experiments were performed.

Chapter 5

5. Results and Discussion

Four basic types of results are presented and discussed:

- Experimental data providing fibre properties for use in modeling.
- Experimental data providing partitioning information under various conditions.
- Modeling results of ion partitioning using ideal Donnan equilibrium.
- Modeling results of ion partitioning using the proposed partitioning model, based on introducing activities to describe the metal ions.

Experiments were performed to determine the fibre properties needed in the partitioning model (K_{a1}' , K_{a2}' , Q_{X1} , Q_{X2} , and F). For the ions of interest, the total NPE content in the pulp is determined as well as qualitative knowledge of the themes in the partitioning data. Acid washed pulp experiments in 150mL and 1L vessels give data over a broad range of pHs for comparison to the partitioning model. The results of the proposed partitioning model (Gibbs-Donnan ion partitioning, obtained with activity coefficients determined by Pitzer's method) are compared to published experimental data, as well as the data obtained here and the ideal model proposed by Towers and Scallan (1996).

5.1 Determining Model Parameters

Fibre properties used in the prediction of NPE partitioning were determined by potentiometric and conductometric titrations and fibre saturation point (FSP) measurements. The experimental procedures have been outlined in Chapter 4. Results are used in the partitioning model; they are not needed to obtain the experimental data. The required model parameters are the mass of water in the fibre phase, F , the total charge on the fibres, Q_{X1} and Q_{X2} , and the dissociation

constants, K_{a1}' and K_{a2}' , of the fixed anionic groups on the fibres. Table 3.3.1 shows the use of these parameters in the equations of the proposed and ideal models.

5.1.1 Potentiometric Titration to Determine Fibre Properties

Both the charge on the fibres, Q_{X1} and Q_{X2} , and the dissociation constants, K_{a1}' and K_{a2}' , of the charged groups can be determined from potentiometric titration data. Experimental data from the titration of acid washed kraft pulp fibres with a NaCl and HCl background are plotted in Figure 5.1.1 and listed in Table A.1. The difference between the titration of a blank (containing only HCl and NaCl) and titration of fibres in the presence of the same quantity of HCl and NaCl is clearly evident in the graph. The curves lie on top of one another while the added NaOH neutralizes the HCl in solution. As the charged groups (likely carboxyl) on the fibres begin to loose protons the two curves separate, and the distance between the two curves is a measure of the quantity of unprotonated sites on the fibres.

It is evident from Figure 5.1.1 that the distance between the two curves is constantly changing as the pH increases, implying that the quantity of charge on the fibres is increasing from a pH of 2.5 to at least 11. The continual increase in charge verifies that kraft pulp fibres act as polyelectrolytes. It is difficult to accurately describe fibres with only one or two dissociation constants, an entire spectrum of dissociation constants would be needed to follow the experimental titration curve obtained. If the fibres could be described by only one dissociation constant, the fibre experimental data would be parallel to the blank curve before and after the pH at which the dissociation constant had it's effect.

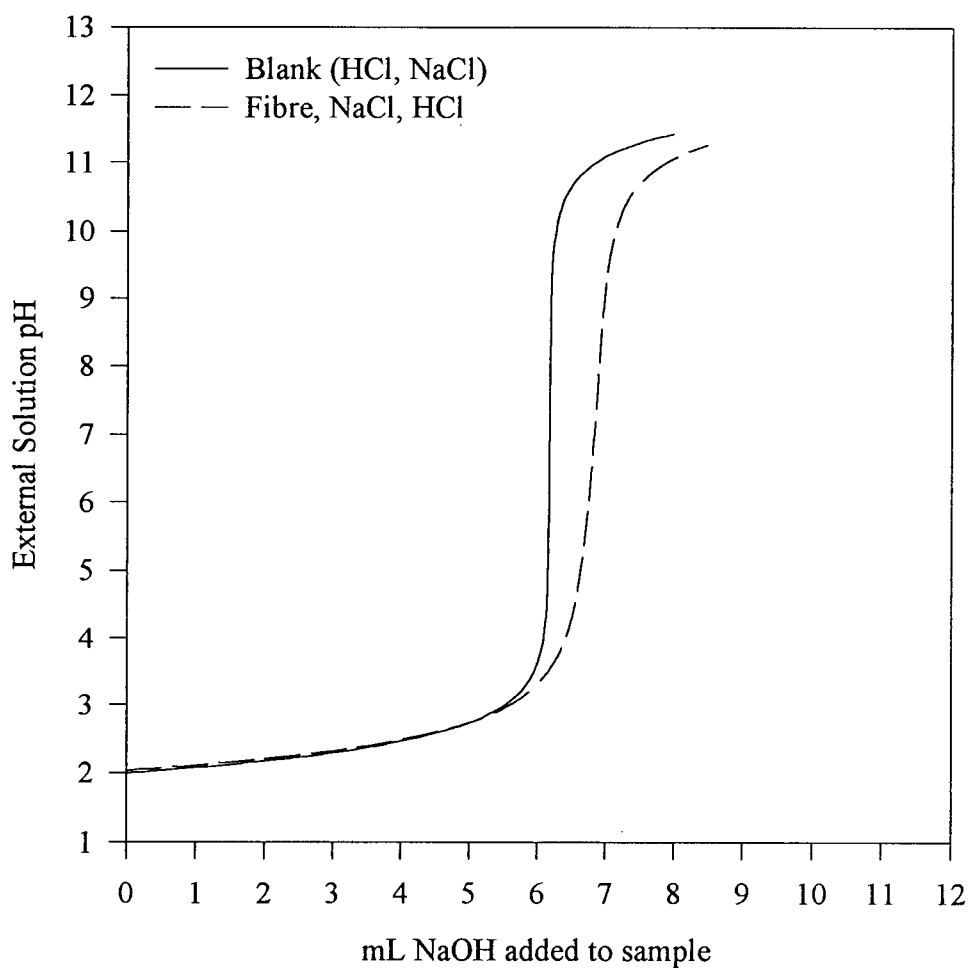


Figure 5.1.1: Potentiometric titration of kraft pulp fibres. Two curves are shown, representing the titration of a blank solution containing only the background of NaCl and HCl, and the titration of kraft fibres within the same background of NaCl and HCl.

Chemically, the two important dissociating groups within the fibres are the carboxyl and phenolic hydroxyl. Although the kraft fibres used in this work cannot be accurately described by two dissociation constants it is reasonable to assume that two constants can do an acceptable job and give a good approximation to the experimental data. A computer algorithm has been used to minimize the square of the error between the experimental pH and the pH predicted by the algorithm in the external solution (S). Both the quantity of charge and dissociation constant of each group was obtained, giving the following results.

$$K_{a1}' = 1.6e-4 \quad Q_{X1} = 95 \text{ mmol/kg od fibre}$$

$$K_{a2}' = 1.1e-8 \quad Q_{X2} = 55 \text{ mmol/kg od fibre}$$

$$Q_X = Q_{X1} + Q_{X2} = 150 \text{ mmol/kg od fibre}$$

A plot of the resulting prediction compared to the experimental data is shown in Figure 5.1.2. Two dissociation constants do an acceptable job of following the experimental data, but a closer representation can be obtained. It is possible to develop a continuous charge distribution on the fibres from the experimental data and fit a curve to this continuous charge distribution. The fit curve gives the quantity of charge on the fibres at any given internal phase (F) pH, and provides a convenient function to obtain the exact charge on the fibres.

A computer algorithm has been used to determine the quantity of charge necessary in the fibre phase to reproduce the experimental results using a Donnan equilibrium, two phase model (see Appendix G). The volume of NaOH at each data point was input to the model, and the quantity of charge was varied to give the same external solution pH as obtained in the experiments. A cubic equation was fit to this data to give a continuous function providing the exact quantity of charge within the kraft fibres. The resulting cubic equation has been plotted in Figure 5.1.3 along with the charge that is predicted by the model employing two dissociation constants.

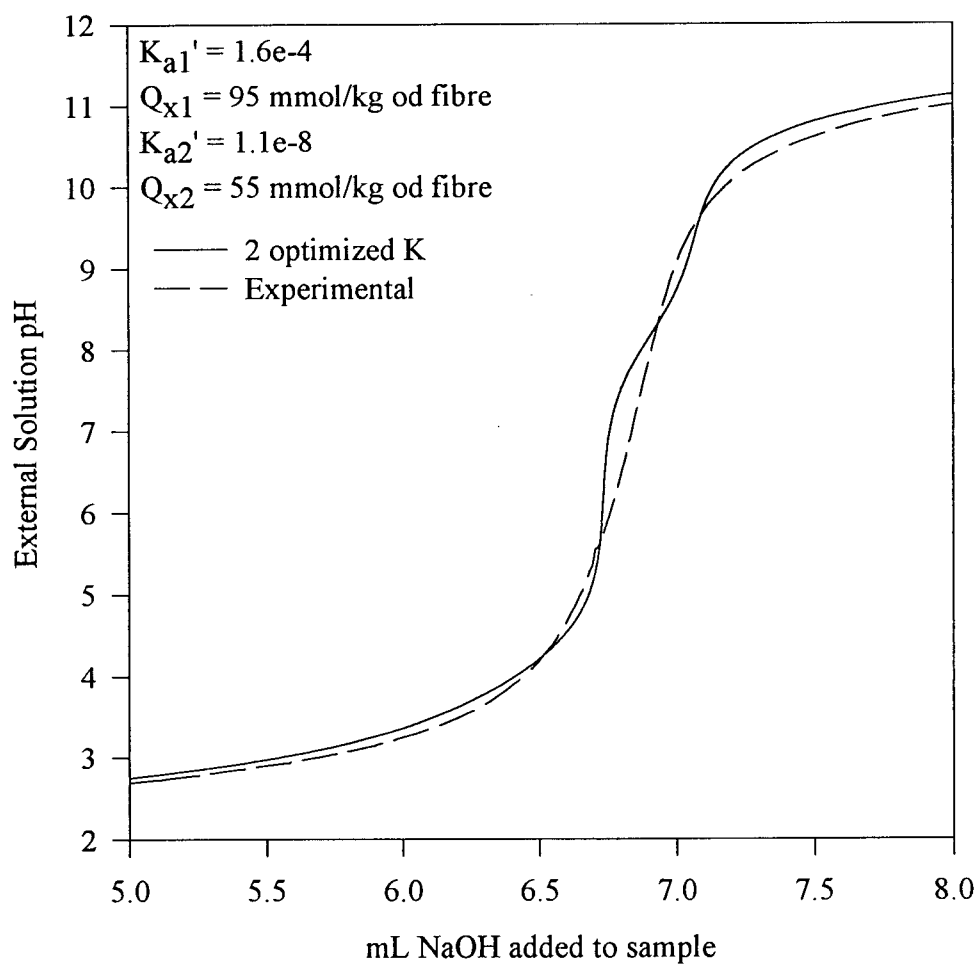


Figure 5.1.2: Comparison of theoretical curve for two calculated dissociation constants with experimental potentiometric titration data.

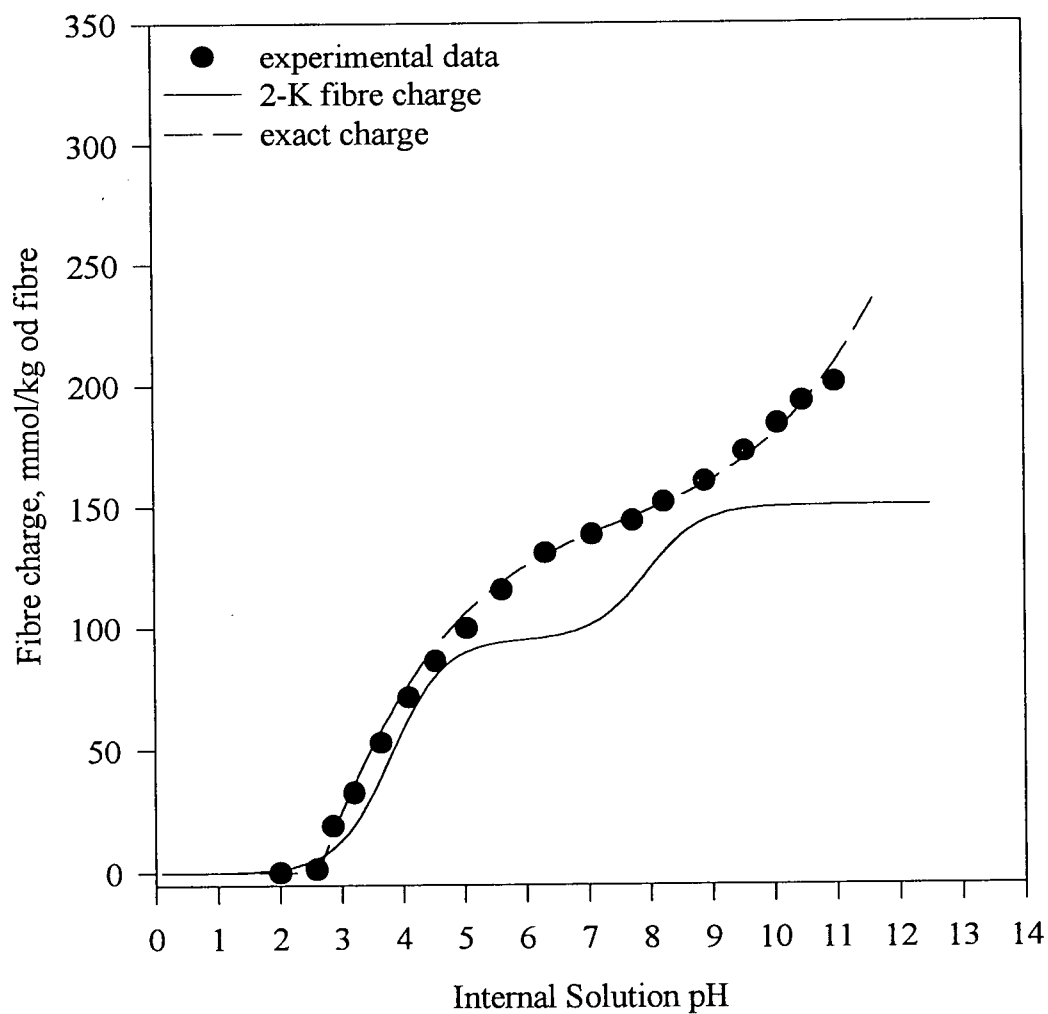


Figure 5.1.3: Fibre charge as a function of pH within the fibres. Two methods of modeling the fibre charge give very different curves. The exact charge model gives a cubic approximation to the dissociating behaviour of the fibres.

The relation used to generate the exact charge curve (cubic approximation) in Figure 5.1.3 is:

$$\text{pH}^F \leq 2.6 \quad Q_x = \frac{\text{mmol ch arg e}}{\text{kg od fibre}} = 0$$

$$\text{pH}^F > 2.6 \quad Q_x = \frac{\text{mmol ch arg e}}{\text{kg od fibre}} = -280.83 + 146.30\text{pH}^F - 17.78(\text{pH}^F)^2 + 0.773(\text{pH}^F)^3$$

This same relationship is also used to generate the metal ion partitioning curves shown later in this chapter. The two curves in Figure 5.1.3 both rise significantly from a pH of 3-5. This indicates that both models of the charge on fibres represent a significant amount of charge at conditions where carboxyl groups are likely to be dissociating ($\text{pK} = 4$); convincing evidence that large quantities of carboxyl groups are present in post-brown stock pulps. The slope of the cubic equation (exact charge model) increases again at pHs above 10, where hydroxyl groups are likely to be dissociating. The 2-K model shows a second rise in the pH range of 7-9. This is somewhat low for the phenolic hydroxyl groups, but does account for increased charge at higher pHs.

The difference between the curves is quite large at all pHs above 5, so the predictions made with these two models should be quite different, as will be seen in subsequent sections. Independent titration data is being used to model the charge on the kraft pulp fibres, not fitting to the experimental NPE partitioning results. The charge on the fibres is a critical parameter in the partitioning model and accurate charge models are needed to provide good predictions within the Donnan equilibrium framework, since charge is the driving force for all NPE partitioning.

Humic acids display similar titration curves to that obtained for the acid washed pulp. The shape of the curves is explained by Stumm and Morgan on page 141 (1996).

...because of the polyfunctionality of the the humic acid (the functional -COOH and -OH groups are present in different configurations and thus have somewhat different pK_a values; carboxylic acid groups and phenolic groups have pK values between 4 and 6, and between 9 and 11 respectively). A further effect is due to the polyelectric nature of the humic acid; by titrating with base, the molecule becomes progressively more negatively charged and the protolysis of H^+ ions is rendered more difficult with increasing pH values.

Stumm and Morgan (1996) also compare the titration curves of humic acid and an equimolar mixture of acetic acid and phenol, reproduced in Figure 5.1.4. The titration of humic acid is very similar to the titration of kraft pulp fibres. The polyfunctionality and polyelectric nature of kraft pulp fibres are the reasons for the relatively poor result of fitting multiple dissociation constants to the fibres. Variation in the dissociation constant causes significant changes in the predictions of the partitioning model, as will be discussed in Section 5.5.

5.1.2 Conductometric Titration

Monitoring the conductivity of the external solution while titrating with NaOH allows the carboxyl content of fibres, Q_x^{carboxyl} , to be determined. A titration of 1.31 od grams of kraft pulp has been performed. A graph of the results is shown in Figure 5.1.5, and is shown in tabular form in Appendix A. The temperature of the experiment was 26.4°C, and the final pH of the solution was 10.1. The shape of the curve is as expected, and the “flat” initial portion is read off the graph as 118 mmol NaOH/kg od fibre in length. The flat initial portion occurs as hydrogen leaves the fibres and is neutralized by the added OH^- . When no further H^+ leaves the fibres, the specific conductance begins to rise with NaOH addition.

This method of titration may over predict the quantity of weak acidic groups in the pulp, since the initial decreasing portion of the curve is unexpected but still attributed to the weakly acidic carboxyl groups. Katz (1984) explains that the initial drop is due to “...the repression of the

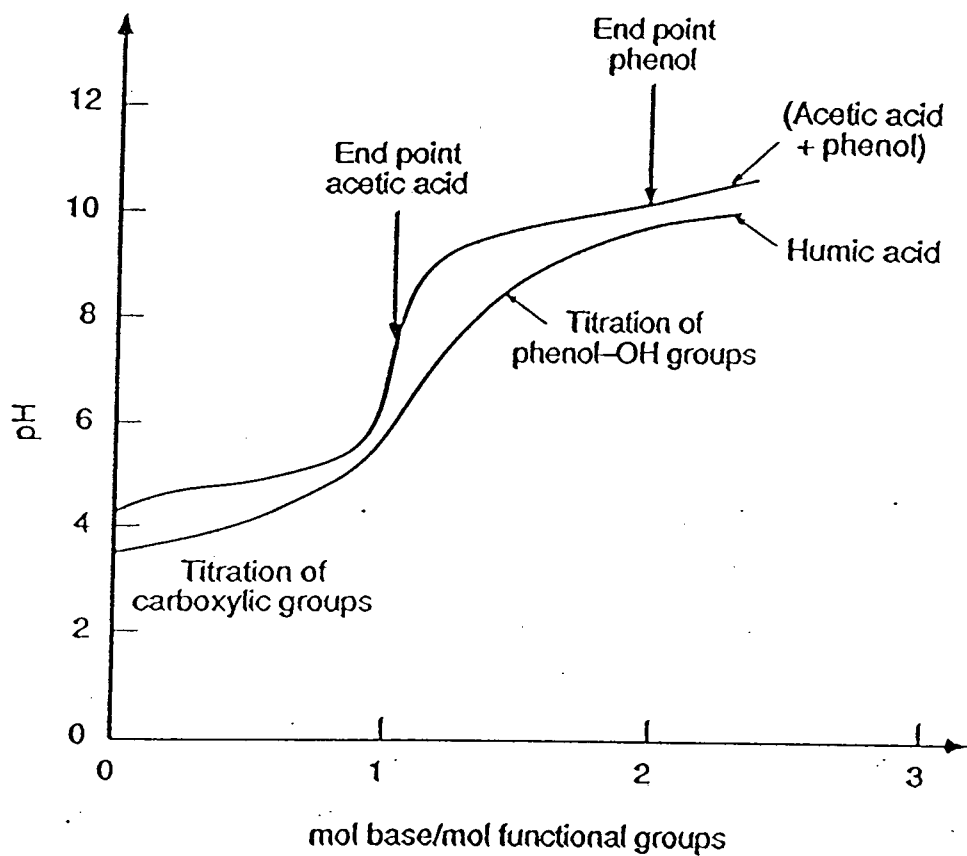


Figure 5.1.4: Comparison of alkalimetric titration of an equimolar (10^{-4} M) acetic acid ($pK_a=4.8$) and phenol ($pK_a=10$) with titration of humic acid containing $\sim 10^{-4}$ mol carboxylic groups (Stumm and Morgan, 1996).

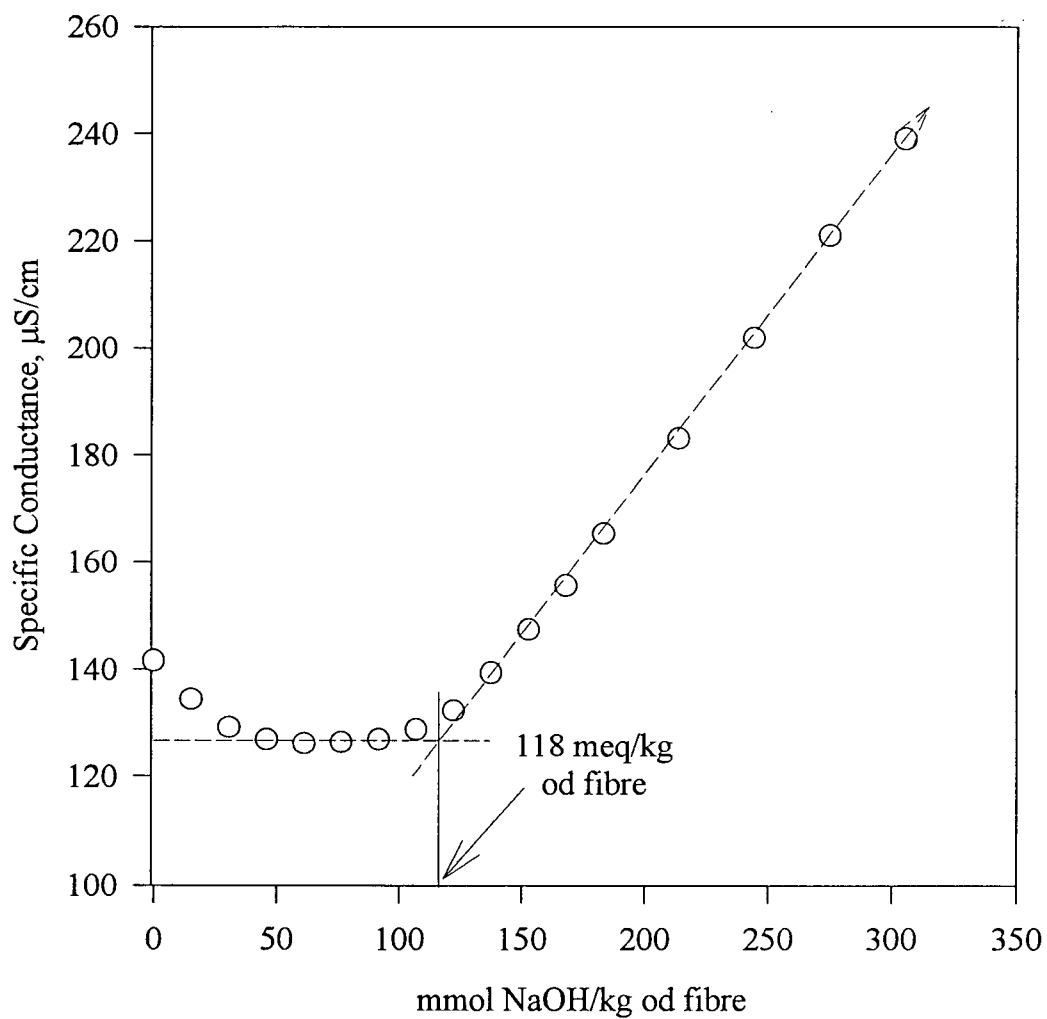


Figure 5.1.5: Specific conductance during the titration of kraft pulp with NaOH. The intersection of the lines indicates the point at which all charged groups on the fibres have been titrated and free hydroxyl ions begin increasing solution conductance.

dissociation of the acid by the anions of the acid that have already been neutralized.” The decreasing portion of the curve can be intentionally created by adding a strong acid to the system. The curve falls as the strong acid is titrated by the strong base, then flattens as the weak acidic groups in the fibres are changed from H^+ to Na^+ form. A rise again occurs when no further H^+ remains in the fibres.

Two different values of Q_X have been obtained; 150 and 118 meq/kg of fibre. No Q_X value is obtained from the variable charge model, since the model gives Q_X as a function of pH within the fibres. Total charge content should only depend on the treatment of the fibres and all fibres are acid washed in the same fashion. Hence, a single value describes the total available charge on the fibres under any condition of pH or mobile ion concentration. Conductometric titration gives only the quantity of carboxyl groups on the fibres, and this is not the total available charge on the fibres, so Q_X^{carboxyl} underpredicts the value Q_X .

5.1.3 Fibre Saturation Point

Figure 5.1.6 presents the effect of pH on the fibre saturation point, which is also shown in Table 5.1.1. The fibre saturation point (FSP) increases with pH, as is expected. Values of 1.4 g/g are not obtained until pHs of 8-9. The average FSP over the range of pH is somewhat lower than the approximate value used by Towers and Scallan (1996) for kraft pulp fibres. Linear regression of the data gives the relation, $FSP = 0.03 \text{ pH} + 1.1$. Linear approximation is likely not valid above a pH of 10, where the FSP will become constant, or may even begin to fall (Grignon and Scallan, 1980). Also, below a pH of 3, it is unlikely the FSP will continue to fall, as a linear model will require.

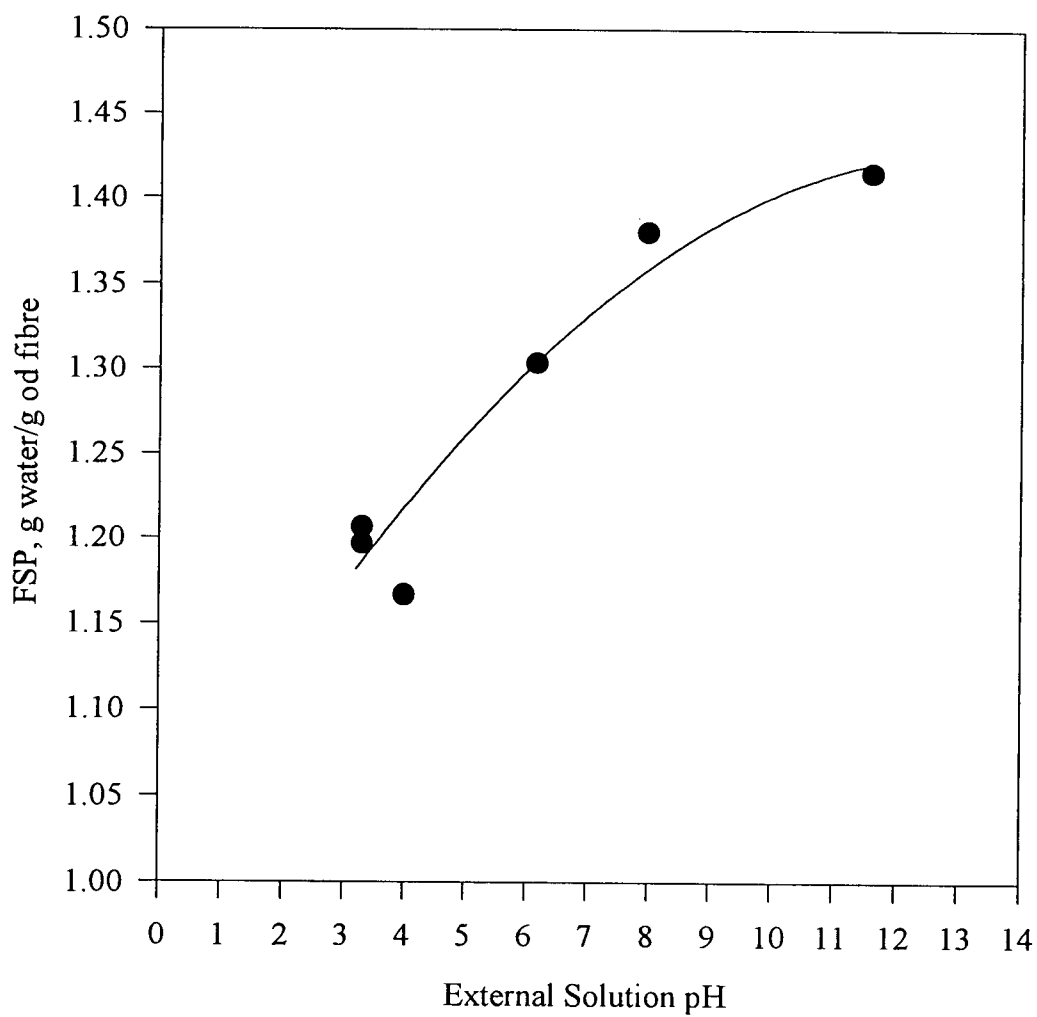


Figure 5.1.6: Fibre saturation point (FSP) over the relevant pH range. Quadratic interpolation through the data gives an approximate relation between the FSP and pH for acid washed fibres.

pH	Average g water / g od fibre	Standard Deviation, σ
3.30	1.20	0.031
3.30	1.21	0.015
4.00	1.17	0.042
6.16	1.30	0.015
7.97	1.38	0.020
11.6	1.42	0.092
As Received	1.34	0.010

Table 5.1.1: Fibre saturation point dependence on pH

To account for these concerns at low and high pHs, a quadratic model is used. A maximum FSP exists for fibres because physically they will be restricted by the bonds holding the matrix of cellulose together. Incorporating this idea into the representation of the data, the quadratic model should not increase significantly above pHs of 11. At low pHs, the model will be considered constant, as the average of the points obtained at the 3.3 and 4 pHs. Regression of the data (Devore, 1991) gives the line shown in Figure 5.1.5, described mathematically below. The prediction error in the curve, measured by the standard deviation (s), is 0.035 g water/g od fibre.

$$\text{pH} < 3.2 \quad \text{FSP} = 1.18 \text{ g H}_2\text{O} / \text{g od fibre}$$

$$\text{pH} \geq 3.2 \quad \text{FSP} = -0.0024(\text{pH}^2) + 0.064 \text{ pH} + 1.001 \text{ g H}_2\text{O} / \text{g od fibre}$$

The purpose of the fibre saturation point relation is to provide a critical parameter in the Donnan equilibrium model for the brown stock washed kraft pulp used in the experiments. The curve is not a general description of the mass of water within all kraft pulps at an input pH. The FSP is a critical parameter within the model because molalities (moles/kg water) are used to describe the concentrations in each phase, are input to Pitzer's activity coefficient model, and are the

parameters used within the Donnan relations to describe the partitioning of each ion. An increase of the FSP from 1.18 to 1.41 causes the quantity of water within the fibres to increase almost 20%. This causes a considerable change in the molality of the fixed charged groups (modeled as A_1^- and A_2^-) in the fibres.

The quality of the data, obtained by centrifuging pulp under specific conditions to give a water retention value equal to the FSP, is good. Besides the variation at a pH of 11.6, the standard deviations are relatively small and the trend in the data makes sense from a physical understanding of what is occurring within the fibres as the pH increases. Another method of obtaining the FSP is through solute exclusion. The increased complexity of solute exclusion experiments were not warranted in this work, because the FSP is likely not exactly the quantity need in the Donnan partitioning model. The FSP was used as an approximation to the value F in the Donnan partitioning model. F is the mass of water in the fibre phase; the water in intimate contact with the fibres such that it has different properties from the water of the external solution. FSP measures the water within the fibre wall and perhaps a small quantity of water trapped by capillary forces in the collapsed lumen of the fibres. Although the FSP is an approximation to the parameter F of the Donnan partitioning model, it is clear from the model predictions, to be presented in the next sections, that FSP does a good job of approximating F .

To convert the quantity of NPEs within the fibres from units of mg/kg of fibre to mg/kg FSP water, the FSP must be used. The error in the FSP (standard deviation of 0.035g water/g of fibre) increases the error in the experimental data considerably, sometimes doubling the relative width of the 95% confidence interval. The only larger error in the experiments is the error in the analysis of the quantity of metal ions in solution. Data are presented in units of mg/kg FSP

water so that concentrations within the fibres and outside the fibres are presented in the same units. This makes it very clear that the concentrations at low pHs are the same within the fibres and in the external solution.

Fibre swelling has generated interest because of the papermaking properties of swollen fibres (Grignon and Scallan, 1980; Katz, Liebergott, and Scallan, 1981; Scallan and Tigerstrom, 1992). Scallan and Tigerstrom deal with fibre swelling as a function of the ions that enter the fibre. These ions set up an osmotic system between the fibre and solution. The fibre wall is thought to swell until the elastic force of the fibre wall is equal to the osmotic force within the fibre. For kraft pulps, the fibre saturation point typically varies from 1.27 to ~1.5 g/g depending on the type of ions adsorbed onto the fibres. Sodium causes the greatest swelling in single ion systems. At low pH, the relationship developed here falls below 1.27 g/g, but 1.18 g/g still seems to be a reasonable value. Having obtained the necessary fibre properties for use in the partitioning model it is now possible to examine its ability to predict the trends of experimental data.

5.2 Comparison of Partitioning Model with Ideal Donnan Model and Published Data

The results of the proposed partitioning model (Gibbs-Donnan ion partitioning, obtained with activity coefficients determined by Pitzer's method), give a reasonably good fit to experimental data. Model results are first compared to ideal Donnan partitioning and the published results of Towers and Scallan (1996) and Bryant and Edwards (1996). Comparisons to data in the literature allow the general properties of the partitioning curves and the trends in the published data to be examined.

Figure 5.2.1 shows results of calcium ion partitioning onto fibres from external solution at various pHs. The curves correspond to the salt contents and fibre properties of Towers and Scallan (1996). Curves for both the model developed in this work and ideal predictions are shown. Experimental data in Figure 5.2.1 shows similar trends to the data obtained in this work. Above a pH of 7 the model results under-predict the experimental data, when only a single dissociation constant is used to model the charge present on the fibres.

Figure 5.2.2 shows calcium adsorption curves over a range of pHs compared to Bryant and Edwards' experimental data (Bryant and Edwards, 1996). In this case, the total charge on the fibres was taken as 105 mmol/kg of fibre and the dissociation constant was assumed to be $K_a' = 1 \times 10^{-4}$. Only a single dissociation constant was used. Both the ideal and non-ideal models do a good job of predicting the concentrations over the pH range of the experimental data. Considering the dissociation constant had to be "guessed" for the post-oxygen fibres, the model does an exceptional job of predicting the partitioning behaviour.

5.2.1 Explanation of Partitioning Curves

There are several important observations that can be made from the partitioning predictions and the comparison of these predictions with experimental data.

- Introducing activity coefficients (γ) leads to increased prediction of the content of calcium within the fibres, compared to ideal predictions.
- The model predicts a drop in the calcium content on the fibres at pHs above 10. In the experiments, the calcium content is constant and one would expect that all charged fibre groups would be ionized. This raises the question, why do the curves fall?

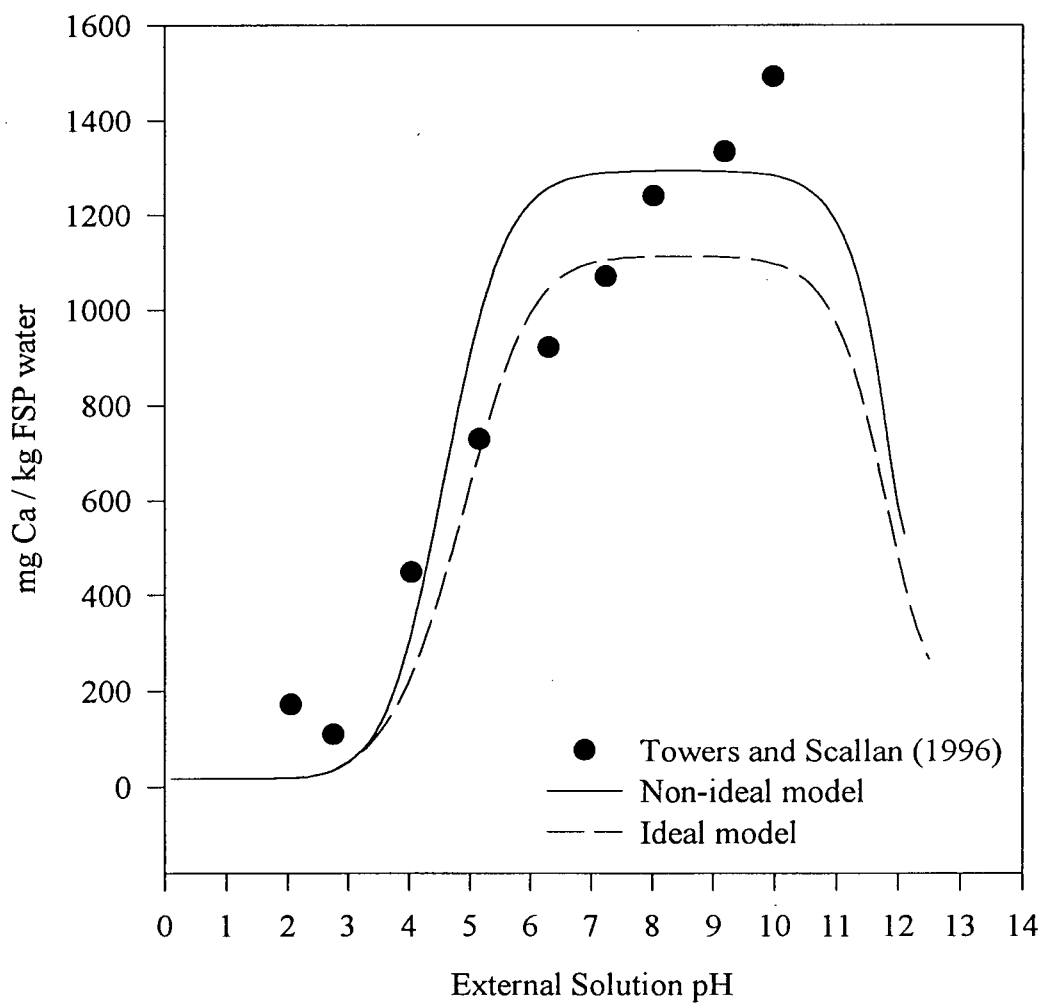


Figure 5.2.1: Fibre concentration of calcium (Ca^{+2}) over a range of pHs. The fibre saturation point (FSP) is assumed constant at 1.4, for comparison to the experimental data of Towers and Scallan (1996).

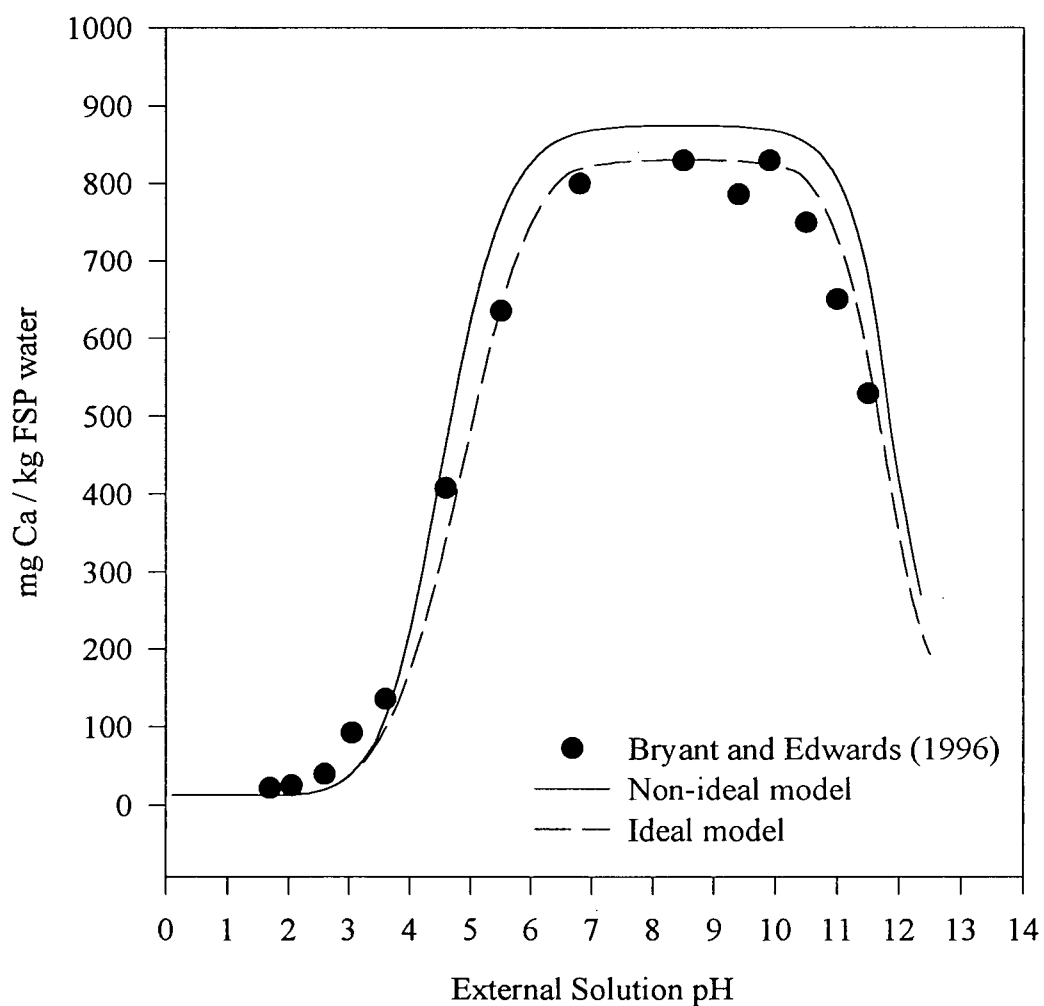


Figure 5.2.2: Fibre concentration of calcium (Ca^{+2}) over a range of pHs. The fibre saturation point (FSP) is assumed constant at 1.4. Data obtained from Bryant and Edwards (1996).

- There are two different themes in the literature data. Both agree that in the pH range of 3-7 the amount of calcium (or any other cationic NPE) on the fibres increases with increasing pH. Above a pH of 7 Towers' data indicates that the concentration of calcium will continue to increase, while Bryant shows that the amount of calcium begins to fall above a pH of 10. Possible reasons for this difference need to be examined. It should be noted that the pulp sample of Towers and Scallan is taken after the last brown stock washer and before the bleach plant while that of Bryant and Edwards is taken after the second oxygen delignification washer.

An attempt is made here to elucidate the above points. The molality of calcium in the activity coefficient case rises 14% above the ideal prediction, at a pH of 8 for Towers and Scallan's experimental conditions (see Figure 5.2.1). The Donnan distribution coefficient (λ = solution phase activity/fibre phase activity) at the same point is 0.070 for ideal predictions and 0.087 for activity coefficient predictions. The molalities within the fibre are able to rise due to the influence of the activity coefficients, even though the distribution coefficient also rises. The activity coefficients for calcium at a pH of 8 are 0.32 in the fibre solution and 0.89 in the external solution. Thus, for the distribution coefficient to rise only a small amount, the concentration within the fibres must increase to offset the low activity coefficient of 0.32 in the fibre phase.

Consider the Donnan relation:

$$\left(\frac{\gamma_j^\alpha m_j^\alpha}{\gamma_j^\beta m_j^\beta} \right)^{\frac{1}{z_j}} = \left(\frac{\gamma_k^\alpha m_k^\alpha}{\gamma_k^\beta m_k^\beta} \right)^{\frac{1}{z_k}} = \left(\frac{\gamma_l^\alpha m_l^\alpha}{\gamma_l^\beta m_l^\beta} \right)^{\frac{1}{z_l}} = \dots = \lambda \quad (26)$$

For the specific example considered here,

$$\left(\frac{\gamma_{Ca^{+2}}^S m_{Ca^{+2}}^S}{\gamma_{Ca^{+2}}^F m_{Ca^{+2}}^F} \right)^{1/2} = \lambda$$

For the ideal case (i.e. λ' rather than λ), the concentrations obtained from the model are 5.40 mg Ca^{+2} /kg external solution and 1112 mg Ca^{+2} /kg internal (FSP) solution. These can be converted to millimolal units by dividing by the molecular weight of calcium. Substituting gives:

$$\left(\frac{5.40 / 40.08 \text{ mmolal}}{1112 / 40.08 \text{ mmolal}} \right)^{1/2} = 0.0697 = \lambda'$$

Introducing activity coefficients changes the equilibrium condition. The same calculation for the activity coefficient concentrations in the external solution and fibre phases gives:

$$\left(\frac{0.89 \times 3.50 / 40.08 \text{ mmolal}}{0.32 \times 1293 / 40.08 \text{ mmolal}} \right)^{1/2} = 0.0868 = \lambda$$

Thus, the increasing concentration within the fibre, and subsequent drop in the external solution are the results of introducing activity coefficients. Although only the Donnan relation depends on activity coefficients, the simultaneous solution of the model equations result in significantly different results when activity coefficients are introduced. The increased concentration of cations within the fibres means more anions will also be present in the fibre phase to maintain electroneutrality.

The experimental data of Bryant and Edwards do not show as large a deviation between the ideal and activity coefficient model predictions. This is due to the dependence of activity coefficients on ionic strength, $I = \frac{1}{2} \sum_j m_j z_j^2$. Roughly half the total calcium is present in the experiments of Bryant and Edwards compared to those of Towers and Scallan. The lower ionic

strength gives activity coefficients closer to unity and the difference between the two predictive models is reduced.

The predicted calcium concentrations drop at high pH due to the addition of sodium (as sodium hydroxide) used to change the pH of the system. In experiments, NaOH or HCl are added to the pulp suspensions to alter the pH. The Na^+ "competes" with Ca^{+2} for the charged sites on fibres. To maintain the electrochemical equilibrium of the system, Ca^{+2} must be driven from the fibre phase to the external solution and replaced by the Na^+ (which is in excess in solution due to added NaOH), maintaining electroneutrality. Thus, at pHs above ~ 10 , Na^+ increases in the fibre phase and Ca^{+2} decreases.

The experimental data of Bryant agrees with the trend that Ca^{+2} content in the fibres should drop at the high pHs. An increasing concentration of Ca^{+2} in the fibre phase can be explained by calcium precipitation onto the fibres, primarily in the form of calcium carbonate, CaCO_3 . At high pHs (starting above ~ 10) Ca^{+2} ceases to be an ion and becomes an insoluble precipitate which no longer participates in the Donnan equilibrium framework because the complex does not have charge. Additional calcium must enter the fibre phase to maintain electrochemical equilibrium and this results in a total amount of calcium in the fibre that rises above the Donnan prediction. The total calcium includes both soluble ionized calcium and insoluble precipitate such as calcium carbonate. When this fibre is ashed and analyzed for Ca content (or filtrate concentrations are measured and back calculation is employed), this total calcium value is obtained. Another possible explanation of the increasing concentration within the fibres is that the single dissociation constant used in the work of Towers and Scallan is not adequate to describe the charge on the fibres at any pH.

From these results it is clear that the two different pulps have distinctly different behaviours above a pH of 7. The pulp obtained after the brown stock washers but before oxygen delignification continues to increase in calcium content, even after it is expected that all fixed anionic groups on the fibres have ionized. Pulp obtained after oxygen delignification plateaus above a pH of 7, following the predictions of Donnan equilibrium very closely. Differences in the partitioning behaviour may be caused by the chemical changes occurring in the fibres during the bleaching processes. Specifically, oxygen delignification decreases the lignin within fibres. Lignin contains large quantities of phenolic hydroxyls which typically begin dissociating at pHs above 9. Lignin removal in the early stages of the bleach plant decreases the phenolic hydroxyl charge, considerably changing the partitioning behaviour at pHs above 9. At pHs above 9, a post-oxygen pulp, would be expected to show a plateau in experimental results because few charged groups would remain in the fibres to deprotonate.

5.3 Metal Ion Partitioning with Post Brown Stock Pulp

Four types of experiments were performed with the post brown stock pulp, as received from the mill. Equilibrium at 1% consistency, added calcium, lower and higher consistencies, and acidification experiments were carried out, as has been discussed in the Chapter 4. The results are required to determine the quantities of sodium, calcium, and magnesium present on the post brown stock pulp so similar amounts of ions can be re-added in the acid washed equilibriums. Also, the principles of Donnan equilibrium are qualitatively compared with the results. Model predictions cannot be compared to the post brown stock results because the quantity of every ion in the pulp is not known. Partitioning predictions require knowledge of the total ion content of all mobile ions present.

The Na, Ca, and Mg partitioning data shown in Table 5.3.1 can be explained by the principles of Donnan equilibrium. The pH of the experiments is ~ 10 (except for the acidified equilibrium), so the weak acidic groups (carboxyls) are ionized, and the fibres are attracting cations into their internal solution (FSP solution). Thus, the cations should show a tendency to be partitioned strongly between the fibres and external solution. The significance of each experiment is discussed in the following sections.

5.3.1 1% Consistency Equilibrium and Metal Profile of Original Pulp

The basic experiment to which all other tests are compared is a 1% consistency equilibrium at room temperature, atmospheric pressure, and the pH naturally occurring upon dilution for the as-received pulp. Concentrations of ions on the fibres are given in mg/kg FSP water to allow easy comparison to the concentrations in the external solution. It is common to give NPE concentrations based on the mass of oven dry fibre, so these values are also included in Table 5.3.1 (related to the other values through the FSP). The results indicate that all cations are present in much higher concentration in the fibre solution than in the external solution with ideal distribution coefficients (λ') of:

$$1535.7 \text{ mg Na / kg FSP water} / 201.7 \text{ mg Na / kg water} = 7.61 \text{ for Na (std.dev. = 0.34)}$$

$$\left(1129.4 \text{ mg Ca / kg FSP water} / 3.5 \text{ mg Ca / kg water} \right)^{1/2} = 18.0 \text{ for Ca (std.dev. = 6.3)}$$

$$\left(169.3 \text{ mg Mg / kg FSP water} / 0.95 \text{ mg Mg / kg water} \right)^{1/2} = 13.4 \text{ for Mg (std.dev. = 6.1)}$$

	Na	σ	Ca	σ	Mg	σ
1 % consistency equilibrium (pH = 10.3)						
external solution, mg / kg water	201.7	5.9	3.5	0.8	0.95	0.3
mg / kg FSP water	1535.7		1129.4		169.3	
mg / kg od fibre	2167.1	35.4	1593.9	207.8	238.0	19.6
1 % consistency acidified equilibrium (pH = 2.2)						
external solution, mg / kg water	210.7	4.4	20.4	1.4		
mg / kg FSP water	160.9		72.6			
mg / kg od fibre	226.1	13.7	85.7	6.2		
1 % consistency equilibrium with 0.3106 g CaCl₂ added (pH=10.2)						
external solution, mg / kg water	222.0		83.3		1.20	
mg / kg FSP water	591.30		3022.8		107.2	
mg / kg od fibre	830.2		4244.4		150.5	
1 % consistency equilibrium with 0.6042 g CaCl₂ added (pH=10.3)						
external solution, mg / kg water	218.0		190.3		2.18	
mg / kg FSP water	495.4		4027.5		101.7	
mg / kg od fibre	696.4		5661.0		143.0	
0.46 % consistency equilibrium (pH =10.3)						
external solution, mg / kg water	98.3		2.9		0.46	
mg / kg FSP water	1257.3		974.9		189.3.0	
mg / kg od fibre	1767.2		1370.3		266.0	
1.95 % consistency equilibrium (pH = 10.3)						
external solution, mg / kg water	422.6		2.5		1.62	
mg / kg FSP water	2560.4		1255.9		181.3	
mg / kg od fibre	3598.8		1765.2		254.8	

Table 5.3.1: Partitioning of ions in post brown stock pulp under various conditions. Standard deviations were obtained only for the first two experiments. Other experiments were not duplicated.

Initially it is apparent that ideal Donnan equilibrium is not obeyed by the ions considered since the distribution coefficient is not the same for all ions. Including the errors given by the standard deviations of the λ 's shows that all the confidence regions overlap, and it is quite possible from this data that the ions do obey the ideal Donnan partitioning. The large errors in the concentrations of Ca^{+2} and Mg^{+2} in the external solution contribute a great deal to the very large

confidence intervals obtained. Reasonable errors were obtained for the concentrations in the fibre solution, but very large uncertainties accompany the external solution concentrations of calcium and magnesium. Dividing the internal and external solution concentrations causes the large external solution error to propagate to the error in the final value. Behaviour contradicting Donnan equilibrium could be due to precipitation within the fibres or bonds being formed between the NPEs and groups within the fibres.

From the results in Table 5.3.1 the total metal content in the pulp can be calculated, knowing the masses of the internal and external solutions. Table 5.3.2 shows these total metal contents calculated from 1% consistency equilibriums (at pHs 10.3 and 2.2) and the high and low consistency experiments (0.46% and 1.95%). Each of these experiments provides the total metal contents on the pulp and the average is displayed in Table 5.3.2. The pulp contains a much larger amount of sodium than expected, likely due to inadequate washing of pulping chemicals from the fibre in the brown stock washers. Quantities of calcium and magnesium are similar to those obtained by other experimenters (Towers and Scallan, 1996; Bryant and Edwards, 1996). The high ionic strength, due to sodium, decreases the magnitude of the Donnan distribution coefficients in all experiments.

Total Metal Contents in pulp as received mg / kg od fibre		Standard Deviation σ
Na	24500	4280
Ca	1990	170
Mg	330	50

Table 5.3.2: Measured NPE contents in post brown stock pulp (as-received)

5.3.2 Acidified 1% Consistency Equilibrium

Hydrochloric acid was added to the suspension of original pulp to decrease the pH to 2.2. Under these conditions the weak acidic groups bound to the pulp should not be ionized, and the solution within the pulp fibres should be very similar in concentration to the external solution. Table 5.3.1 shows that this is indeed the case, and the sodium concentration within the fibres even falls below that of the external solution. Acid addition causes ions to leave the fibre phase, increasing the concentration of ions in the external solution. The trend of very large decreases of metal ions within the fibres and moderate increases in the external solution are present for both Na and Ca. The large mass of the external solution (V-F) relative to the fibre phase mass (F) yields the small change in external concentration while large changes in concentration are observed within the fibres.

5.3.3 Elevated Calcium 1% Consistency Equilibrium

Increasing the calcium in the system drives magnesium and sodium out of the fibres and into the external solution. The addition of calcium causes a new equilibrium in which sodium and magnesium are a smaller fraction of the total mobile ions in the system. Since the fixed charge on the fibres has not changed, calcium will replace sodium and magnesium within the fibres so the distribution coefficient can remain the same for all ions. Sodium in the fibres falls from 1500 mg/kg FSP water to 600, then 500 as calcium increases from 1100 to 3000 to 4000 mg /kg FSP water. This indicates the principle of Donnan equilibrium is obeyed.

Increasing the calcium in the system also shows that increasing the ionic strength of the system decreases the Donnan distribution coefficient. The distribution coefficient is decreased because the fixed charge within the fibres attracts a specified amount of charged mobile species. If there

are few mobile cations, they are partitioned very strongly to satisfy electroneutrality of the fibre phase. With increased cation content, the same number of cations are needed in the fibre, but these make up a smaller fraction of the total mobile ions, and the distribution coefficient falls.

5.3.4 0.46% and 1.95% Consistency Equilibriums

Changing the consistency causes a new equilibrium since the external solution mass remains very similar in each experiment, while the mass of charge containing fibre and quantity of metal ions varies. Table 5.3.3 shows the Donnan distribution ratios of sodium and calcium in the fibre solution to the external solution for the three different consistencies.

Consistency %	Sodium Donnan Ratio Na in fibre/Na in external solution	Calcium Donnan Ratio (Ca in fibre/Ca in external solution) ^{1/2}
0.458	12.8 (std. dev. = 0.57)	18.4 (std. dev. = 6.2)
1	7.6 (std. dev. = 0.34)	18.0 (std. dev. = 6.3)
1.948	6.1 (std. dev. = 0.27)	22.5 (std. dev. = 7.6)

Table 5.3.3: Donnan distribution coefficients (λ') at various consistencies.

The decreasing ratio as consistency increases is what is expected from Donnan equilibrium theory. When there are less total ions present (at low consistency), the sodium ions should be present in higher concentrations within the fibres. Calcium does not appear to obey this principle as the Donnan ratio does not change a great deal regardless of the consistency. Estimates in the standard deviations of the concentrations of the 0.458% and 1.948% consistency experiments were obtained by assuming the coefficients of variation were the same as those in the 1% consistency experiments. Including the uncertainty of these errors it is impossible to make any sure statements about the trends in the Donnan distribution coefficients for the calcium data. This is again due to the low concentrations and uncertainty in calcium measurements in the external solution.

Many of the discrepancies in the distribution coefficient could be due to the very low concentrations of divalent cations in the external solution. Magnesium concentrations, for example, do not rise above 2.2 mg/kg water (2.2 ppm). This is a very low concentration, testing the limits of AA, especially when the external solution contains dissolved organics from the pulping process. The large standard deviations in Table 5.3.1 indicate the scatter in the external solution concentrations of calcium and magnesium.

5.4 Metal Ion Partitioning with Acid Washed Pulp

Two different NPE concentrations were used in the equilibrium experiments that were performed. One set of experiments was performed using the same concentrations of NPEs found in the original pulp from the brown stock washers, the other at an elevated concentration of magnesium. Experiments were performed in both the 150mL and 1L vessels, and both EGTA/EDTA and AA were used to determine metal ion concentrations (for Ca^{+2} , Mg^{+2} , and Na^{+}). The significance, importance, and relationship between each experiment will be discussed in turn.

5.4.1 Brown Stock Pulp Ion Contents in 150 mL Vessels

Figures 5.4.1, 5.4.2, and 5.4.3 show the filtrate concentrations of calcium, magnesium, and sodium from 150 mL vessel experiments obtained by EGTA, EDTA, and AA measurements, respectively. Tables 5.4.1, 5.4.2, and 5.4.3 list the plotted data, along with the standard errors (s/\sqrt{N}) of the values (three concentration measurements at each pH). The curves fall as cations are drawn from the external solution into the fibres to maintain electroneutrality. Calcium results agree up to a pH of 7, where experimental data continue to fall, while the 2-K model predictions indicate that a plateau is expected. The exact charge model follows the

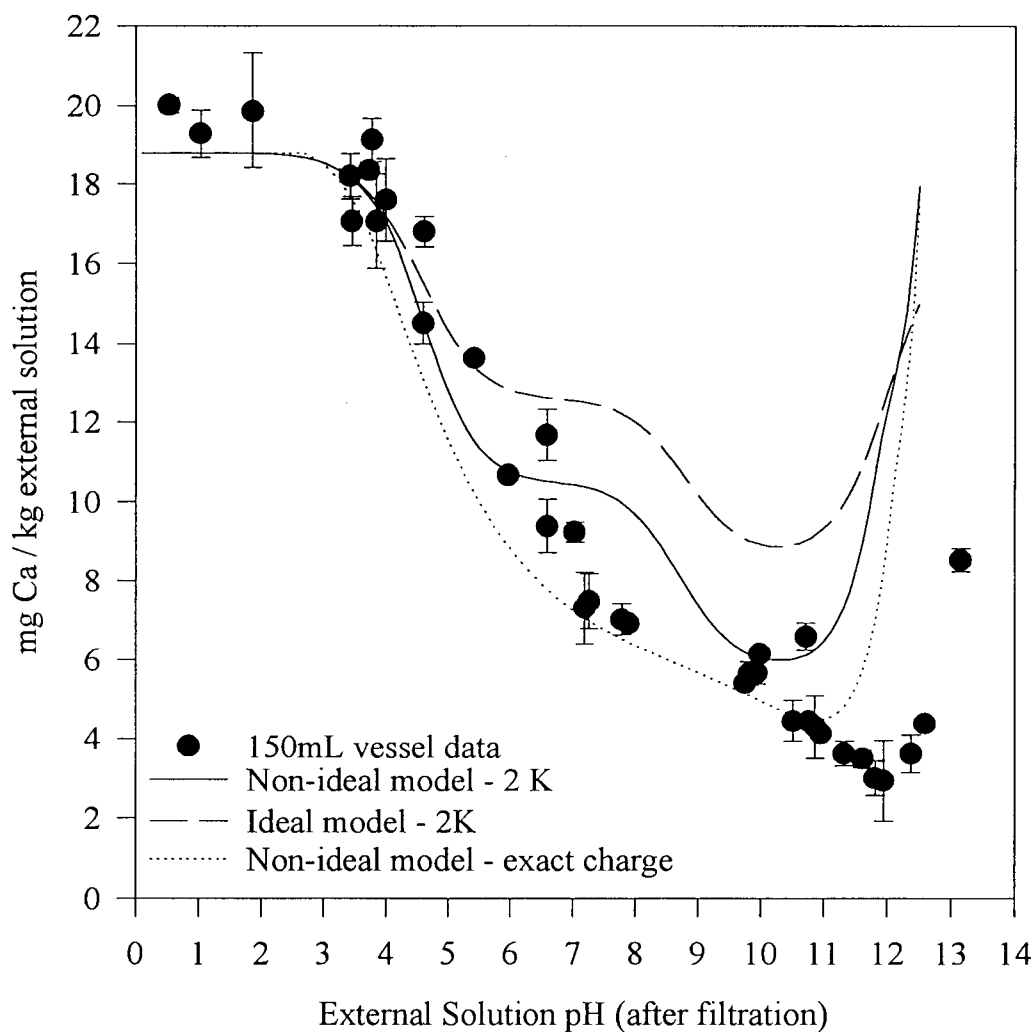


Figure 5.4.1: External solution concentration of calcium (Ca^{+2}) over a range of pHs. Dissociated groups on the fibres draw the cations into the fibres, causing the concentration to decrease in the external solution.

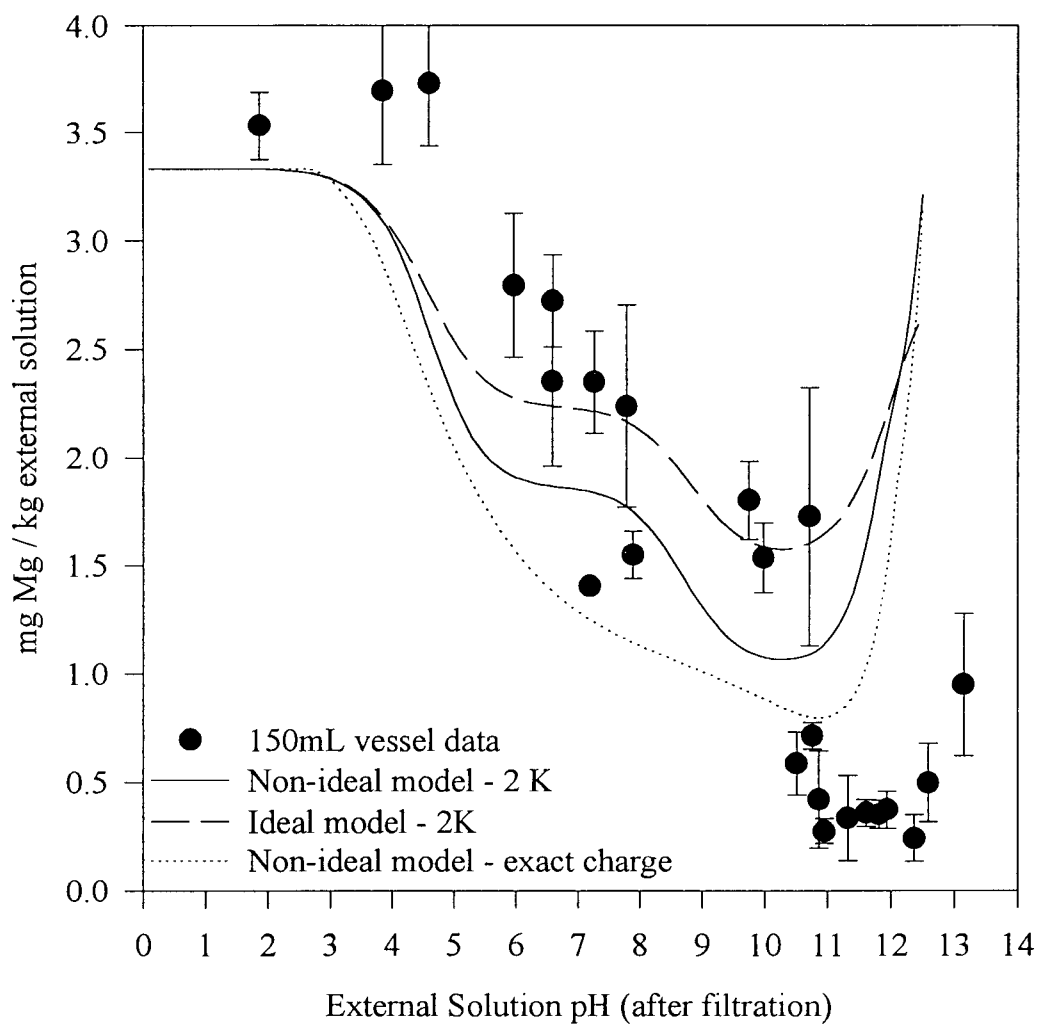


Figure 5.4.2: External solution concentration of magnesium (Mg^{+2}) over a range of pHs. Dissociated groups on the fibres draw the cations into the fibres, causing the concentration to decrease in the external solution.

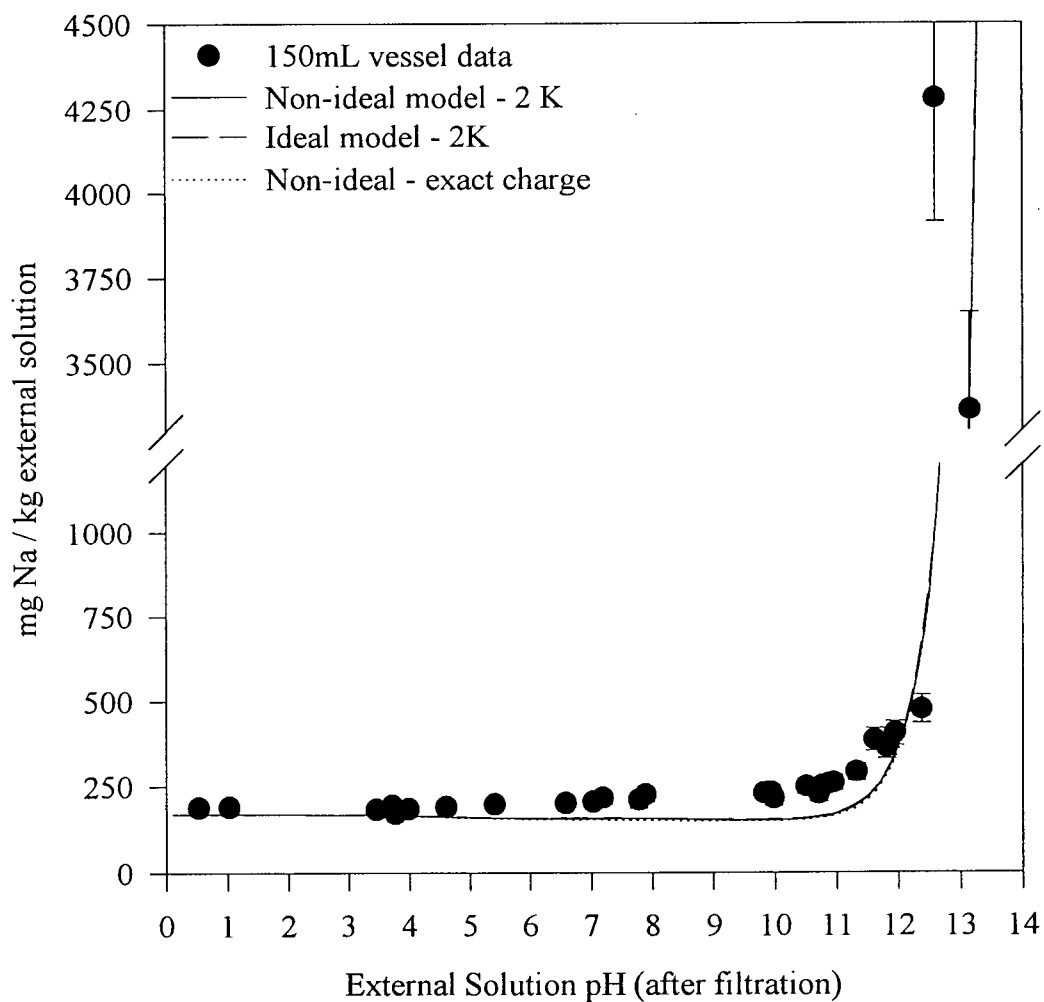


Figure 5.4.3: External solution concentration of sodium (Na^+) over a range of pHs. Sodium hydroxide is used to increase the pH of the fibre suspension, so the amount of sodium is constantly increasing.

pH	mg Ca / kg external solution		mg Ca / kg od fibre		mg Ca / kg FSP water	
0.53	20.0	(0.044)	-57	(7.1)	-49	(6.1)
1.03	19.3	(0.140)	18	(14.2)	15	(12.0)
1.86	19.9	(0.338)	-25	(32.1)	-21	(27.2)
3.42	18.2	(0.133)	128	(14.2)	108	(12.1)
3.45	17.1	(0.144)	212	(14.8)	178	(12.7)
3.72	18.3	(0.046)	108	(7.3)	90	(6.2)
3.77	19.1	(0.131)	26	(14.2)	21	(11.8)
3.84	17.1	(0.275)	230	(26.6)	190	(22.2)
3.99	17.6	(0.242)	165	(24.4)	135	(20.2)
4.59	14.5	(0.120)	480	(12.9)	386	(12.1)
4.61	16.8	(0.089)	234	(10.7)	188	(9.1)
5.41	13.6	(0.009)	557	(6.1)	436	(8.4)
5.96	10.7	(0.012)	870	(6.5)	671	(11.6)
6.58	11.7	(0.150)	721	(15.3)	547	(14.3)
6.59	9.4	(0.158)	970	(16.3)	730	(16.7)
7.03	9.2	(0.060)	950	(8.3)	720	(12.5)
7.19	7.3	(0.210)	1130	(20.5)	850	(20.0)
7.26	7.5	(0.167)	1100	(16.9)	820	(17.7)
7.78	7.0	(0.093)	1180	(11.2)	880	(15.5)
7.89	6.9	(0.004)	1180	(6.4)	870	(13.8)
9.75	5.4	(0.008)	1320	(6.6)	950	(14.5)
9.82	5.7	(0.068)	1300	(9.2)	930	(15.0)
9.93	5.7	(0.065)	1360	(9.4)	970	(15.6)
9.98	6.2	(0.008)	1260	(6.7)	900	(13.8)
10.51	4.4	(0.123)	1470	(14.0)	1040	(17.9)
10.71	6.6	(0.079)	1440	(11.9)	1020	(16.9)
10.76	4.4	(0.013)	1420	(7.0)	1010	(15.2)
10.86	4.3	(0.185)	1480	(19.5)	1050	(20.4)
10.95	4.1	(0.018)	1480	(7.4)	1050	(15.9)
11.32	3.6	(0.072)	1520	(10.2)	1070	(16.9)
11.61	3.5	(0.050)	1520	(8.7)	1070	(16.4)
11.81	3.0	(0.102)	1530	(11.9)	1080	(17.5)
11.94	2.9	(0.235)	1540	(23.3)	1080	(22.4)
12.37	3.6	(0.111)	1450	(12.3)	1020	(16.8)
12.59	4.4	(0.000)	1370	(6.6)	960	(14.4)
13.15	8.5	(0.068)	1160	(10.9)	810	(13.8)

Table 5.4.1: Calcium partitioning in 150 mL equilibrium vessels. Concentration in the external solution determined by EGTA titration. Negative values result from back calculation with the known total calcium content in the system. Standard errors are given in brackets. Data determined in triplicate.

pH	mg Mg / kg external solution		mg Mg / kg od fibre		mg Mg / kg FSP water	
3.45	3.6	(0.218)	-16	(20.7)	-13	(17.3)
3.77	3.6	(0.485)	-6	(47.3)	-5	(39.2)
3.84	3.7	(0.081)	-21	(7.7)	-17	(6.4)
3.99	3.7	(0.156)	-17	(15.3)	-14	(12.6)
4.59	3.7	(0.070)	-25	(6.8)	-20	(5.5)
4.61	2.7	(0.229)	80	(22.7)	65	(18.3)
5.41	3.1	(0.374)	38	(37.0)	30	(29.0)
5.96	2.8	(0.077)	66	(7.9)	50	(6.1)
6.58	2.4	(0.091)	109	(8.7)	82	(6.7)
6.59	2.7	(0.049)	73	(4.8)	55	(3.7)
7.03	2.6	(0.261)	88	(24.6)	66	(18.5)
7.19	1.4	(0.002)	194	(1.1)	145	(2.3)
7.26	2.4	(0.045)	101	(4.4)	76	(3.5)
7.78	2.2	(0.109)	121	(10.6)	90	(8.0)
7.89	1.6	(0.025)	190	(2.6)	140	(2.9)
9.75	1.8	(0.042)	160	(4.0)	110	(3.3)
9.82	0.9	(0.140)	260	(13.2)	180	(9.8)
9.93	0.9	(0.161)	270	(15.6)	190	(11.5)
9.98	1.5	(0.037)	190	(3.7)	130	(3.3)
10.51	0.6	(0.034)	290	(3.6)	210	(3.9)
10.71	1.7	(0.138)	200	(15.0)	140	(10.8)
10.76	0.7	(0.014)	270	(1.8)	190	(3.1)
10.86	0.4	(0.052)	300	(5.3)	210	(4.8)
10.95	0.3	(0.013)	320	(1.9)	230	(3.5)
11.32	0.3	(0.046)	300	(4.6)	210	(4.5)
11.61	0.4	(0.014)	300	(1.9)	210	(3.3)
11.81	0.4	(0.015)	290	(1.9)	200	(3.2)
11.94	0.4	(0.020)	290	(2.3)	200	(3.3)
12.37	0.2	(0.025)	300	(2.6)	210	(3.5)
12.59	0.5	(0.042)	270	(4.1)	190	(3.9)
13.15	1.0	(0.076)	280	(8.0)	200	(6.3)

Table 5.4.2: Magnesium partitioning in 150mL equilibrium vessels. Concentration in the external solution determined by EDTA and EGTA titration. Negative values result from back calculation with the known total magnesium content in the system. Standard errors are given in brackets. Data determined in triplicate.

pH	mg Na / kg external solution	
0.53	187	(3.7)
1.03	189	(4.0)
3.45	182	(3.7)
3.72	192	(4.0)
3.77	170	(0.7)
3.99	183	(3.5)
4.61	189	(3.5)
5.41	196	(2.1)
6.58	200	(2.3)
7.03	205	(3.5)
7.19	215	(4.4)
7.78	209	(5.1)
7.89	224	(4.6)
9.82	229	(4.6)
9.93	231	(4.6)
9.98	213	(4.9)
10.51	246	(4.9)
10.71	226	(5.8)
10.76	248	(5.1)
10.86	254	(5.1)
10.95	258	(5.1)
11.32	290	(5.8)
11.61	386	(7.9)
11.81	362	(7.4)
11.94	405	(8.1)
12.37	475	(9.5)
12.59	4280	(86.0)
13.15	3360	(67.4)

Table 5.4.3: Sodium partitioning in 150 mL equilibrium vessels. Concentrations determined by AA. All back calculated fibre values were negative and have not been tabulated. Standard errors are given in brackets. Data determined in triplicate.

experimental data more closely and shows no plateau between a pH of 7 and 8. It can be seen that the accurate charge distribution given by the cubic equation provides much better predictive ability than the two dissociation constant model. At pHs above 12 both the models and the experimental data indicate that calcium and magnesium are driven from the fibres back into the

external solution. This is due to the amount of sodium in the system (Figure 5.4.3) which causes the divalent cations to be replaced within the fibres by the very high concentrations of sodium.

In the figures, the 95 % confidence interval has been plotted with the experimental data. This is calculated using the standard error from the relation,

$$\bar{x} - t \frac{s}{\sqrt{N}} < \mu < \bar{x} + t \frac{s}{\sqrt{N}} \quad (57)$$

where: μ is the average of the population.

\bar{x} is the average of the sample.

s is the standard deviation of the sample.

N is the number of data points in the sample.

t is the value of Student's t distribution for the given confidence interval and degrees of freedom. For three data points and a 95% confidence interval, t is 4.303 (Mandel, 1984).

Sample error calculations are shown in Appendix D. The standard error (s/\sqrt{N}) , was tabulated because it is a fundamental quantity of the data and from it any confidence interval can be determined. The largest errors occur in the experimental determination of the concentrations of the metal ions (using EDTA and EGTA) and the curve approximating the fibre saturation point. Other errors in measurements of mass and volume are much smaller and have little effect on the final errors obtained. For clarity on the plot of magnesium concentrations in the external solution not all the data points have been included. It was arbitrarily decided that data points with 95% confidence intervals greater than 0.6mg/kg external solution would not be plotted. This is partially justified by noting that the purpose of figures is to clearly display results. The large error bars of 8 of the 31 data points significantly reduce the clarity of Figure 5.4.2, so those 8 points have not been plotted.

The trends of the magnesium experimental results differ from those of calcium primarily in the magnitude of scatter and error in the data. Both sets of data decrease as the pH increases. At a pH above 12 both the calcium and magnesium data begin to fall. The magnesium data are not as close to the shape of the exact charge model as the calcium data, due to the larger errors in the magnesium data. The low solution concentrations of magnesium and the use of the difference between the EDTA and EGTA titration results to obtain the Mg concentrations result in much greater uncertainty in the experimental data. Magnesium concentrations are below 5 ppm in the external solution; quite low for accurate EDTA-EGTA analysis.

The model predictions in Figure 5.4.3 do a moderately good job of estimating the sodium in the system at a given pH. Model results tend to under-predict the experimental data between the pHs of 3 and 8 because the "buffering" effect of the fibres has not been taken into account. That is, the H^+ leaving the fibres upon NaOH addition is not taken into account in predicting the resulting pH. The pH change that occurs when NaOH is added to the pulp suspension is assumed to be the same as that which would occur if the NaOH was added to pure water.

The main reason for treating the pulp suspension as water when considering the pH change caused by NaOH addition is that the sodium content of the system has its greatest effect at pHs above 10. At this point many of the charged groups on the fibres are dissociated and the pulp suspension behaves very much like water, as far as the pH change caused by NaOH addition is concerned. The continuing rise in the exact charge on the fibres at pHs above 10 is completely overshadowed by the large amounts of NaOH added to the system. The rapid increase in

sodium content in the system decreases the Donnan partitioning ratio, decreasing the quantity of divalent cations in the fibres and increasing them in the external solution.

Input concentrations of NPEs to the acid washed pulp for these experiments are as follows:

$$\text{Ca}^{+2} = 1860 \text{ mg / kg od fibre}$$

$$\text{Mg}^{+2} = 330 \text{ mg / kg od fibre}$$

$$\text{Na}^{+} = 16650 \text{ mg / kg od fibre}$$

Comparison of these values with Table 5.3.2 indicates that less sodium (Na^{+}) is added to the system than the 24500 mg/kg od fibre found present in the post brown stock pulp. Acid washed experiments begin at a pH of 3.7 and sodium hydroxide is added to increase the pH. The data in Table 5.3.2 is for the post brown stock pulp, with a pH of 10.3. Increasing the pH of the acid washed pulp from 3.7 to 10.3 with sodium hydroxide has been accounted for in the value above by subtracting from 24500 mg Na^{+} /kg od fibre the average NaOH added to 1% consistency pulp suspensions to achieve the pH change (7850 mg/kg od fibre). At a pH of 10.3 the pulp suspension in these acid washed experiments contains very similar amounts of Na^{+} , Ca^{+2} , and Mg^{+2} .

The standard errors shown in Tables 5.4.1, 5.4.2, and 5.4.3 provide some idea of the variability in the data but another good measure is to examine the scatter of data points at similar pHs. For calcium, the data in Table 5.4.1 between pHs 10.5 and 11 show that the difference between data points taken at the same condition can be up to 2 mg/kg external solution. The variability with magnesium is even more pronounced. In the same alkaline pH range the data points range in value from 1.7 to 0.3 mg Mg/kg external solution. This scatter is likely partially introduced by the variability of pulp and partially due to the analysis of magnesium at concentrations below 1

ppm (1 mg/kg external solution). Although errors are significant, the important conclusion is that both calcium and magnesium data lie in a definite band which is predicted well by the exact charge model over all pHs, and predicted well by the 2-K model at pHs below 7.

Back-calculation of the fibre concentrations from the filtrate concentrations and the known total salt in the system gives the divalent ion concentrations in fibres, as shown in Figures 5.4.4 and 5.4.5 (from the data in Tables 5.4.1, 5.4.2, and 5.4.3). Negative values due to back calculation have been included and the 95% confidence intervals on the plots show that some of these values have large enough deviations to also possibly be positive. There is again the difference in the 2-K model predictions and experimental data at pHs above 7 for both calcium and magnesium. The exact charge model makes much better predictions, due to other charged groups that dissociate at higher pHs (likely phenolic hydroxyls). The exact charge model includes the effect of these groups, and the increased total charge causes more cations to be drawn into the fibres at the high pHs. Thus, it seems that accurate modeling of the charge in the fibres is all that is needed to closely follow the experimental data of NPE partitioning.

Data corresponding to sodium contents in the fibres have not been plotted because back calculation consistently gave negative values of sodium within the fibres. Over-prediction of the sodium content in the external solution by only a few percent causes the mass balance to give negative sodium contents within the fibres, due to the large total content of sodium in the system. The total sodium includes the sodium added as a NPE with calcium and magnesium, and the sodium added as NaOH to increase the pH of the pulp suspension. Both concentrations must be known exactly for back-calculation to be successful.

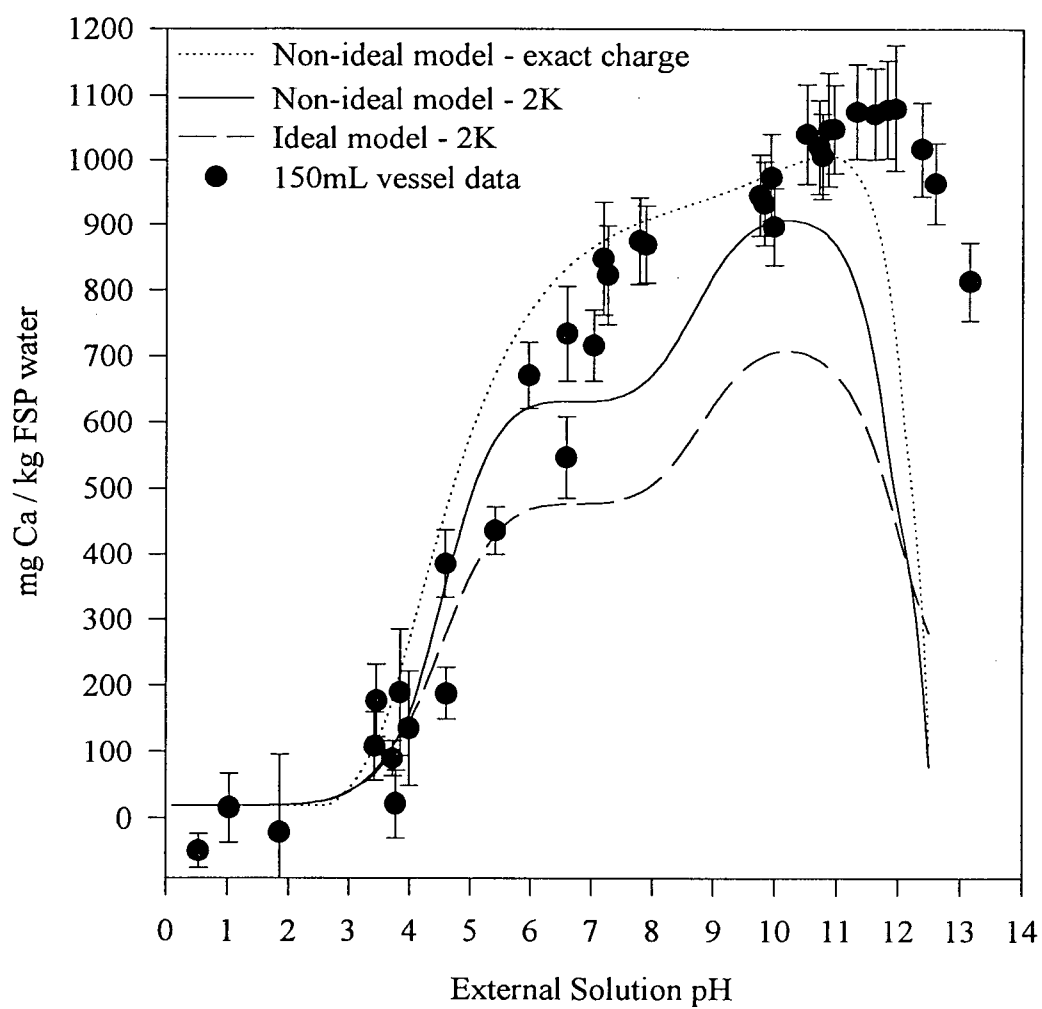


Figure 5.4.4: Fibre phase concentration of calcium over the pH range 1-13.

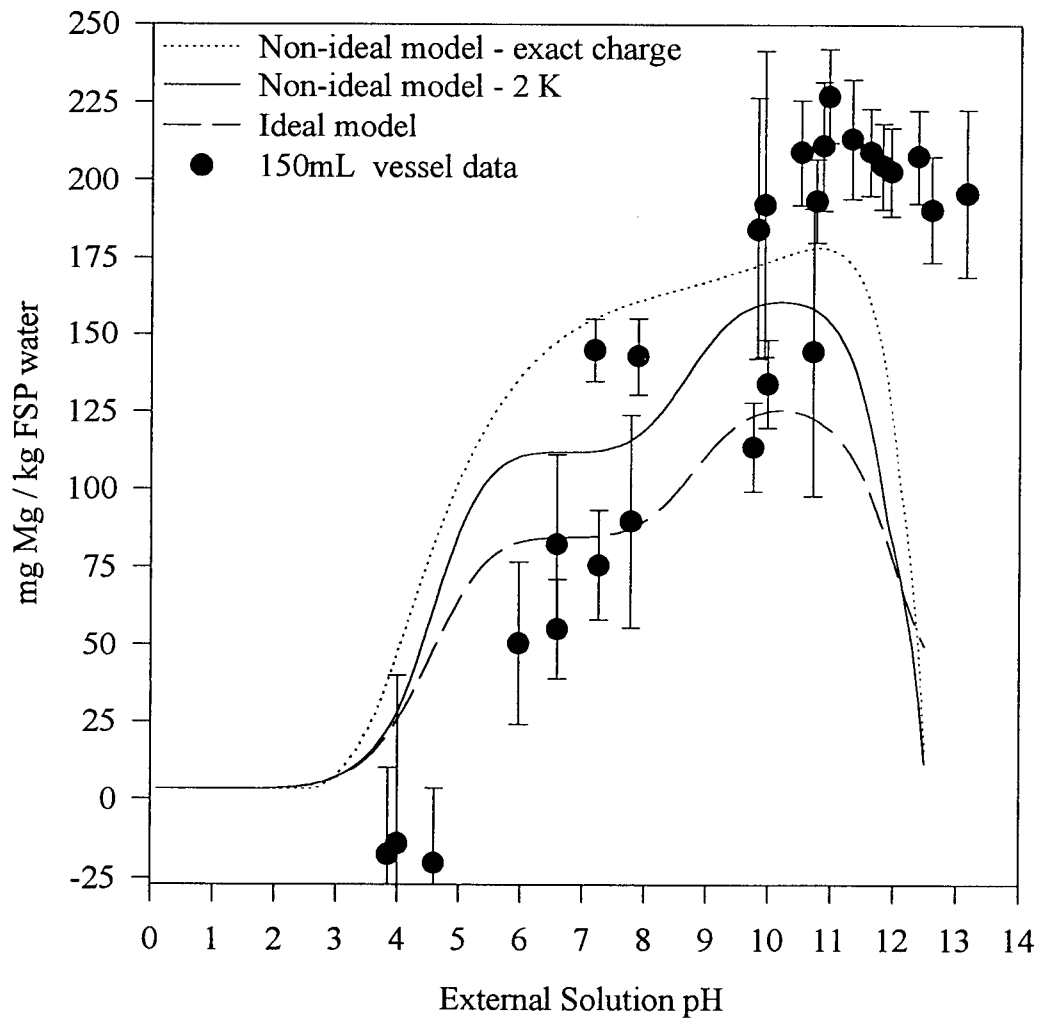


Figure 5.4.5: Fibre phase concentration of magnesium over the pH range 3-13.

Again, the magnesium experimental data shows much larger errors and scatter than the data of calcium within the fibres. The back-calculation experimental method employed is very effective for calcium, while the large errors in the magnesium external solution propagate through the calculation and remain very large in the internal solution. The back-calculation method is very dependent on the accuracy of the external solution concentrations. Poor accuracy results in negative values, which is seen in the data points at pHs below 3 in Table 5.4.1.

A second explanation for the 2-K partitioning model under-predicting Ca or Mg contents at high pHs is precipitation of calcium and magnesium within the fibres. The Donnan model does not account for precipitation phenomena but precipitated compounds within the fibres would increase the experimental results above model predictions. Precipitation can explain why Donnan equilibrium principles disagree with the data obtained for the original pulp in Section 5.3. Results presented there indicate that calcium and magnesium have higher distribution coefficients (λ') than sodium, while Donnan equilibrium requires that the distribution coefficient of all mobile ions must be the same. The data are obtained at a pH of 10.3; high enough that precipitation could be significant within the fibres. Also, these fibres are not acid washed, so the quantity of carbonates, oxalates, and phosphates could be much higher than in the acid washed pulp used here. Distribution coefficients of calcium and magnesium are higher than that of sodium, which would be expected if calcium and magnesium had precipitated within the fibres.

In Section 5.3 it also appears that changing the consistency does not significantly change the calcium distribution coefficient. This could be another indication that calcium within the fibres is in a precipitated, rather than soluble, form. The post brown stock washer pulp is likely to have many of the anions that can cause precipitation (carbonates, oxalates, and phosphates), which is

further reason to consider the possibility of the phenomenon. Although these are valid concerns, after acid washing the fibres and at the concentrations of NPEs found in the post brown stock washer pulp, it seems that precipitation is not a concern. The electrostatics of Donnan equilibrium describe the partitioning of calcium and magnesium between the fibres and external solution.

The negative values of NPE contents in the fibre phase obtained at low pH for both calcium and magnesium curves indicates there is more calcium or magnesium in the system than expected or the EDTA and EGTA titrations consistently over-predict the divalent metal ion contents. Tests were performed on acid washed pulp to determine the residual ion contents. These were found to be below detection limits for calcium and magnesium and very low for sodium. This points out the major weakness of the back-calculation method used in 150mL experiments. Relying on the mass balance and external solution concentrations can lead to poor results when external solution concentrations are not accurate. This is particularly evident at low pHs where few unprotonated charge sites exist on the fibres and the concentrations in the internal and external solutions are similar.

5.4.2 Elevated Magnesium Content in 150 mL Vessels

Experiments in 150mL and 1L vessels were performed at elevated magnesium contents to verify the methods are equivalent (i.e. provide the same trends and similar concentrations). The results for the 150mL vessels are presented first. Concentrations of Ca^{+2} and Mg^{+2} in the external solution were analyzed through EGTA and EDTA titration. Results for the 150 mL vessels are shown in Tables 5.4.4, 5.4.5, and 5.4.6 for calcium, magnesium and sodium. Negative concentrations within the fibre result from back-calculation when metal contents in the external

solution are measured higher than the mass balance indicates is possible. The problem occurs only at low pHs for calcium, where few metal ions are in the fibres and the concentrations in both phases are the same (indicated by the model). Sodium concentrations are likely over-predicted by AA since the values are consistently too high to provide positive fibre contents of metal ions, thus none are shown in Table 5.4.6. Another possibility is the existence of residual sodium after acid washing, as mentioned before. This seems unlikely since the amount remaining after acid washing is smaller than the sodium added when increasing the pH from 3 to 4 with NaOH.

pH	mg Ca/kg external solution		mg Ca/kg od fibre		mg Ca/kg FSP water	
1.45	31.5	(0.23)	-208	(24.6)	-191	(23.0)
3.4	30.4	(0.35)	-98	(34.4)	-82	(28.8)
3.59	31.0	(0.28)	-131	(29.3)	-109	(24.4)
3.83	30.0	(0.16)	-46	(20.5)	-38	(17.0)
4.02	29.3	(0.00)	15	(9.3)	12	(7.7)
4.5	29.6	(0.12)	3	(15.1)	3	(12.3)
6.31	27.6	(0.14)	200	(16.7)	153	(13.0)
8.59	25.5	(0.02)	396	(9.3)	288	(7.9)
9.39	25.2	(0.09)	438	(12.8)	315	(10.2)
9.88	23.6	(0.33)	581	(31.8)	415	(23.5)

Table 5.4.4: Calcium partitioning in 150 mL vessels with elevated Mg contents. Concentration in the external solution determined by EGTA titration. Negative values result from back calculation with the known total calcium content in the system. Standard errors are given in brackets. Data determined in triplicate.

Metal ion concentrations for the elevated magnesium experiments are very different from the metals originally present on the pulp. Values added are as follows:

$$\text{Ca}^{+2} = 2990 \text{ mg / kg od fibre}$$

$$\text{Mg}^{+2} = 11900 \text{ mg / kg od fibre}$$

$$\text{Na}^{+} = 25700 \text{ mg / kg od fibre}$$

pH	mg Mg/kg external solution		mg Mg/kg od fibre		mg Mg/kg FSP water	
1.45	109.2	(0.21)	830	(41.8)	760	(39.5)
3.4	107.4	(0.65)	940	(72.0)	790	(62.7)
3.59	109.7	(0.88)	850	(95.3)	710	(79.0)
3.83	107.0	(0.21)	1220	(46.5)	1000	(41.8)
4.02	107.5	(1.23)	1000	(132.5)	820	(109.2)
4.5	104.1	(1.53)	1360	(155.7)	1100	(125.5)
6.31	102.9	(0.95)	1470	(102.3)	1120	(79.0)
8.59	100.8	(0.09)	1650	(37.2)	1200	(32.5)
9.39	96.3	(0.21)	2120	(39.5)	1520	(37.2)
9.88	62.8	(1.30)	5340	(130.1)	3820	(109.2)

Table 5.4.5: Magnesium partitioning in 150 mL vessels with elevated Mg contents. Concentration in the external solution determined by EDTA and EGTA titration. Standard errors are given in brackets. Data determined in triplicate.

pH	mg Na / kg external solution	
1.45	265	(0.23)
3.4	263	(2.09)
3.59	274	(0.23)
3.83	275	(0.93)
4.02	280	(0.93)
4.5	285	(0.70)
6.31	295	(0.46)
8.59	310	(0.46)
9.39	317	(2.32)
9.88	388	(1.39)

Table 5.4.6: Sodium external solution concentrations in 150 mL vessels with elevated Mg contents. Concentrations determined by AA. Standard errors are given in brackets. Data determined in triplicate.

In these experiments calcium and magnesium are present in 60% and 3600% higher concentrations respectively. Sodium is present at the concentration of the brown stock pulp (no adjustment made for the pulp suspension being at pH 3.7). When the pH is increased, sodium

content will also rise above the brown stock pulp value. It is probable that these concentrations will encourage precipitation of the divalent cations.

Elevated magnesium experiments were performed to cause precipitation within the fibres and to simulate the conditions within a closed mill using MgSO_4 prior to its bleaching stages. The magnesium content is between 4 and 15 times the amount typically added to pulps, which is 0.05 - 0.1% Mg^{+2} on od fibre. Magnesium is added prior to oxygen delignification stages as a protector to prevent cellulose degradation (McDonough, 1996). Hydrogen peroxide bleaching stages also use magnesium to reduce decomposition of the hydrogen peroxide by transition metals. In a closed mill it is conceivable that magnesium levels could become quite high due to recycle of bleach plant effluents.

5.4.3 Elevated Magnesium Content in 1L Vessel: AA analysis

Metal contents in the 1L mixing vessel were typically determined by AA. Two uses of the data are possible; using both external solution and ash concentrations to determine the metal contents in the fibres or using only the external solution concentration and knowledge of the total ion contents to back calculate the fibre concentrations. Data from both types of analysis are shown in Tables 5.4.7 - 5.4.11.

Data in Tables 5.4.4, 5.4.5, and 5.4.6 can be compared to the data of Tables 5.4.7, 5.4.8, and 5.4.9 to see the difference in results when 150 mL vessels and back-calculation are used as opposed to a 1L vessel with analysis of both the ash and external solution is carried out. Figures 5.4.6 - 5.4.9 show the concentrations of calcium and magnesium in the external solution and fibres for these elevated magnesium experiments. It can be seen that both methods give similar results, implying that both back-calculation and ash and external solution analysis methods are

valuable in determining metal profiles. Experiments with 150mL vessels avoid the time consuming and error prone steps of ashing and dissolving, while 1L vessel experiments (using both ash and external solution) allow the total quantity of a given metal ion to be determined.

pH	mg Ca / kg external solution	mg Ca / kg od fibre	mg Ca / kg FSP water
3.15	27.7 (0.07)	76 (2.1)	64 (2.1)
3.17	28.3 (0.86)	93 (3.5)	78 (3.3)
6.17	26.1 (0.63)	361 (9.5)	277 (8.6)
9.64	25.1 (0.51)	574 (11.9)	412 (10.5)
10.53	15.1 (0.44)	911 (30.0)	647 (23.2)
11.93	2.2 (0.07)	1810 (42.8)	1272 (35.1)

Table 5.4.7: Calcium partitioning in 1L vessel with high Mg. AA used to analyze filtrate and ash NPE contents. Values use both filtrate and ash concentrations to calculate contents on fibres. Standard errors are given in brackets. Data determined in triplicate.

pH	mg Mg / kg external solution	mg Mg / kg od fibre	mg Mg / kg FSP water
3.15	101 (0.93)	281 (2.1)	238 (2.1)
3.17	107 (0.46)	295 (3.7)	250 (3.5)
6.17	95 (1.39)	829 (17.7)	635 (14.2)
9.64	94 (0.46)	1224 (14.6)	878 (12.1)
10.53	10 (0.23)	6532 (34.2)	4637 (26.0)

Table 5.4.8: Magnesium partitioning in 1L vessel with high Mg. AA used to analyze filtrate and ash NPE contents. Values use both filtrate and ash concentrations to calculate contents on fibres. Standard errors are given in brackets. Data determined in triplicate.

The common trend in the results is that both calcium and magnesium fibre phase concentrations lie above the Donnan equilibrium predictions at the pHs above 10. Also, it appears that at this point there is a strong tendency for Ca^{+2} and Mg^{+2} to rapidly enter the fibre. The reason for this is likely the precipitation of the cations as carbonates or hydroxides. Magnesium concentrations are much higher than in the brown stock pulp, bringing the system closer to the precipitation condition. The partitioning model does not incorporate precipitation phenomena, thus it does

not follow the trend of the experimental data. The assumption that all mobile ions are soluble over the pH range is violated when the magnesium content is increased. Precipitation occurs

pH	mg Na / kg external solution	mg Na / kg od fibre	mg Na / kg FSP water
3.15	305 (1.63)	512 (2.6)	434 (2.6)
3.17	293 (6.74)	570 (4.0)	483 (3.7)
6.17	344 (3.02)	764 (11.2)	585 (9.5)
9.64	368 (0.93)	897 (7.2)	643 (7.9)
10.53	563 (3.72)	919 (33.2)	652 (25.3)
11.93	687 (9.53)	4220 (51.1)	2960 (39.5)
12.75	3420 (16.73)	6640 (93.0)	4650 (67.4)

Table 5.4.9: Sodium partitioning in 1L vessel with high Mg. AA used to analyze filtrate and ash NPE contents. Values use both filtrate and ash concentrations to calculate contents on fibres. Standard errors are given in brackets. Data determined in triplicate.

pH	mg Ca / kg external solution	mg Ca / kg od fibre	mg Ca / kg FSP water
3.15	27.7 (0.07)	45.0 (5.3)	38.2 (4.6)
3.17	28.3 (0.86)	-6.4 (4.8)	-5.4 (4.3)
6.17	26.1 (0.63)	61.4 (28.1)	47.1 (22.1)
9.64	25.1 (0.51)	418 (23.2)	299 (17.7)
10.53	15.1 (0.44)	1200 (46.2)	852 (34.2)
11.93	2.2 (0.07)	2421 (65.1)	1701 (49.3)

Table 5.4.10: Calcium partitioning in 1L vessel with high Mg. AA used to analyze filtrate and only the filtrate concentration and the known total salts added are used to calculate NPE contents on fibres. Standard errors are given in brackets. Data determined in triplicate.

pH	mg Mg /kg external solution	mg Mg / kg od fibre	mg Mg / kg FSP water
3.15	101.2 (0.91)	984 (3.8)	834 (3.4)
3.17	106.6 (0.40)	493 (5.3)	418 (4.7)
6.17	95.2 (1.42)	1222 (26.7)	936 (20.9)
9.64	93.7 (0.51)	1651 (21.6)	1184 (16.7)
10.53	9.8 (0.12)	9496 (43.7)	6740 (32.3)

Table 5.4.11: Magnesium partitioning in 1L vessel with high Mg. AA used to analyze filtrate and only the filtrate concentration and the known total salts added are used to calculate NPE contents on fibres. Standard errors are given in brackets. Data determined in triplicate.

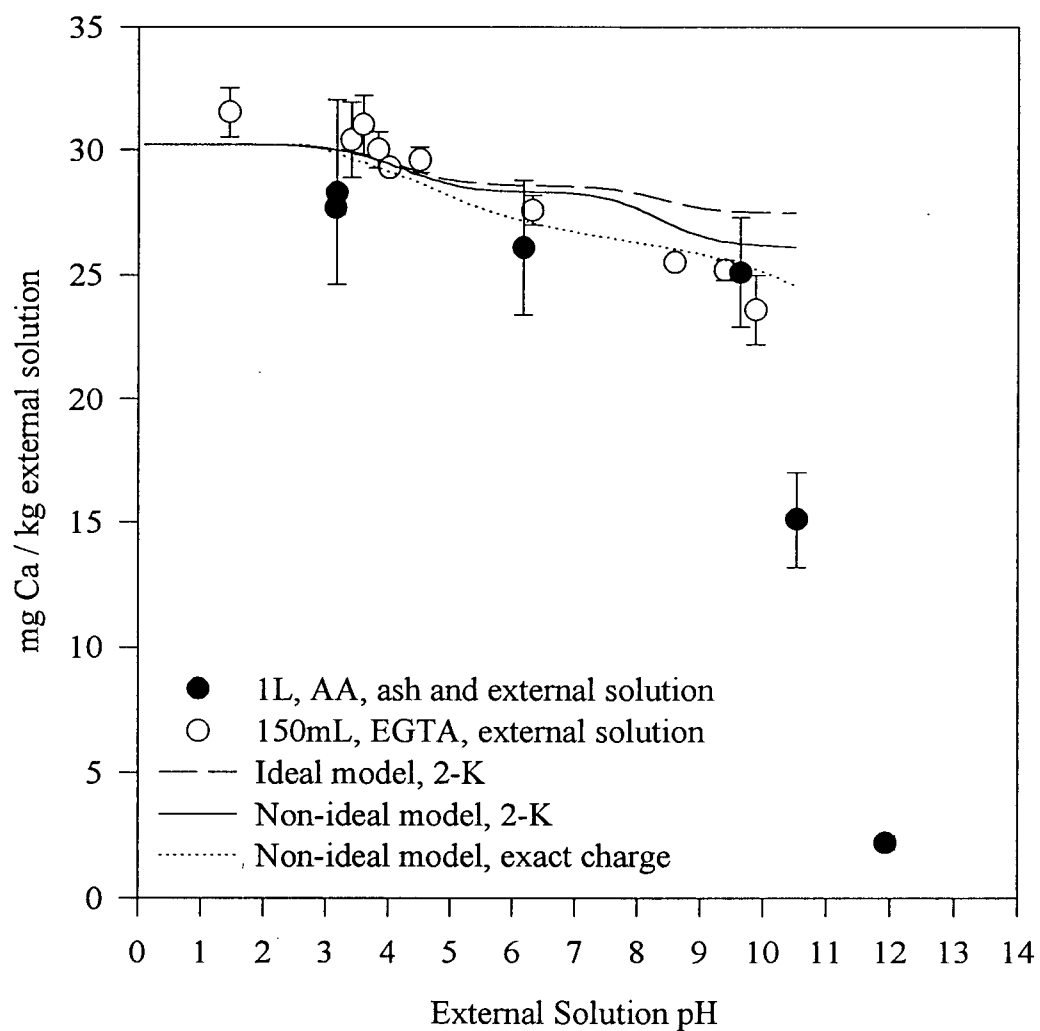


Figure 5.4.6: External solution concentration of calcium with 1L and 150mL vessels

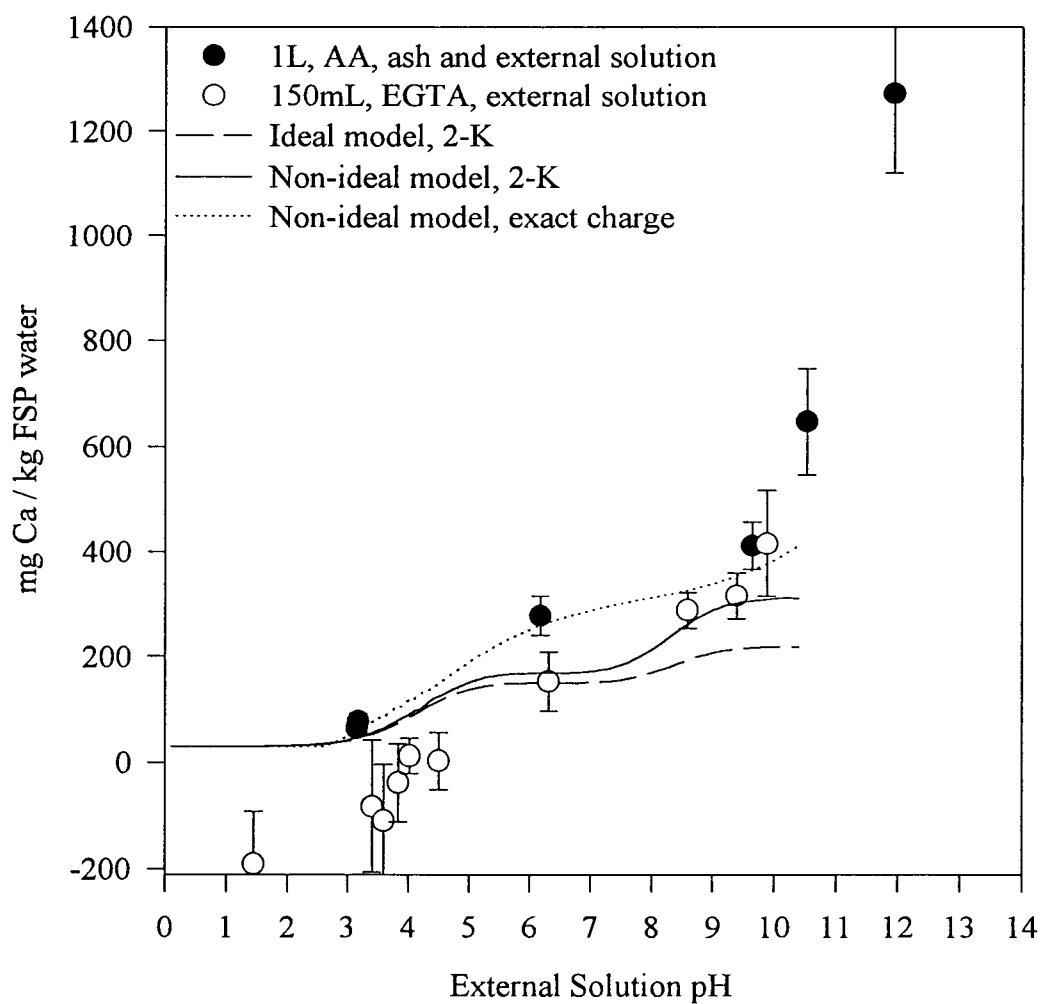


Figure 5.4.7: Fibre phase concentration of calcium with 1L and 150mL vessels

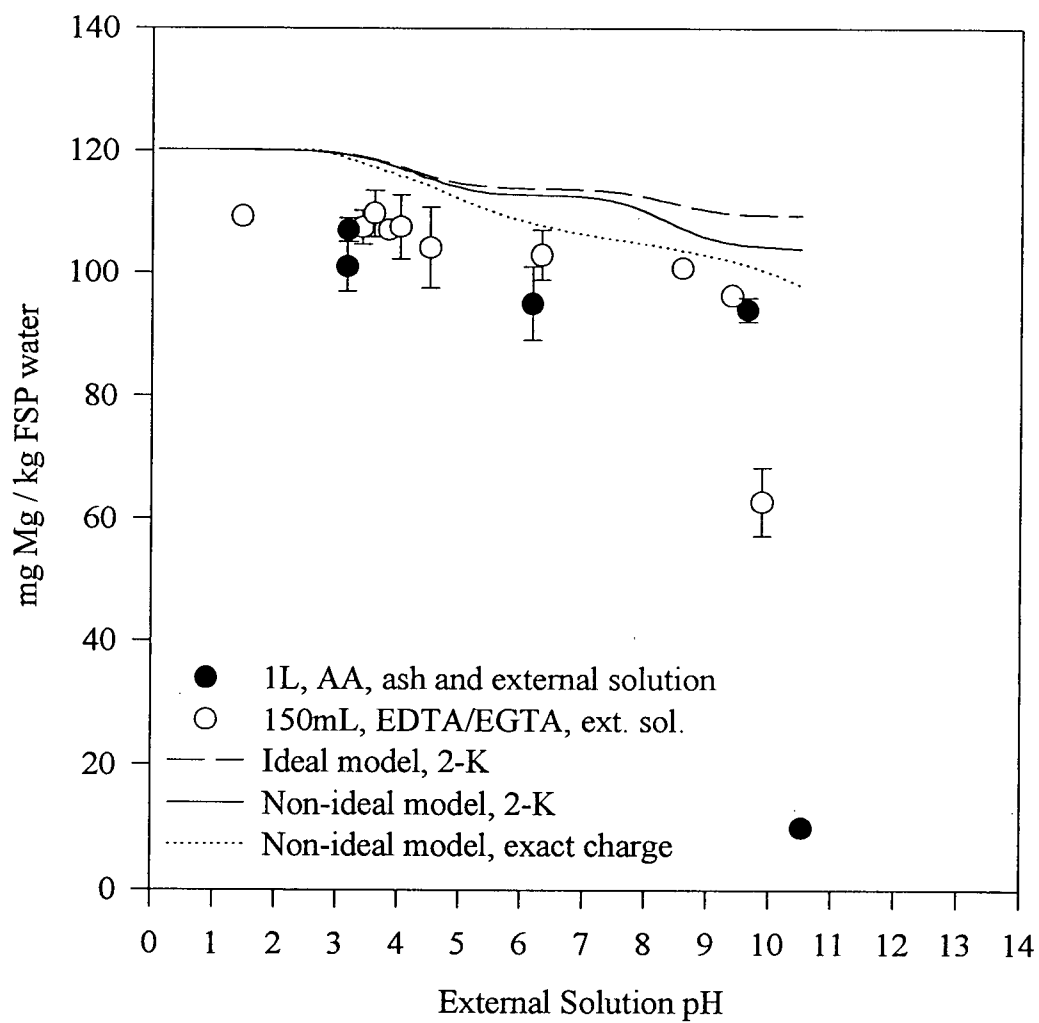


Figure 5.4.8: External solution concentration of magnesium with 1L and 150mL vessels

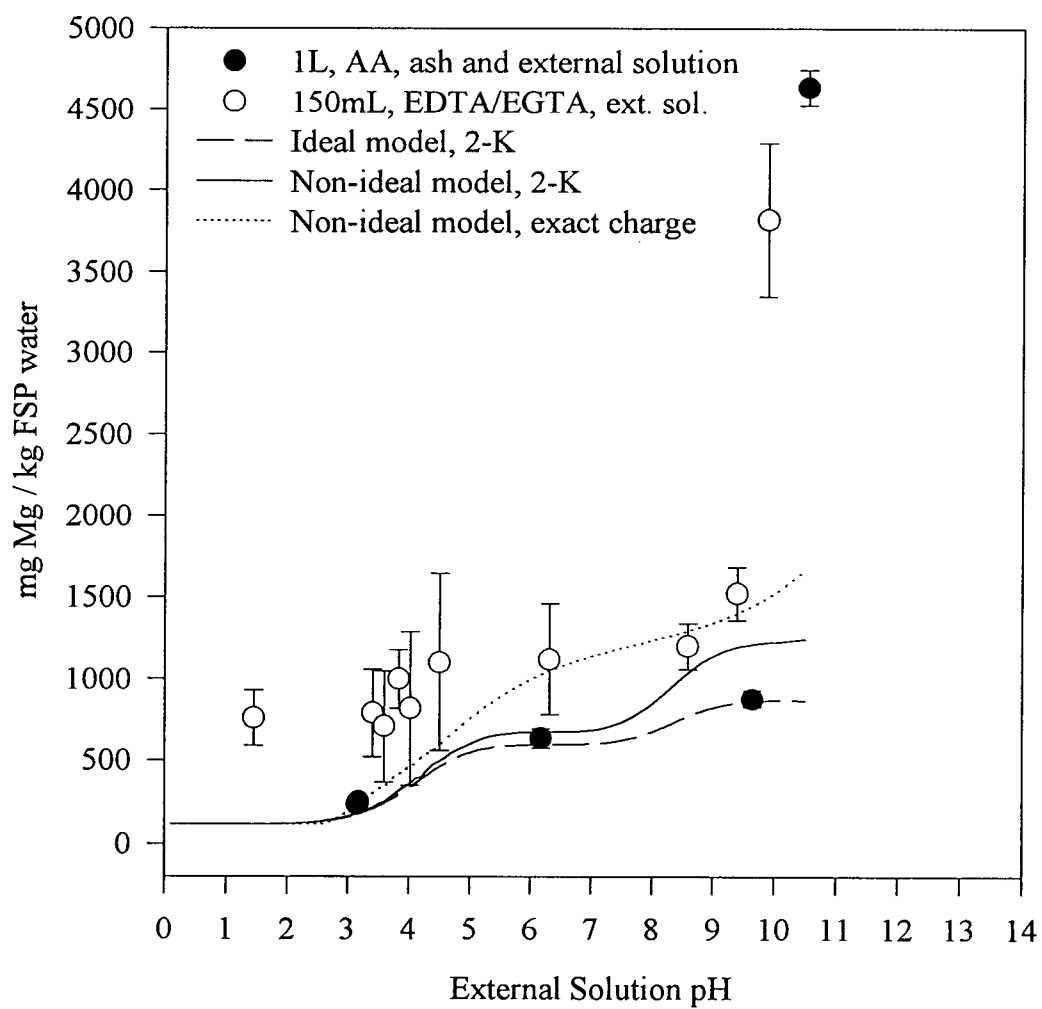


Figure 5.4.9: Fibre phase concentration of magnesium with 1L and 150mL vessels

when magnesium levels are increased and Donnan equilibrium no longer describes the system (once the pH where precipitation occurs has been reached). In a mill, the Donnan equilibrium model will be adequate for most partitioning predictions because the tests at high magnesium levels represent a situation of very extreme build up of magnesium within the fibre line.

Model predictions have been stopped at a pH of 10.5 because the model is no longer applicable when precipitation begins and algorithm convergence becomes a problem with the very high ionic strengths. Precipitation is not included within the model developed. The predictive curves do not follow the experimental data (and are not intended to) so they have been stopped at a pH of 10.5. Also, the values the algorithm converges to between pHs of 10.8 and 11.4 are not correct. The convergence of the algorithm becomes difficult at the high ionic strengths when the trends in the curves are beginning to turn down as the NaOH content becomes high.

Predictions of the partitioning model, both for ideal and activity coefficient cases, do a similar job of representing the experimental data. The activity coefficient model predicts higher concentrations within the fibres than the ideal model, but it is difficult to say which prediction is better because of the differences in the experimental data from the 150mL and 1L vessels. The quality of the experimental data is again a concern, even though analysis of both the fibres and external solution has been used and AA as well as EDTA-EGTA analysis have been used to obtain solution concentrations. It is very clear that obtaining reliable experimental data is a major obstacle in effective NPE partitioning modeling. The figures clearly show the proposed model lacks the ability to predict the trends above a pH of 10 at elevated magnesium concentrations.

The possibility of precipitation can be explored using solubility products for the common precipitates of calcium and magnesium and the maximum concentrations of calcium and magnesium from the partitioning model (Lide, 1996). From the 2-K activity coefficient predictions in Figures 5.4.7 and 5.4.9 the maximum concentrations are 310 mg Ca^{+2} /kg FSP water and 1240 mg Mg^{+2} /kg FSP water. Table 5.4.12 shows the necessary concentration of anionic species for precipitation to occur. The precipitates of calcium carbonate, calcium oxalate, calcium phosphate, and magnesium hydroxide seem probable.

	K_{sp}^a	Anion, mol / kg FSP water
calcium carbonate, CaCO_3	4.96E-09	6.41E-07
calcium fluoride, CaF_2	1.46E-10	1.37E-04
calcium hydroxide, Ca(OH)_2	4.68E-06	2.46E-02
calcium iodate, $\text{Ca(IO}_3)_2$	6.47E-06	2.89E-02
calcium iodate 6-hydrate, $\text{Ca(IO}_3)_3 \cdot 6\text{H}_2\text{O}$	7.54E-07	4.60E-02
calcium oxalate 1-hydrate, $\text{CaC}_2\text{O}_4 \cdot \text{H}_2\text{O}$	2.34E-09	3.03E-07
calcium phosphate, $\text{Ca}_3(\text{PO}_4)_2$	2.07E-33	6.69E-14
calcium sulfate, CaSO_4	7.10E-05	9.18E-03
	K_{sp}^b	Anion, mol/ kg FSP water
magnesium carbonate, MgCO_3	6.82E-06	1.34E-04
magnesium carbonate 3-hydrate, $\text{MgCO}_3 \cdot 3\text{H}_2\text{O}$	2.38E-06	4.67E-05
magnesium carbonate 5-hydrate, $\text{MgCO}_3 \cdot 5\text{H}_2\text{O}$	3.79E-06	7.43E-05
magnesium fluoride, MgF_2	7.42E-11	3.81E-05
magnesium hydroxide, Mg(OH)_2	5.61E-12	1.05E-05

Table 5.4.12: Common precipitates of calcium and magnesium. The concentration of anion necessary to cause precipitation is calculated assuming ideal solution behaviour.

Note a: Calcium concentration is 310 mg/kg FSP water or 0.00774 mol/kg FSP water.

Note b: Magnesium concentration is 1240 mg/kg FSP water or 0.0510 mol/kg FSP water.

An advantage of the 1L vessel experiments is that no negative values are obtained on back calculation, which can be a problem when only the filtrate is analyzed. As far as the trends in the

data are concerned, both experimental methods are very similar. The data in Table 5.4.7 is compared to the data in Table 5.4.10 in Figure 5.4.10. This displays the difference caused by ignoring analysis of the fibre mat and using back calculation to obtain concentrations in the fibre phase. There is significant scatter in the data, but the theme in both sets of data is of steady increase as the pH increases. It is difficult to say if one method is superior in obtaining good partitioning data.

5.4.4 Elevated Magnesium Content Experiments in 1L Vessel: EDTA / EGTA analysis

Two vessel volumes were used in experiments, 150mL and 1L. The effect of volume can be examined by comparing Tables 5.4.13 and 5.4.14 (1L vessel) to Tables 5.4.4 and 5.4.5 (150mL vessel), presented previously. Both data sets use EGTA/EDTA to analyze the external solution concentrations of calcium and magnesium. Results for calcium from Tables 5.4.13 are also shown in Figure 5.4.10. The data lie in the same band as data obtained by other methods, indicating the size of the vessel does not significantly effect the quality of the data.

pH	mg Ca / kg external solution		mg Ca / kg od fibre		mg Ca / kg FSP water	
3.15	28.8	(0.07)	-71.0	(9.6)	-60.2	(8.2)
3.17	28.6	(0.58)	-37.1	(57.2)	-31.4	(48.5)
6.17	26.2	(0.35)	48.4	(36.9)	37.1	(28.3)
9.64	24.4	(0.23)	485	(21.8)	347	(16.5)
10.53	15.6	(0.23)	1152	(23.2)	818	(20.2)
11.93	10.7	(0.19)	1624	(17.9)	1141	(20.7)
12.75	13.6	(0.74)	1367	(68.6)	958	(50.0)

Table 5.4.13: Calcium Partitioning in 1L vessel with high Mg. EDTA and EGTA used to analyze external solution concentration. Standard errors are given in brackets. Data determined in triplicate.

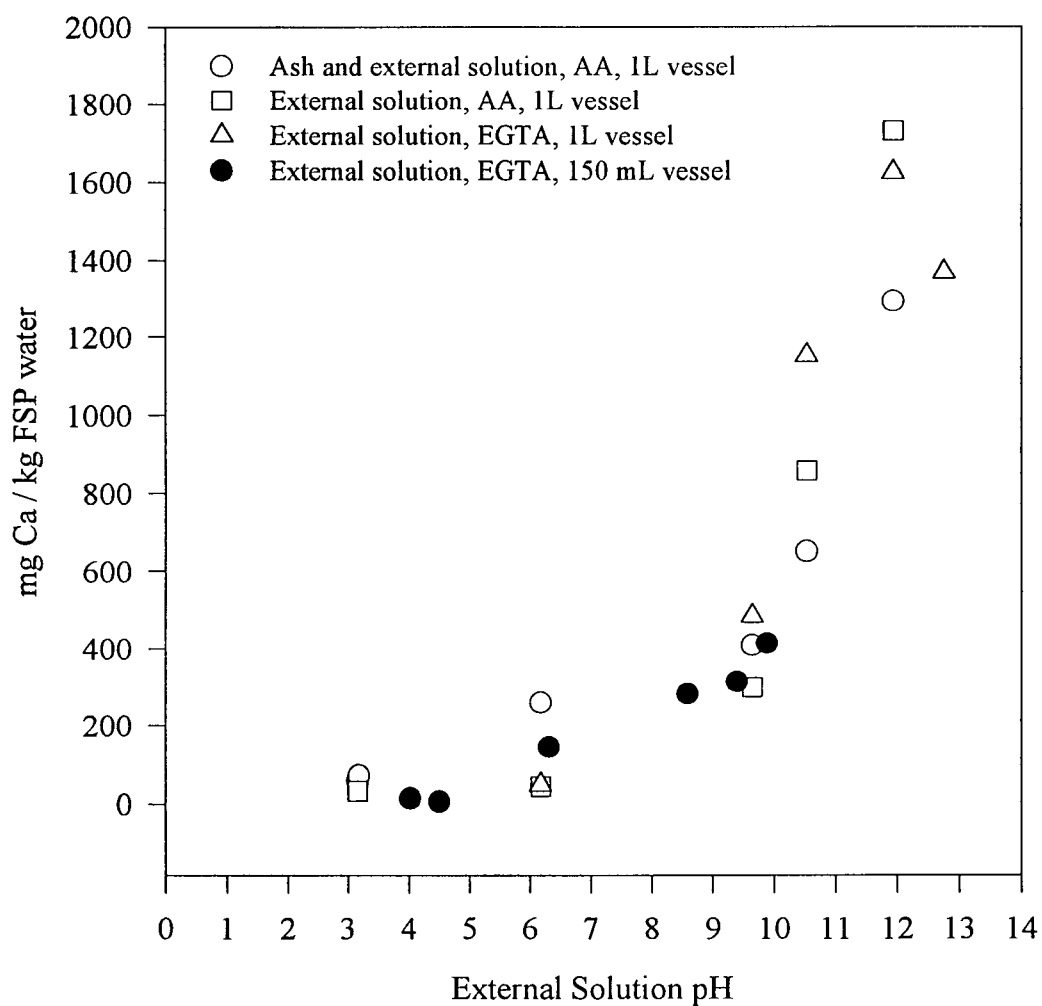


Figure 5.4.10: Comparison of calcium contents within the fibres for elevated magnesium equilibrium experiments. Data plotted for different vessel volumes and metal ion analysis methods.

pH	mg Mg / kg external solution		mg Mg / kg od fibre		mg Mg / kg FSP water	
3.15	126.7	(1.00)	-1620	(93.0)	-1370	(79.0)
3.17	129.9	(1.79)	-1800	(153.4)	-1530	(134.8)
6.17	118.3	(4.23)	-1170	(388.1)	-890	(297.5)
9.64	117.4	(1.21)	-610	(104.6)	-440	(76.7)
10.53	9.6	(2.18)	9520	(134.8)	6760	(130.1)

Table 5.4.14: Magnesium Partitioning in 1L vessel with high Mg. EDTA and EGTA used to analyze external solution concentrations. Standard errors are given in brackets. Data determined in triplicate.

5.5 Sensitivity to Model Parameters

Calcium activity coefficients over a range of pHs are shown in Figure 3.3.1. The curves show that the fibre system is far from ideal as the activity coefficients in the fibre and in solution deviate a great deal from one. Using Pitzer's method to determine the activity coefficients is a worthwhile endeavour because suspensions of fibres in electrolyte solutions are far from ideal systems. The fibre phase has activity coefficients that are furthest from one, especially at very low and high values of pH. Activity coefficient predictions lie above the ideal predictions and, in some cases, provide much better prediction of the concentrations within the fibres (see Figure 5.4.4).

Figure 5.5.1 demonstrates the importance of the dissociation constant, K_a' , of the fibre charged groups (assuming a single dissociation constant can be used). It dramatically changes the pH at which the ions begin to strongly partition between the fibres and solution. Larger values of K_a' cause ions to partition more strongly at a lower pH ($pK_a' = -\log K_a'$). The shape of the rising portion of the curve is the same in all cases, and the value of K_a' has no effect on the point at

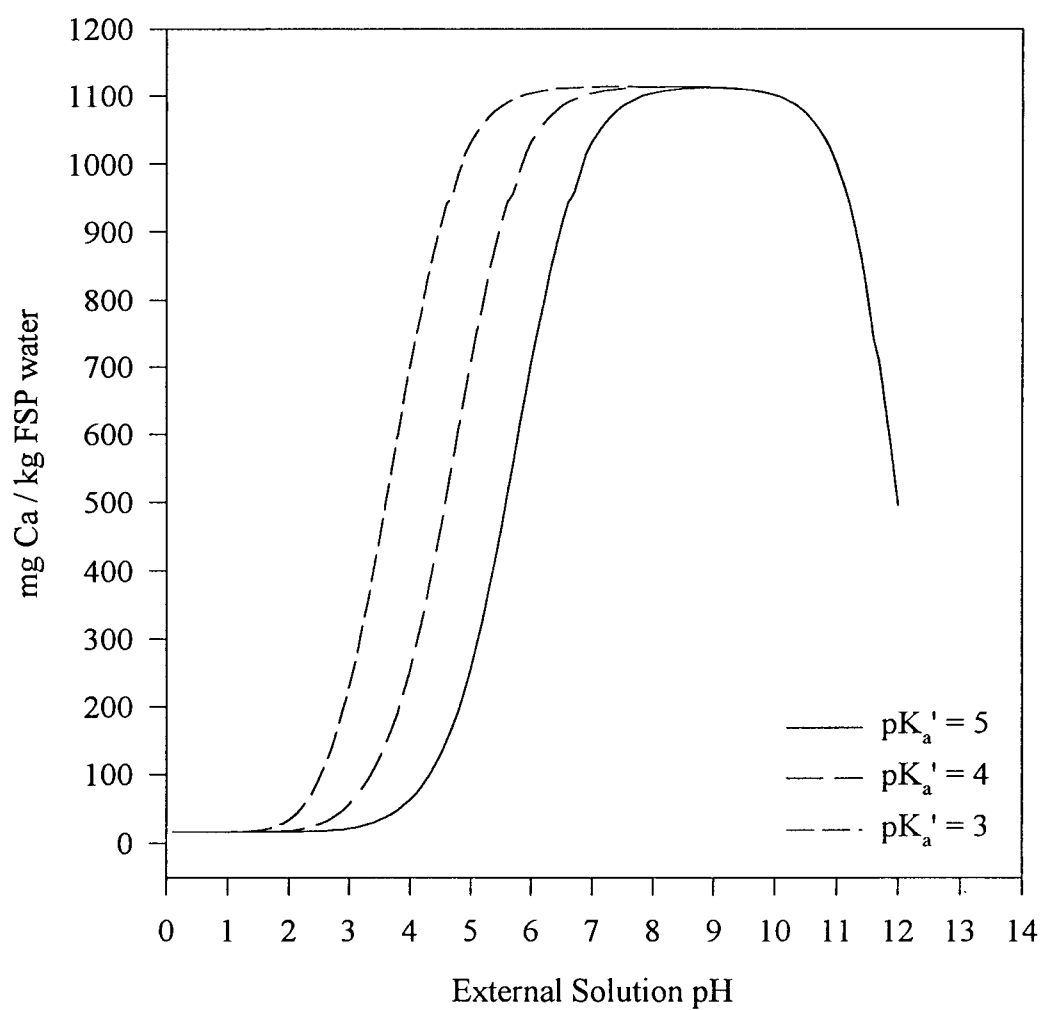


Figure 5.5.1: Dissociation constant effect on partitioning predictions.

which soluble calcium is driven from the fibres (above a pH of 10). The dissociation constant determines under what conditions the charged groups will dissociate, but not the total charge on the fibre. At pHs above 10, all charged groups on the fibres are ionized and the dissociation constant of those groups is un-needed in determining the partitioning behaviour.

Figure 5.5.2 shows the difference between the non-ideal and ideal predictions of NPE partitioning obtained with the exact charge model. The difference is the same as between the non-ideal and ideal 2-K models. The non-ideal model predicts higher concentrations within the fibres at a given pH. Experimental data for calcium makes it clear there is significant value in considering the system as non-ideal at pHs above 7. There is much closer agreement between the experimental data and the non-ideal model than the data and the ideal model. Pitzer's models appears to work well within the fibres, even though the fibre phase contains many charged groups that alter the nature of the electrostatic interactions between ions.

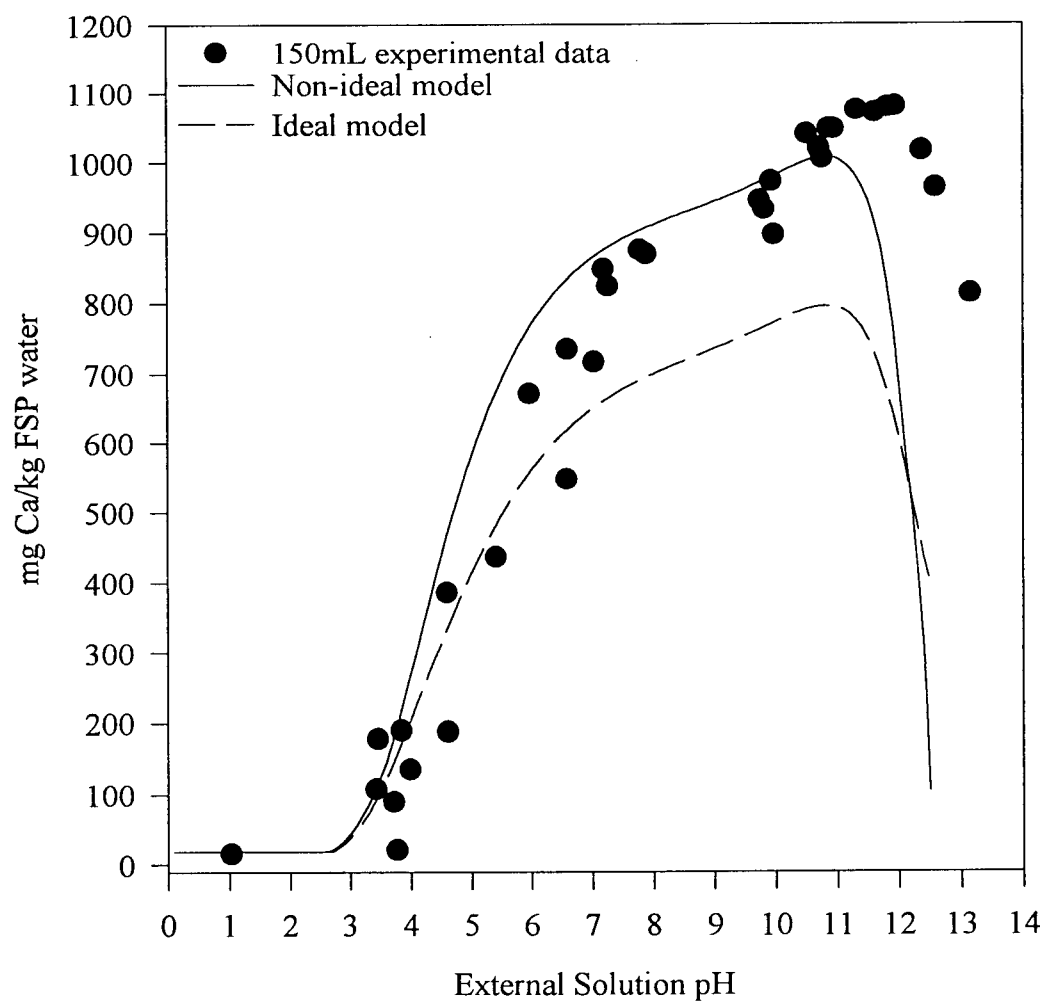


Figure 5.5.2: Non-ideal and ideal predictions by the exact charge model.

Chapter 6

6. Summary, Conclusions, and Recommendations

A thermodynamics based model to predict the partitioning of NPEs between kraft fibres and water in a pulp suspension was developed. It is based on the Donnan equilibrium framework. The non-ideality of the phases is taken into account by introducing activity coefficients. Comparing the proposed partitioning model (with a single dissociation constant) to the experimental results of Bryant and Edwards (1996) shows that very good agreement is possible. Bryant and Edwards used softwood pulp obtained after the second post oxygen washer. Oxygen delignification reduces the lignin within the fibres so that a definite plateau occurs in the data at pHs above 7 (see Figure 5.2.2) due to the lack of charged groups dissociating at the higher pHs. This means that the partitioning is governed by ionic equilibrium only.

Experimental results obtained for post-brown stock fibres show different partitioning behaviour at pHs above 7. Cations continue to be drawn from the external solution into the internal solution of the fibres as the pH rises above 7. The partitioning data for calcium and magnesium give curves that rise continuously from a pH of 3 to 11. This behaviour is due to the polyfunctionality of the post brown stock kraft fibres. The various configurations of the carboxylic and phenolic groups on the fibres yield complex de-protonation behaviour which would require a spectrum of K_a s to model adequately.

Three basic properties of the kraft pulp fibres were obtained by independent experiments; the total charge on the fibres, Q_{X1} and Q_{X2} , the dissociation constants, K_{a1}' and K_{a2}' , and the mass of water within the fibres, F . Inclusion of fibre saturation point (F) as a function of pH improves

the accuracy of the model by giving more precise molalities for use in the equilibrium and activity coefficient relationships. The quantity of total charge on the fibres and the dissociation constant of those charged groups are critical parameters in the model. Using two dissociation constants does not adequately model the dissociating behaviour of the fibres, so an exact charge model, developed from the potentiometric titration of a pulp sample, has also been employed. It models the fibres as highly polyfunctional species by fitting a cubic equation to the experimental data and provides good NPE partitioning predictions from a pH of 2 - 13. This indicating again that electrostatics are the dominant mechanism of NPE partitioning and Donnan equilibrium is a good framework in which to consider the partitioning phenomena.

At a pH of 12, both the partitioning model and calcium experimental data show a decreasing concentration of calcium is expected within the fibres as the concentration of sodium in the system becomes large. In the region above a pH of 7 the proposed 2-K model under-predicts experimental results. Two possible explanations for this behaviour are precipitation within the fibres or the need for more dissociation constants to be used in modeling the fixed anionic charges in the fibres. From the predictions of the exact charge model it is clear that precipitation is not significant at the concentrations of NPEs present in post brown stock washer kraft pulp.

Experiments with elevated magnesium levels give very different experimental results. At pHs above 10, precipitation appears to dominate the equilibrium, resulting in very dramatic rises in the fibre concentrations of both calcium and magnesium. This behaviour was expected due to the larger amounts of the divalent cations bringing the partitioning system closer to (and beyond) the conditions necessary for precipitation. Solubility products for various calcium and

magnesium precipitates indicate that calcium carbonates, oxalates, phosphates, and magnesium hydroxides are likely the precipitated materials.

Experimental data obtained for magnesium consistently displayed large errors, making it difficult to compare with the predicted partitioning curves. Large errors are due to the low concentrations of magnesium in the external solution at all pHs, and the use of EDTA and EGTA titration to determine the quantity of magnesium and calcium in the system. Magnesium contents are determined by the difference in the moles of EDTA and EGTA needed to titrate a sample, thus the errors in each titration add giving a final value with significant error. The data of calcium contained much less error and scatter and verifies that the back-calculation method used to determine the quantities of NPEs in the fibres is a useful tool for quickly determining the partitioning behaviour.

6.1 Conclusions

- Incorporating activity coefficients into the partitioning model is a worthwhile endeavor, as the predictions follow more closely the trends observed in the experimental data.
- Including only two dissociation constant, K_{a1}' and K_{a2}' , does not capture the functional behaviour of the post brown stock pulp used for experiments in this work. Using an exact charge distribution gives good prediction of the partitioning of calcium and magnesium, indicating that electrostatics are the dominant force in the equilibrium system.
- Model predictions are poor at pHs above 10 when elevated concentrations of calcium and magnesium are examined, likely due to chemical precipitation. In particular, precipitation of calcium carbonate and magnesium hydroxide is a possibility in the experiments conducted. The Donnan equilibrium model developed does not account for precipitation.
- Fibre properties and state (i.e. post oxygen or post brown stock) have a large effect on the type of partitioning data obtained.
- Obtaining reliable experimental data on NPE partitioning is a difficult task with systems of fibres in water. Ions present in low concentrations (such as magnesium) show large errors.
- The Donnan framework is effective in describing the partitioning of metal ions in a pulp suspension, assuming no chemical precipitation occurs.

6.2 Recommendations

- Obtain partitioning data for the "cleaner" fibres after bleaching stages (i.e. post oxygen or post chlorine dioxide).
- Investigate possible lab techniques to verify the formation of precipitates within the fibres.
- Develop fast, accurate methods for obtaining experimental data on NPE partitioning in the external and internal solutions of a pulp suspension.
- Obtain experimental partitioning information for other NPEs of interest. Important soluble ions not considered in this work are manganese (Mn^{+2}), potassium (K^{+}), and phosphorous (PO_4^{-3}). These ions are generally in the next highest concentrations behind sodium, calcium, and magnesium. Manganese is involved in the decomposition of bleaching chemicals and potassium participates in process equipment corrosion.

7. References

- Ampulski R.S., "The Equilibrium for the Na/Ca Ion-Exchange Reaction of Bleached Northern Softwood Kraft Pulp", *Nordic Pulp and Paper Research Journal*, 4(1), p. 38-42, 1989.
- Arnson T.R. and Stratton, R.A., "The Adsorption of Complex Aluminum Species by Cellulosic Fibers", *TAPPI Journal*, 66(12), p.72-75, 1983.
- Athanasopoulos, N., "Flame Methods Manual for Atomic Absorption", GMC Operators Manual, Australia, 1993.
- Barnes, F. and Reid, B., "Zero Effluent at Millar Western Pulp (Meadow Lake) Ltd. - Four Years Later", *Pacific Paper* '95, 104 - 108, Oct. 1995.
- Been, J. and Oloman, J.W., "Electical Conductivity of Pulp Suspensions Using Donnan Equilibrium Theory", *J. Pulp Paper Sci.* 21(3):80, 1995.
- Biermann, C.J., "Handbook of Pulping and Papermaking", Academic Press, USA, 1996.
- Bihani, B.G., "Goal of Closed-Cycle Operation hinges on Fiberline Developments", *Pulp and Paper*, p. 87-90, July 1996.
- Bryant P.S. and Edwards L.L., "Cation Exchange of Metals on Kraft Pulp", *Journal of Pulp and Paper Science*, Vol. 22, No. 1, p. J37-J42, 1996.
- Bryant, P.S., "Metals Management in the Fibreline", 1996 TAPPI Minimum Effluent Mills Symposium, p. 95-100, 1996.
- Butler, J.N., "Ionic Equilibrium A Mathematical Approach", Addison-Wesley Publishing Company, Inc., Reading, Massachusetts, 1964.
- Dence, C.W., "Chemistry of Chemical Pulp Bleaching", p. 125-159 in "Pulp Bleaching: Principles and Practice", Dence, C.W. and Reeve, D.W., Editors, TAPPI Press, Atlanta, 1996.
- Devore, J.L., "Probability and Statistics for Engineering and the Sciences", 3rd Ed., Brooks/Cole Publishing Company, Pacific Grove, California, 1991.
- Diniz J.M.B.F., "Application of Chemical Equilibrium to Wood Pulps", *Holzforschung*, Vol. 50, No. 5, p. 429-433, 1996.
- Donnan, F.G. and Harris, A.B., "The Osmotic Pressure and Conductivity of Aqueous Solutions of Congo-Red, and Reversible Membrane Equilibria", *J. Chem. Soc.*, 99:1554, 1911.
- Eisenberg, H., *Biological Macromolecules and Polyelectrolytes in Solution*, Clarendon Press, Scotland, 1976.

- Frederick, W.J., "Managing Non-process Elements Flows in Pulp-Mill Chemical Cycles", in "The Impact of Energy and Environmental Concerns on Chemical Engineering in the Forest Products Industry", H.N. Rosen, AIChE Symposium Series, 80(239), p. 21-29, 1984.
- Galloway, L., "Closed-cycle technologies for bleached kraft pulp mills", National Pulp Mills Research Program Technical Report No. 7, 1994.
- Gilbert, A., and Rapson, H., "Accumulation of potassium in a closed cycle mill", Pulp and Paper Canada, 81(2):T43., 1980.
- Gleadow, P., Hastings, C., Barynin, J., Schroderus, S., and Warnqvist, B., "Towards closed-cycle kraft: ECF versus TCF case studies", Pulp and Paper Canada, 98:4, p. T100-T110, 1997.
- Grignon, J. and Scallan, A.M., "Effect of pH and Neutral Salts upon the Swelling of Cellulose Gels", Journal of Applied Polymer Science, Vol. 25, p. 2829-2843, 1980.
- Guggenheim, E.A., "Thermodynamics", 6th Ed., North - Holland Publishing Company, New York, 1977.
- Guggenheim, J. Phys. Chem., 33, 842, 1929.
- Haglund, I.A.K., Kringstad, K.P., and Almin, K., "Donnan equilibria in pulping and bleaching; some considerations", Proceedings of the 1989 TAPPI Wood and Pulping Chemistry Conference, p. 635-640, 1989.
- Hardland, C.E., "Ion Exchange Theory and Practice", 2nd Ed., The Royal Society of Chemistry, Bath, GB, 1994.
- Harris, D.C., "Quantitative Chemical Analysis", W.H. Freeman and Company, 1991.
- Hatsopoulos, G.N. and Keenan, J.H., "Principles of General Thermodynamics", John Wiley & Sons Inc., New York, 1965.
- Helferich, F., "Ion Exchange", Dover Publications, Inc., New York, 1995.
- Jeffery, G.H., Bassett, J., Mendham, J., and Denney, R.C., "Vogel's Textbook of Quantitative Chemical Analysis", 5th Ed., John Wiley & Sons, Inc., New York, 1989.
- Katchalsky, A. and Curran, P.F., "Nonequilibrium Thermodynamics in Biophysics", Harvard University Press, Cambridge 1967.
- Katz, S., Beatson, R.P., and Scallan, A.M., "The determination of strong and weak acidic groups in sulfite pulps", svensk papperstidning, no. 6, p. R48-R53, 1984.

- Katz, S., Liebergott, N., and Scallan, A.M., "A mechanism for the alkali strengthening of mechanical pulps", TAPPI Journal, Vol. 64, No. 7, 1981.
- Keitaanniemi, O. and Virkola, N.E., "Undesirable elements in causticizing systems", TAPPI Journal, 65(7), p. 89-92, 1982.
- Lapierre, L., Bouchard, J., Berry, R.M., and Van Lierop, B., "Chelation Prior to Hydrogen Peroxide Bleaching of Kraft Pulps: An Overview", Journal of Pulp and Paper Science, Vol. 21, No. 8, p. J268-J273, 1995.
- Lide, D.R. (Editor), "CRC Handbook of Chemistry and Physics", 76th Ed., CRC Press, Boca Raton, 1995.
- Magnusson, H., Mork, K., and Warnqvist, B., "Non-process chemical elements in the kraft recovery system", Proceedings of the 1979 TAPPI Pulping Conference, p. 77-83, November 1979.
- Mandel, J., "The Statistical Analysis of Experimental Data", Dover Publications, Inc., New York, 1984.
- Marinsky, J.A. and Marcus, Y., "Ion Exchange and Solvent Extraction", Vol 1, Marcel Dekker, p. 237 - 334 1993.
- McDonough, T.J., "Oxygen Delignification", p. 213-239 in "Pulp Bleaching: Principles and Practice", Dence, C.W. and Reeve, D.W., Editors, TAPPI Press, Atlanta, 1996.
- Minor, J.L., "Production of Unbleached Pulp", p. 25-57 in "Pulp Bleaching: Principles and Practice", Dence, C.W. and Reeve, D.W., Editors, TAPPI Press, Atlanta, 1996.
- PAPRICAN, "Conductometric Titration", Experimental Method document, June 1988.
- PAPRICAN, "The Water Retention Value", Fibre Chemistry Section Method, 1979.
- Park, H., PhD Dossier, 1996.
- Pitzer K.S., "Thermodynamics of Electrolytes. 1. Theoretical Basis and General Equations" Journal of Physical Chemistry, 77(2), p. 268-277, 1973.
- Pitzer, K.S., "Activity Coefficients in Electrolyte Solutions", 2nd Ed., CRC Press, Boca Raton, FL, 1991.
- Rasanen, E. and Stenius, P., "The Sorption of Na^+ , Ca^{++} , Mg^{++} and Mn^{++} on cellulose fibres: prediction and analysis of sorption equilibrium with electrostatic models", Proceedings of the 9th International Symposium on Wood and Pulping Chemistry", p. 94-1 - 94-5, 1997.

- Reeve, D.W., Rowlandson, G., Kramer, J.D., and Rapson, W.H., "The closed-cycle bleached kraft pulp mill - 1978", TAPPI Journal, 62(8), p. 51-54, 1979.
- Ricketts, J.D., "Considerations for the closed-cycle mill", TAPPI Journal, Vol. 77, No.11, p. 43-49, 1994.
- Rosen A., "Adsorption of sodium ions on kraft pulp fibers during washing", TAPPI Journal, 58(9), p. 156-161, 1975.
- Scallan, A.M. and Carles, J.E., The correlation of water retention value with the fibre saturation point, Svensk Papperstidning 75, 17, p. 699 - 703, 1972.
- Scallan, A.M., Katz, S., and Argyropoulos, D.S., "The Conductometric Titration of Cellulosic Fibres" in "Cellulose and Wood", Schuerch, C., Ed., John Wiley & Sons, New York, p.1457, 1989.
- Scallan, A.M. and Tigerstrom, A.C., "Swelling and Elasticity of the Cell Walls of Pulp Fibres", Journal of Pulp and Paper Science, Vol. 18, No. 5, p. J188-J192, 1992.
- Skoog, D.A., Leary, J.J., "Principles of Instrumental Analysis", 4th Ed., Saunders College Publishing, New York, 1992.
- Smook, G.A., "Handbook for Pulp and Paper Technologists", 2nd Ed., Angus Wilde Publications, Vancouver, 1994.
- Stumm, W. and Morgan, J.J., "Aquatic Chemistry: Chemical Equilibria and Rates in Natural Waters", 3rd Ed., John Wiley & Sons, Inc., New York, 1996.
- Tanford, C., Physical Chemistry of Macromolecules, John Wiley and Sons, New York, 1961.
- Technical Association of the Pulp and Paper Industry (TAPPI) Useful Methods, UM 256, p. 54-56, 1991.
- Tiemann, H.D., Bull No. 70, U.S. Dept. Agr. Forest Serv., 1906
- Tombs, M.P. and Peacocke, A.R., "The Osmotic Pressure of Biological Macromolecules", Oxford University Press, Belfast 1974.
- Towers M. and Scallan A.S., "Predicting the Ion-Exchange of Kraft Pulps Using Donnan Theory", Journal of Pulp and Paper Science, Vol. 22, No. 9, p. J332-J337, 1996.
- Towers, M., "System Closure in Bleached Kraft Mills", Course Notes, 1997.
- Tran, H.N., "How does a kraft recovery boiler become plugged?", Tappi Journal, p.102-106, November, 1986.

Ulmgren, P., "Consequences of Build-up of Non-process Chemical Elements in Closed Kraft Recovery Cycles - Aluminosilicates Scaling, a Chemical Model", Journal of Pulp and Paper Science, 8(2), TR27 - TR32, 1982.

Ulmgren, P., "Non-process elements in a bleached kraft pulp mill with increased system closure" 1996 TAPPI Minimum Effluent Mills Symposium, 17-26, 1996.

Whitten, K.W., Gailey, K.D., and Davis, R.E., "General Chemistry", 3rd Ed., Saunders College Publishing, New York, p 740, 1988.

Zemaitis, J.F. et al., "Handbook of Aqueous Electrolyte Thermodynamics", American Institute of Chemical Engineers, New York 1986.

Appendix A: Titration data for kraft pulp fibres

This section contains the experimental data obtained through potentiometric and conductometric titrations of fibres. The data in Table A.1 is plotted in Figure 5.1.5.

Time	ml NaOH added to sample	Conductance, mS/cm
1:45	0	141.6
1:50	0.2	134.4
1:55	0.4	129.1
2:00	0.6	126.8
2:05	0.8	126
2:10	1	126.3
2:15	1.2	126.8
2:20	1.4	128.7
2:25	1.6	132.3
2:30	1.8	139.3
2:35	2	147.4
2:40	2.2	155.6
2:45	2.4	165.3
2:50	2.8	183.1
2:55	3.2	202
3:00	3.6	221
3:05	4	239

Table A 1: Conductometric titration results for kraft pulp fibres without the addition of a strong acid.

mL NaOH	pH	mL NaOH	pH	mL NaOH	pH	mL NaOH	pH
0	2.035	3.465	2.398	6.495	4.271	6.945	8.651
0.005	2.035	3.565	2.412	6.510	4.324	6.955	8.778
0.01	2.036	3.665	2.429	6.530	4.418	6.965	8.902
0.015	2.038	3.765	2.446	6.540	4.458	6.975	9.018
0.025	2.038	3.865	2.465	6.560	4.551	6.985	9.122
0.045	2.040	3.965	2.484	6.570	4.608	6.995	9.219
0.085	2.043	4.065	2.503	6.580	4.665	7.005	9.300
0.165	2.050	4.165	2.524	6.590	4.719	7.015	9.378
0.265	2.057	4.265	2.547	6.605	4.817	7.025	9.450
0.365	2.064	4.365	2.567	6.615	4.885	7.035	9.520
0.465	2.073	4.465	2.592	6.625	4.954	7.045	9.585
0.565	2.080	4.565	2.618	6.635	5.015	7.055	9.644
0.665	2.087	4.665	2.644	6.650	5.136	7.070	9.729
0.765	2.095	4.765	2.671	6.660	5.187	7.080	9.776
0.865	2.102	4.865	2.701	6.680	5.362	7.100	9.871
0.965	2.113	4.965	2.732	6.690	5.449	7.110	9.912
1.065	2.121	5.065	2.765	6.700	5.552	7.130	9.993
1.165	2.130	5.165	2.801	6.710	5.627	7.145	10.044
1.265	2.137	5.265	2.839	6.725	5.788	7.170	10.127
1.365	2.147	5.365	2.880	6.735	5.876	7.190	10.184
1.465	2.156	5.465	2.931	6.745	5.967	7.220	10.265
1.565	2.166	5.565	2.984	6.755	5.964	7.245	10.326
1.665	2.177	5.665	3.041	6.765	6.173	7.275	10.388
1.765	2.185	5.765	3.109	6.775	6.287	7.315	10.462
1.865	2.196	5.855	3.178	6.785	6.417	7.355	10.528
1.965	2.206	5.935	3.247	6.795	6.524	7.405	10.600
2.065	2.216	6.005	3.313	6.805	6.652	7.455	10.663
2.165	2.228	6.070	3.384	6.815	6.791	7.520	10.734
2.265	2.241	6.125	3.451	6.825	6.912	7.590	10.801
2.365	2.251	6.175	3.520	6.835	7.066	7.675	10.872
2.465	2.261	6.220	3.588	6.845	7.216	7.770	10.941
2.565	2.273	6.265	3.669	6.855	7.361	7.870	11.005
2.665	2.287	6.290	3.711	6.865	7.501	7.970	11.059
2.765	2.298	6.335	3.806	6.875	7.652	8.070	11.109
2.865	2.311	6.355	3.849	6.885	7.807	8.170	11.152
2.965	2.325	6.385	3.923	6.895	7.961	8.270	11.192
3.065	2.339	6.410	3.986	6.905	8.101	8.370	11.230
3.165	2.353	6.440	4.074	6.915	8.268	8.470	11.265
3.265	2.369	6.455	4.124	6.925	8.397		
3.365	2.382	6.475	4.193	6.935	8.532		

Table A 2: Potentiometric titration results. The data in Table A.2 is plotted in Figure 5.1.1.

Appendix B: Pitzer's Equations

Pitzer's model was developed to provide improved solution property estimation compared to Debye-Huckel theory. Debye-Huckel theory ignores the kinetic effect of the hard cores of ions on electrolyte solution properties. Pitzer proposes that a more accurate model of electrolyte solutions will contain an electrostatic term plus a virial coefficient series. The virial coefficients can be functions of the ionic strength of the solution.

The excess Gibbs energy for a solution can be expressed in terms of molalities as:

$$\frac{G^{ex}}{w_w RT} = f(I) + \sum_i \sum_j m_i m_j \lambda_{ij}(I) + \sum_i \sum_j \sum_k m_i m_j m_k \mu_{ijk} + \dots \quad (\text{B-1})$$

where: w_w is the number of kilograms of solvent

m_i, m_j, m_k, \dots are the molalities of all solutes

I is the ionic strength given by $I = \frac{1}{2} \sum_i m_i z_i^2$ where the summation is taken over all solute species i .

z_i is the charge number of the i^{th} solute

The first term of equation (B-1) contains the Debye-Huckel limiting law and is a function of ionic strength, temperature, and solvent properties but not on individual solute molalities. The second term accounts for short range interactions between solutes i and j . The third term accounts for triple interactions between ions. It is worth noting here that while the form of the equations Pitzer's adopts are based in thermodynamics, the virial coefficients for all species are determined empirically.

The differentiation of $(G^{ex}/w_w RT)$ gives the activity coefficient for ion i .

$$\ln \gamma_i = \left[\frac{1}{w_w RT} \frac{\partial G^{ex}}{\partial m_i} \right]_{n_w} \quad (\text{B-2})$$

$$\ln \gamma_i = \left(\frac{z_i^2}{2} \right) f' + 2 \sum_j m_j \lambda_{ij} + \left(\frac{z_i^2}{2} \right) \sum_j \sum_k m_j m_k \lambda'_{jk} + 3 \sum_j \sum_k m_j m_k \mu_{ijk} + \dots \quad (\text{B-3})$$

In equations (B-2) and (B-3), f' and λ' represent the ionic strength derivatives of f and λ . The actual working form of Pitzer's equations are modified forms of equation (B-3) to account for electroneutrality in solution. To make summations simpler to understand, "a" is used to represent the summation over all anion species and "c" indicates the summation should be made over all cation species.

For mixed electrolyte solutions the activity coefficients of the cation M and the anion X are:

$$\ln \gamma_M = z_M^2 F + \sum_a m_a (2B_{Ma} + Z C_{Ma}) + \sum_c m_c \left(2\Phi_{Mc} + \sum_a m_a \psi_{Mca} \right) + \sum_a \sum_{a'} m_a m_{a'} \psi_{Maa'} + z_M \sum_c \sum_a m_c m_a C_{ca} + 2 \sum_n m_n \lambda_{nM} + \dots \quad (\text{B-4})$$

$$\ln \gamma_X = z_X^2 F + \sum_c m_c (2B_{cX} + Z C_{cX}) + \sum_a m_a \left(2\Phi_{Xa} + \sum_c m_c \psi_{cXa} \right) + \sum_c \sum_{c'} m_c m_{c'} \psi_{cc'X} + |z_X| \sum_c \sum_a m_c m_a C_{ca} + 2 \sum_n m_n \lambda_{nM} + \dots \quad (\text{B-5})$$

where: z_M and z_X are the charges on the cation and anion species
 m_i is the molality of species i , mol/kg solvent

The F in the first term of equations (B-4) and (B-5) is an extended Debye-Huckel term given by:

$$F = f' + \sum_c \sum_a m_c m_a B'_{ca} + \sum_c \sum_{c'} m_c m_{c'} \Phi'_{cc'} + \sum_a \sum_{a'} m_a m_{a'} \Phi'_{aa'} \quad (\text{B-6})$$

$$f' = -A_\phi \left[\frac{I^{1/2}}{(1+bI^{1/2})} + \frac{2}{b} \ln(1+bI^{1/2}) \right] \quad (\text{B-7})$$

where: Φ' is the ionic strength derivative of Φ

I is the ionic strength of the solution given by:

$$I = \frac{1}{2} \sum_i m_i z_i^2 \quad (\text{B-8})$$

A_ϕ is the Debye-Huckel osmotic coefficient given by:

$$A_\phi = \frac{1}{3} \left(\frac{2\pi N_o d_w}{1000} \right)^{1/2} \left(\frac{e^2}{\epsilon k T} \right)^{3/2} \quad (\text{B-9})$$

N_o is Avagadro's number

d_w is the density of the solvent

e is the charge on an electron

k is Boltzmann's constant

T is the absolute temperature of the system

ϵ is the dielectric constant of the solvent

b is a universal parameter with the value of $1.2 \text{ (kg.mol)}^{1/2}$

The relationships for B and B' used in equations (B-4), (B-5), and (B-6) are:

$$B_{MX} = \beta_{MX}^{(0)} + \beta_{MX}^{(1)} g(\alpha_1 I^{1/2}) + \beta_{MX}^{(2)} g(\alpha_2 I^{1/2}) \quad (\text{B-10})$$

$$g(x) = \frac{2[1 - (1+x)\exp(-x)]}{x^2} \quad (\text{B-11})$$

$$B'_{MX} = \frac{[\beta_{MX}^{(1)} g'(\alpha_1 I^{1/2}) + \beta_{MX}^{(2)} g'(\alpha_2 I^{1/2})]}{I} \quad (\text{B-12})$$

$$g'(x) = \frac{-2[1 - (1 + x + x^2/2)\exp(-x)]}{x^2} \quad (\text{B-13})$$

where: $\beta_{MX}^{(0)}$ is a tabulated parameter specific to the salt MX
 $\beta_{MX}^{(1)}$ is a tabulated parameter specific to the salt MX
 $\beta_{MX}^{(2)}$ is a parameter to account for the ion pairing effect of 2-2 salts
 $g(x)$ and $g'(x)$ are functions accounting for the ionic strength dependence of B_{MX} and B'_{MX}

For best fit with experimental data the two alpha parameters are given the value:

$$\alpha_1 = 1.4$$

$$\alpha_2 = 12$$

The parameter C_{MX} is determined by the tabulated parameter C^ϕ in the equation:

$$C_{MX} = \frac{C^\phi}{2|z_M z_X|^{1/2}} \quad (\text{B-14})$$

The effects of unsymmetrical mixing (interaction of ions of different charge) are accounted for by the parameters Φ and Φ' . These values are generally expected to be small since they account for the short range interaction of like charged ions. The relationships are:

$$\Phi_{ij} = \theta_{ij} + {}^E\theta_{ij}(I) \quad (\text{B-15})$$

$$\Phi'_{ij} = {}^E\theta'_{ij}(I) \quad (\text{B-16})$$

where: ${}^E\theta_{ij}(I)$ and ${}^E\theta'_{ij}(I)$ depend on the charges of the ions i and j , the total ionic strength, and solvent properties

θ_{ij} is a tabulated parameter specific to the salt ij

Pitzer's parameters ($\beta_{MX}^0, \beta_{MX}^1, \beta_{MX}^2, C^\phi$, and θ_{ij}) needed to determine the activity coefficients for the system of Na^+ , Ca^{+2} , Mg^{+2} , H^+ , OH^- and Cl^- are mostly available in the literature. The values of calcium hydroxide and magnesium hydroxide were not obtained, just as the θ_{ij} parameters were not available for manganese.

Appendix C: Unknowns and Equations of Gibbs-Donnan Equilibrium

List of Unknowns

Basically it is the molalities of all species in each phase and the Donnan partitioning ratio (distribution coefficient) that are unknown. The 15 parameters used to solve the system are listed below, including the pH of the external solution which is also used in solution of the equations.

$$m_{Na^+}^S, m_{Ca^{+2}}^S, m_{Mg^{+2}}^S, m_{H^+}^S, m_{Cl^-}^S, m_{OH^-}^S$$

$$m_{Na^+}^F, m_{Ca^{+2}}^F, m_{Mg^{+2}}^F, m_{H^+}^F, m_{Cl^-}^F, m_{OH^-}^F, m_{X^-}^F$$

λ , and pH^S , the pH in the external solution.

List of Equations and Solution Method

The first equation relates the external solution pH to the molality of H^+ in the external solution.

$$m_{H^+}^S = \frac{10^{-pH^S}}{\gamma_{H^+}^S} \quad (C-1)$$

Iteration is based on the distribution coefficient, λ , in the computer algorithm. The relations of Donnan equilibrium for each mobile ion are:

$$\lambda = \left(\frac{\gamma_{Na^+}^F m_{Na^+}^F}{\gamma_{Na^+}^S m_{Na^+}^S} \right) \quad (C-2)$$

$$\lambda^2 = \left(\frac{\gamma_{Ca^{+2}}^F m_{Ca^{+2}}^F}{\gamma_{Ca^{+2}}^S m_{Ca^{+2}}^S} \right) \quad (C-3)$$

$$\lambda^2 = \left(\frac{\gamma_{Mg^{+2}}^F m_{Mg^{+2}}^F}{\gamma_{Mg^{+2}}^S m_{Mg^{+2}}^S} \right) \quad (C-4)$$

$$\lambda = \left(\frac{\gamma_{H^+}^F m_{H^+}^F}{\gamma_{H^+}^S m_{H^+}^S} \right) \quad (C-5)$$

$$\lambda = \left(\frac{\gamma_{Cl^-}^S m_{Cl^-}^S}{\gamma_{Cl^-}^F m_{Cl^-}^F} \right) \quad (C-6)$$

$$\lambda = \left(\frac{\gamma_{OH^-}^S m_{OH^-}^S}{\gamma_{OH^-}^F m_{OH^-}^F} \right) \quad (C-7)$$

The dissociation constant of water relates the H^+ and OH^- molalities.

$$K_w = a_{H^+} a_{OH^-} = \gamma_{H^+} m_{H^+} \gamma_{OH^-} m_{OH^-}$$

This equation can be written for both phases, but equations (C-5) and (C-7) can be combined to give an equivalent relation. Thus, the dissociation of water is written for only one phase to avoid redundant equations.

$$K_w = \gamma_{H^+}^F m_{H^+}^F \gamma_{OH^-}^F m_{OH^-}^F \quad (C-8)$$

Electroneutrality gives two equations (one for each phase).

$$\sum_j z_j m_j^S = 0$$

$$m_{Na^+}^S + m_{H^+}^S + 2(m_{Ca^{+2}}^S + m_{Mg^{+2}}^S) - m_{OH^-}^S - m_{Cl^-}^S = 0 \quad (C-9)$$

$$\sum_k z_k m_k^F = 0$$

$$m_{Na^+}^F + m_{H^+}^F + 2(m_{Ca^{+2}}^F + m_{Mg^{+2}}^F) - m_{OH^-}^F - m_{Cl^-}^F - m_{X^-}^F = 0 \quad (C-10)$$

Dissociation of the (single) charged group on the fibres gives:

$$m_{X^-}^F = \frac{K_a (Q_X / F)}{m_{H^+}^F + K_a} \quad (C-11)$$

The remaining relations are the mass balances on ions. Beginning with calcium (Ca^{+2}).

$$C_{Ca^{+2}} = F m_{Ca^{+2}}^F + (V - F) m_{Ca^{+2}}^S$$

Rearranging equation (3) and substituting gives:

$$C_{Ca^{+2}} = F m_{Ca^{+2}}^F + (V - F) \left(\frac{\gamma_{Ca^{+2}}^F m_{Ca^{+2}}^F}{\gamma_{Ca^{+2}}^S \lambda^2} \right)$$

Finally solving in terms of the molality of calcium in the fibre, a valuable relationship is obtained.

$$m_{Ca^{+2}}^F = \frac{\lambda^2 C_{Ca^{+2}}}{F \lambda^2 + (V - F) \left(\frac{\gamma_{Ca^{+2}}^F}{\gamma_{Ca^{+2}}^S} \right)} \quad (C-12)$$

Similarly for magnesium:

$$C_{Mg^{+2}} = F m_{Mg^{+2}}^F + (V - F) m_{Mg^{+2}}^S$$

$$m_{Mg^{+2}}^F = \frac{\lambda^2 C_{Mg^{+2}}}{F \lambda^2 + (V - F) \left(\frac{\gamma_{Mg^{+2}}^F}{\gamma_{Mg^{+2}}^S} \right)} \quad (C-13)$$

Also for sodium a very similar relation exists. Since the ion is not divalent the distribution coefficient is not squared in this case.

$$C_{Na^+} = F m_{Na^+}^F + (V - F) m_{Na^+}^S$$

$$m_{Na^+}^F = \frac{\lambda C_{Na^+}}{F\lambda + (V-F)\left(\frac{\gamma_{Na^+}^F}{\gamma_{Na^+}^S}\right)} \quad (C-14)$$

Thus, if the total quantities of calcium, magnesium and sodium ($C_{Ca^{+2}}$, $C_{Mg^{+2}}$, and C_{Na^+} respectively) are known there are 14 unknowns (pH^S has been set) and 14 equations. The system of equations can be solved.

Basic Program Structure

- The pH in the external solution is set and equation (C-1) is used to determine the molality of hydrogen in the external solution.
- A "guess" of λ is given.
- The electroneutrality relations given in equation (C-9) and (C-10) are solved for the molality of chlorine and substituted into equation (C-6).
- Equations (C-5), (C-7), and (C-8) are used to determine the hydrogen and hydroxide ions in both phases.
- Equation (C-11) is solved with the known molality of hydrogen in the fibre phase.

The Donnan relations (equations (C-2), (C-3), and (C-4)) are used along with the mass balance relations (equations (C-12), (C-13), and (C-14)) to express the problem completely in terms of known quantities and λ .

Appendix D: Errors propagation in calculations

General Equations

The variance estimate of a population, $V(x)$, is:

$$V(x) = s^2 = \frac{\sum_i (x_i - \bar{x})^2}{N - 1} \quad (D-1)$$

where: s is the sample estimate of the standard deviation

x_i is known quantity i of the sample

\bar{x} is the average of the sample

N is the size of the sample

The coefficient of variation of x , CV_x , is:

$$CV_x = \frac{s}{\bar{x}} \quad (D-2)$$

The confidence interval of the mean of the population, μ , is given by:

$$\bar{x} - t \frac{s}{\sqrt{N}} < \mu < \bar{x} + t \frac{s}{\sqrt{N}} \quad (D-3)$$

where: t is the value of Student's t distribution for the given confidence interval and degrees of freedom. For three data points and a 95% confidence interval, the value is 4.303 (Mandel, 1984).

Two formulas describe the propagation of errors for statistically independent variables. When values are added or subtracted, such as:

$$u = a x + b y + c z + \dots \quad (D-4)$$

where: x , y , and z are statistically independent variables

a , b , and c are constants

the variance of u is related to the variances of x , y , and z by:

$$V(u) = a^2 V(x) + b^2 V(y) + c^2 V(z) + \dots \quad (D-5)$$

For multiplication or division the law of propagation of errors depends on the coefficient of variation of the variables.

$$u = \frac{x y z \dots}{p q r \dots} \quad (D-6)$$

$$(CV_u)^2 = (CV_x)^2 + (CV_y)^2 + (CV_z)^2 + \dots \\ + (CV_p)^2 + (CV_q)^2 + (CV_r)^2 + \dots \quad (D-7)$$

Errors in Metal Ion Concentration Results

For experiments performed with the 150mL vessels, the following values are measured:

- mass moist pulp
- mass salt solution

- mass NaOH or HCl for pH change
- mass H₂O added to bring to 1% consistency
- pH
- mass oven dry (od) fibre
- mmol EDTA/g sample (determined in triplicate)
- mmol EGTA/g sample (determined in triplicate)\

From the pH, the fibre saturation point (FSP) can be determined, using the quadratic relationship obtained by curve fitting. From these values the total water, water that is external solution, and mmol of Ca, Mg, and Na can be determined. It is easiest to see the method of calculation and error propagation using an example. The data at a pH of 7.26 are:

mass moist pulp = 2.8254 g, s = 0.03 g

mass salt solution = 1.4763 g, s = 0.007 g

mass NaOH solution = 1.8954 g, s = 0.009 g

total mass of system = 100.0283 g, s = 0.30 g

FSP = 1.339 g water/g od fibre, s = 0.035 g/g. This s is the estimate of the standard deviation, obtained from the sum of the squared residuals for the quadratic curve.

mass od fibre = 1.0350 g, s = 0.006 g

The values obtained by photometric titration with EGTA are:

1.81×10^{-4} mmol EGTA/g sample

1.95×10^{-4} mmol EGTA/g sample

1.85×10^{-4} mmol EGTA/g sample

The values for EDTA titration are:

2.87×10^{-4} mmol EDTA/g sample

2.81×10^{-4} mmol EDTA/g sample

2.82×10^{-4} mmol EDTA/g sample

The concentration of calcium in the external solution can be calculated directly from the results of EGTA titration, since EGTA binds calcium, but not magnesium. The values are converted to mg calcium/kg external solution by multiplying by the molar mass. For the first value, this is:

$$1.81 \times 10^{-4} \frac{\text{mmol EGTA}}{\text{g sample}} \left(\frac{40.08 \text{ mg}}{\text{mmol}} \right) \left(\frac{1000 \text{ g}}{\text{kg}} \right) = 7.25 \frac{\text{mg Ca}^{+2}}{\text{kg external solution}}$$

The same calculation for the next two values gives 7.82 and 7.41 mg Ca⁺²/kg external solution. The average of these values is 7.49 and using equation (D-1) gives a standard deviation of 0.29. Equation (D-3) gives the 95% confidence interval of the mean between 6.76 and 8.22 mg Ca⁺²/kg external solution.

It is more complicated to obtain the concentration of magnesium in the external solution because this depends on both the EGTA and EDTA titrations. Unlike EGTA, EDTA binds all divalent cations. In the simple systems considered here that means calcium and magnesium will be bound. Magnesium contents in the external solution can be obtained by:

$$\frac{\text{mmol Mg}}{\text{g filtrate}} = \frac{\text{mmol Ca \& Mg}}{\text{g filtrate}} - \frac{\text{mmol Ca}}{\text{g filtrate}} \quad (\text{D-8})$$

For the first value of EDTA titration, the amount of magnesium in the external solution is:

$$\frac{2.87 \times 10^{-4} \text{ mmol Ca \& Mg}}{\text{g solution}} - \frac{7.49 \text{ mg Ca}}{\text{kg solution}} \left(\frac{\text{mmol}}{40.08 \text{ mg}} \right) \left(\frac{\text{kg}}{1000 \text{ g}} \right) = \frac{1.00 \times 10^{-4} \text{ mmol Mg}}{\text{g solution}}$$

$$\frac{1.00 \times 10^{-4} \text{ mmol Mg}}{\text{g solution}} \left(\frac{24.312 \text{ mg}}{\text{mmol}} \right) \left(\frac{1000 \text{ g}}{\text{kg}} \right) = 2.43 \frac{\text{mg Mg}}{\text{kg external solution}}$$

The same calculation for the other two values of EDTA titration gives 2.29 and 2.31 mg Mg/kg external solution respectively. The average of the three values is 2.34 mg Mg⁺²/kg external solution with a standard deviation of 0.076. The 95% confidence interval is 2.15 to 2.53 mg Mg⁺²/kg external solution.

The amount of metal ions (Ca, Mg, or Na) in the fibres can be obtained from the total ions in the system and the mass of the external solution. In equation form this is:

$$\text{mg ion in fibres} = \text{mg ion total} - \text{mg ion in external solution} \quad (\text{D-9})$$

The total amount of ions added to the system is determined from amount of salt solution added to the 150mL vessel and the concentration of that solution. It is assumed here that the concentration of the salt solution is known exactly. The amount of calcium is 0.031643 mmol/g salt solution and the amount of magnesium is 0.009308 mmol/g salt solution. The total mg of calcium in the 150mL vessel is:

$$1.4763 \text{ g} \left(\frac{0.031643 \text{ mmol Ca}}{\text{g salt solution}} \right) \left(\frac{40.08 \text{ mg}}{\text{mmol}} \right) = 1.872 \text{ mg Ca}^{+2}$$

The covariance of the total Ca⁺² in the system is the same as the covariance of the mass of salt solution, since the concentration of the solution is assumed to have zero variance.

$$(\text{CV}^{\text{total}})^2 = (\text{CV}^{\text{mass}})^2 + (\text{CV}^{\text{concentration}})^2$$

$$(\text{CV}^{\text{total}})^2 = \left(\frac{0.007 \text{ g}}{1.4763 \text{ g}} \right)^2 = 2.25 \times 10^{-5}$$

In terms of standard deviation,

$$(\text{CV}^{\text{total}})^2 = \left(\frac{s^{\text{total}}}{\text{total Ca}^{+2}} \right)^2$$

$$s^{\text{total}} = (\text{CV}^{\text{total}})(\text{total Ca}^{+2})$$

$$s^{\text{total}} = \sqrt{2.25 \times 10^{-5}} \cdot 1.872 \text{ mg Ca}^{+2} = 0.0089 \text{ mg Ca}^{+2}$$

The mass of calcium in the external solution is also determined by a simple formula.

$$\text{mg in external solution} = (V - F) C^{\text{external solution}} \quad (\text{D-10})$$

where: V is the total mass of water in the 150mL vessel (not to be confused with a variance)

F is the mass of water in the fibres

C^{external solution} is the concentration of calcium in the external solution

The total mass of water in the system is the total mass of the system minus the mass of od fibre. This value is;

$$V = 100.0283 \text{ g} - 1.0350 \text{ g} = 98.9933 \text{ g}$$

The error in V is obtained from equation (E-5) for two variables

$$V(V) = V(100.0283) + V(1.0350)$$

$$V(V) = (0.3 \text{ g})^2 + (0.006)^2$$

$$V(V) = 0.090036 \text{ g}^2$$

$$s^V = \sqrt{V(V)} = 0.300 \text{ g}$$

The mass of water in the fibres is the fibre saturation point (FSP). At the pH of 7.26 the FSP is 1.339 g water/g od fibre with a standard deviation, s , of 0.035 g/g. Multiplying the FSP by the mass of oven dry fibre gives F , the mass of water in the fibres.

$$1.339 \frac{\text{g water}}{\text{g od fibre}} (1.035 \text{ g od fibre}) = 1.386 \text{ g water in fibres}$$

The error in this value can be obtained from equation (D-7) from the squares of the covariance.

$$(CV_F)^2 = (CV_{FSP})^2 + (CV_{\text{od fibre}})^2$$

$$(CV_F)^2 = \left(\frac{0.035}{1.339} \right)^2 + \left(\frac{0.006}{1.035} \right)^2 = 7.17 \times 10^{-4}$$

$$CV_F = 0.0268$$

Converting to a standard deviation gives:

$$s_F = CV_F \bar{x}$$

$$s_F = 0.0268 (1.386 \text{ g water in fibres})$$

$$s_F = 0.0371 \text{ g water}$$

Subtracting V from F gives the mass of external solution in the 150mL vessel.

$$(V - F) = 98.9933 \text{ g} - 1.339 \text{ g} = 97.654 \text{ g}$$

The error in this value is determined by adding the variances.

$$V(V - F) = V(V) + V(F)$$

$$V(V - F) = 0.090036 \text{ g}^2 + (0.0371 \text{ g})^2$$

$$V(V - F) = 0.0914 \text{ g}^2$$

$$s_{(V-F)} = \sqrt{V(V - F)} = \sqrt{0.0914 \text{ g}^2} = 0.302 \text{ g}$$

Finally, the mass of ions in the external solution can be determined from equation (D-10).

$$\text{mg in external solution} = (V - F) C^{\text{external solution}}$$

$$\text{mg in external solution} = 97.654 \text{ g} \left(7.25 \frac{\text{mg Ca}^{+2}}{\text{kg ext. sol.}} \right) \left(\frac{\text{kg}}{1000 \text{ g}} \right) = 0.708 \text{ mg Ca}^{+2}$$

The concentration of external solution used here is the first of the three external solution concentrations calculated previously. The average value can also be used and the error present in that value can be carried through to the final solution. A comparison of the two calculation options will be made after the calculations are complete.

The error is obtained from equation (D-7).

$$(CV_{\text{mg Ca}^{+2}})^2 = (CV_{(V-F)})^2 + (CV_C)^2$$

$$(CV_{\text{mg Ca}^{+2}})^2 = \left(\frac{0.302}{97.654} \right)^2 + (0)^2 = 1.61 \times 10^{-3}$$

$$CV_{\text{mg Ca}^{+2}} = 0.00309$$

Converting to a standard deviation gives:

$$s_{\text{mg Ca}^{+2}} = CV_{\text{mg Ca}^{+2}} \bar{x}$$

$$s_{\text{mg Ca}^{+2}} = 0.00309 (0.708 \text{ mg Ca}^{+2})$$

$$s_{\text{mg Ca}^{+2}} = 0.00219 \text{ mg Ca}^{+2}$$

With the above information, equation (D-9) can be used to determine the mass of calcium in the fibres.

$$\text{mg ion in fibres} = \text{mg ion total} - \text{mg ion in external solution}$$

$$\text{mg Ca}^{+2} \text{ in fibres} = 1.872 \text{ mg Ca}^{+2} - 0.708 \text{ mg Ca}^{+2}$$

$$\text{mg Ca}^{+2} \text{ in fibres} = 1.164 \text{ mg Ca}^{+2}$$

Variances are used to determine the error in this value.

$$V(\text{mg Ca}^{+2} \text{ in fibres}) = V(\text{mg Ca}^{+2} \text{ total}) + V(\text{mg Ca}^{+2} \text{ in ext. sol.})$$

$$V(\text{mg Ca}^{+2}) = (0.0089 \text{ mg})^2 + (0.00219 \text{ mg})^2$$

$$V(\text{mg Ca}^{+2}) = 8.4 \times 10^{-5} \text{ mg}^2$$

$$s_{\text{mg Ca}^{+2}} = \sqrt{V(\text{mg Ca}^{+2})} = \sqrt{8.4 \times 10^{-5} \text{ mg}^2} = 0.00916 \text{ mg}$$

Results are most commonly presented per kg of od fibre. Converting to these units gives:

$$\frac{1.164 \text{ mg Ca}^{+2}}{1.035 \text{ g od fibre}} \left(\frac{1000 \text{ g}}{\text{kg}} \right) = 1125 \frac{\text{mg Ca}^{+2}}{\text{kg od fibre}}$$

The error in this value can be calculated from equation (D-7) to give a covariance of 0.00977 and a standard deviation, s , of 11.0 mg Ca²⁺/kg od fibre. For the other two concentrations the values obtained by the same calculation technique are 1071 and 1110 mg Ca²⁺/kg od fibre with standard deviations of 10.9 and 11.0 mg Ca²⁺/kg od fibre respectively. The average concentration from these values is 1102 mg Ca²⁺/kg od fibre. The standard deviation of the three values, s , is 27.7 mg Ca²⁺/kg od fibre. Converted to the 95% confidence interval gives a range of 1102 ± 69 mg Ca²⁺/kg od fibre.

The second method of calculation is to use the average through the calculation and obtain a final standard deviation from the errors in the calculation. This results in an average of 1102, but a slightly larger standard deviation of 29.5 mg Ca²⁺/kg od fibre. Assuming this value came from three samples gives a 95% confidence interval of ± 73 mg Ca²⁺/kg od fibre. There is very little difference in the final error obtained by the two methods. The first method has been adopted for the calculation of all the errors in this thesis.

In terms of the mass of water within the fibres the result is:

$$\frac{1.140 \text{ mg Ca}^{+2}}{1.035 \text{ g od fibre}} \left(\frac{\text{g od fibre}}{1.339 \text{ g water}} \right) \left(\frac{1000 \text{ g}}{\text{kg}} \right) = 822.8 \frac{\text{mg Ca}^{+2}}{\text{kg internal water}}$$

Again, the error in this value can be calculated from equation (D-7) to give a covariance of 0.0370 and a standard deviation, s , of 31.1 mg Ca^{+2} /kg internal water. For the 95% confidence interval, the value is between 822.8 ± 77.3 mg Ca^{+2} /kg internal water.

Calculations for magnesium and sodium are performed in the same way as calcium. When both the ash and external solution are considered in the calculation of metal ion concentrations the same principles are used within a slightly different calculation procedure.

Appendix E: Difference between K_a' and K_a

Rather than treating the charged groups on the fibres as ideal, it is possible to treat their dissociation as non-ideal and obtain the thermodynamic equilibrium constant, K_a . For the dissociation of the acidic charged groups on the non-diffusing species. The general reaction for the dissociation is:



where: X^- is the bound charged group on the non-diffusing species

H^+ is the dissociating group (assumed hydrogen)

If K_a is the dissociation constant, then the activities of the species present can be used to represent the equilibrium that is attained.

$$K_a = \frac{(a_{X^-}^F)(a_{H^+}^F)}{(a_{XH}^F)} \quad (E-2)$$

If Q_X is the moles of fixed charged groups on the fibre, then these charged groups can have two forms, bonded to a hydrogen or dissociated. The relationship can then be written:

$$\frac{Q_X}{F} = m_{XH}^F + m_{X^-}^F \quad (E-3)$$

where: Q_X is the equivalents of fixed charged groups on the fibres

F is the mass of solvent in the fibre (F) phase

m_{XH}^F is the molality of charged groups with hydrogen bound to them

$m_{X^-}^F$ is the molality of charged groups in the dissociated state

Writing equation (E-2) in terms of molalities and activity coefficients, substitution into equation (E-3), and solving for $m_{X^-}^F$ gives:

$$m_{X^-}^F = \frac{K_a (Q_X / F)}{\left(\frac{\gamma_{H^+}^F \gamma_{X^-}^F}{\gamma_{XH}^F} \right) m_{H^+}^F + K_a} \quad (E-4)$$

where: $\gamma_{H^+}^F$ is the activity coefficient of H^+ in the F phase. This value can be determined by Pitzer's activity coefficient model.

$\frac{\gamma_{X^-}^F}{\gamma_{XH}^F}$ is the ratio of the activity coefficients of the unprotonated and protonated sites within the fibres. This is an unknown.

The activity coefficients involving X in equation (E-4) cannot be obtained from Pitzer's method because they refer to charged species attached to the fibres, not free ions.

Equation (E-4) is different from equation (34) by the activity coefficient term in the denominator. When the ratio $\frac{\gamma_{X^-}^F}{\gamma_{XH}^F}$ is taken to be one, equation (E-4) is different from equation (34) by only the activity coefficient of hydrogen. Figure E-1 shows the difference in partitioning predictions caused by including or removing the activity coefficient of hydrogen for a two dissociation constant model. The activity coefficient causes only a minor shift in the graph over the pH range 2-10. Above a pH of 10 there is no difference between the curves.

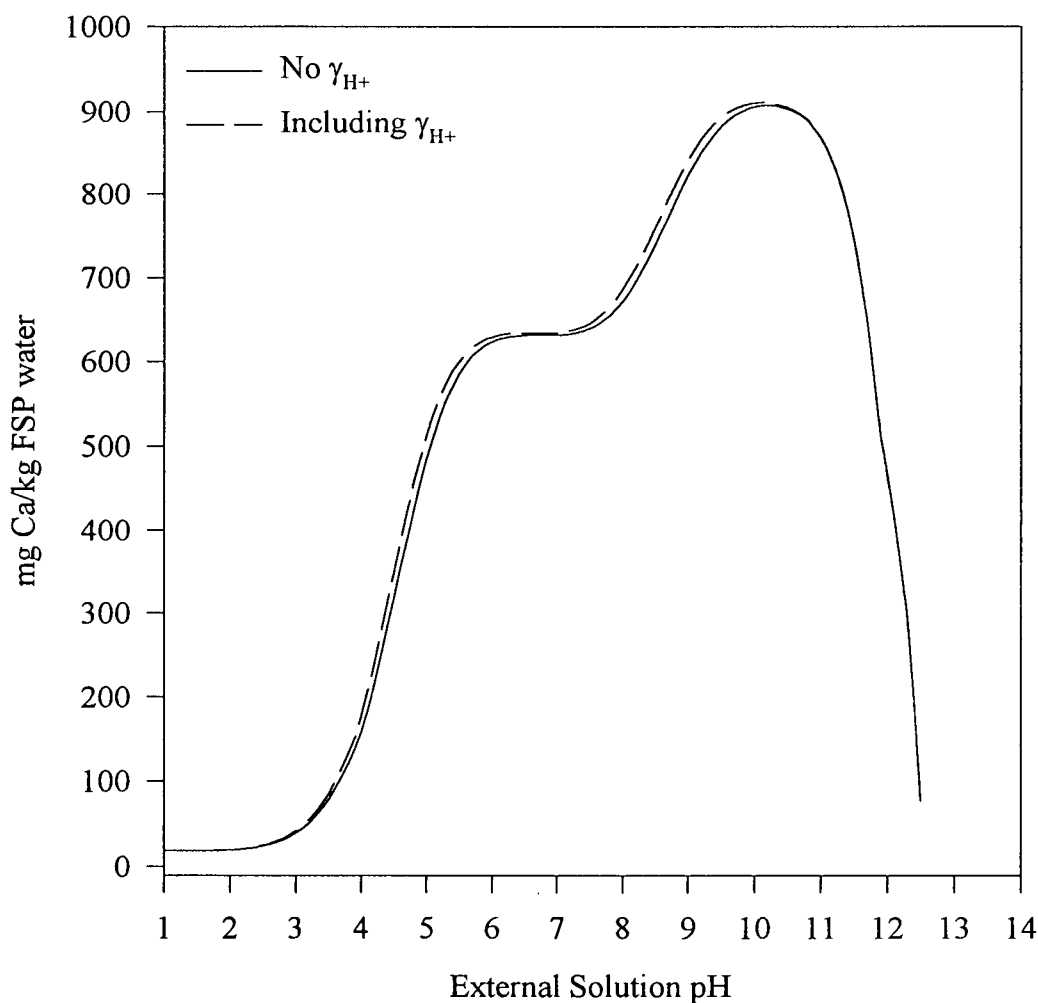


Figure E-1: Partitioning predictions for two dissociation constants including and ignoring the activity coefficient of hydrogen in equation E-4.

Changes in the ratio $\frac{\gamma_{X^-}^F}{\gamma_{XH}^F}$ cause changes in the partitioning predictions as well, as is shown in Figure E-2. Increasing the activity ratio causes the curves to shift to lower concentrations at a given external solution pH. Thus, variation of the fibre activity coefficients over the range of pHs considered could cause significant changes in the shape of the partitioning predictions with two dissociation constants.

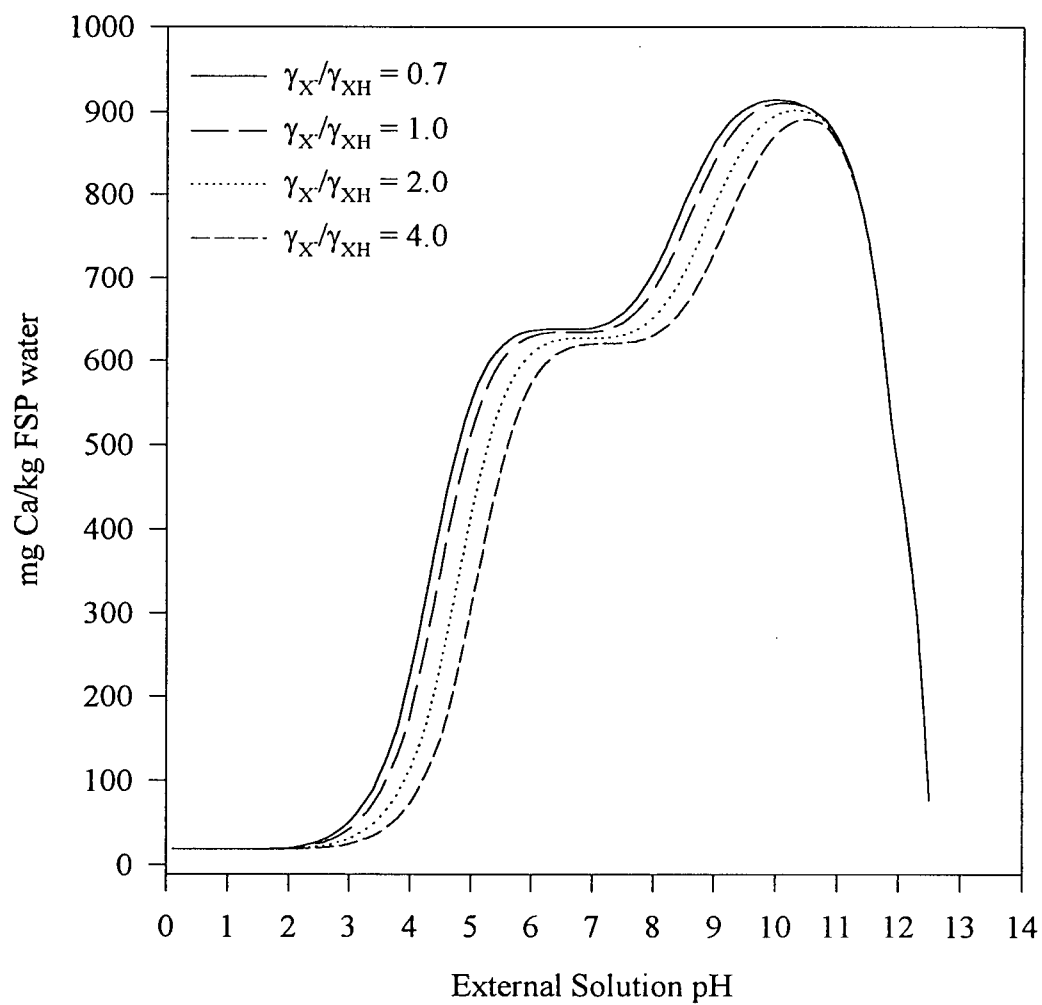


Figure E-2: Partitioning predictions for two dissociation constants at various ratios of the fibre phase activity coefficients.

Appendix F: FORTRAN code for NPE partitioning predictions

```

C PROGRAM NAME: lowmg FOR
C ACTIVITY-DONNAN EQUILIBRIUM ION PARTITIONING
C Model uses a variable charge on the fibres (fit to NaOH tit. data)
C
C implicit double precision (a-h,m-z)
C integer ncat,nani
C parameter (ncat=5,nani=2)
C common o1a,o1c,o2a,o2b,o2c,vf,ak,akw,xkb0,xkb1
C +,xkb2,xkb3
C double precision amc(ncat),ama(nani),bmc(ncat),ph
C +,bma(nani),age(ncat),aga(nani),bge(ncat),bga(nani)
C +,cubmc(ncat),cubma(nani),cuamc(ncat),cuama(nani)
C +,mmc(ncat),mma(nani),fbgam
C
C LIST OF VARIABLES:
C
C O1A: MOLES OF SODIUM, MOL/KG PULP
C O1C: MOLES OF CHLORINE, MOL/KG PULP
C O2A: MOLES OF CALCIUM, MOL/KG PULP
C O2B: MOLES OF MAGNESIUM, MOL/KG PULP
C O2C: MOLES OF MANGANESE, MOL/KG PULP
C V: TOTAL LIQUID, KG SOLVENT/KG PULP
C F: WATER CONTENT OF WALL, KG SOLVENT/KG PULP
C XK: ACID GROUP CONTENT, MOL/KG PULP
C AK: DISSOCIATION CONSTANT, MOL/KG SOLVENT
C akw: dissociation constant of water
C HA: CONCENTRATION OF HYDROGEN, MOL/KG SOLVENT
C DENS: DENSITY OF THE SOLVENT, KG/M3
C AFUNC: SUBROUTINE TO SOLVE EQUATIONS AND RETURN
C THE FUNCTION VALUE, ACTIVITY COEFFICIENTS,
C AND MOLALITIES
C NCAT: NUMBER OF CATIONS
C NANI: NUMBER OF ANIONS
C AMCO: MOLALITY OF CATIONS IN ALPHA PHASE
C BMCQ: MOLALITY OF CATIONS IN BETA PHASE
C AMAQ: MOLALITY OF ANIONS IN ALPHA PHASE
C BMAQ: MOLALITY OF ANIONS IN BETA PHASE
C AGCO: ACTIVITY COEFFICIENT OF CATIONS IN ALPHA PHASE
C BGCO: ACTIVITY COEFFICIENT OF CATIONS IN BETA PHASE
C AGAQ: ACTIVITY COEFFICIENT OF ANIONS IN ALPHA PHASE
C BGAQ: ACTIVITY COEFFICIENT OF ANIONS IN BETA PHASE
C INDICES ARE AS FOLLOWS:
C FOR THE CATIONS:
C 1. SODIUM, Na+
C 2. HYDROGEN, H+
C 3. CALCIUM, Ca+2
C 4. MAGNESIUM, Mg+2
C
C 5. MANGANESE, Mn+2
C FOR THE ANIONS:
C 1. CHLORINE, Cl-1
C 2. hydroxide, OH-1
C PHR: pH OF SOLUTION
C CUBMAQ: mg/kg pulp OF ANIONS IN BETA PHASE
C CUBMCO: mg/kg pulp OF CATIONS IN BETA PHASE
C
C Normal NPE profile, 150 ml vessel
C Na = 16650 mg/kg od fibre
C Ca = 1860 mg/kg od fibre
C Mg = 330 mg/kg od fibre
C
C o1a=0.7242342d0
C o2a=0.04640719d0
C o2b=0.0137354d0
C o2c=0.0000001d0
C o1c=o1a+2.0d0*(o2a+o2b+o2c)
C v=99.0d0
C f=1.18d0
C xkb0=-280.83d0
C xkb1=146.3d0
C xkb2=-17.776d0
C xkb3=0.7731d0
C ak=2.6d-5
C akw=10.0d-14
C dens=1000.0d0
C
C mmc(1)=22.98977d0
C mmc(2)=1.0079d0
C mmc(3)=40.08d0
C mmc(4)=24.305d0
C mmc(5)=54.9380d0
C mma(1)=35.453d0
C mma(2)=15.999d0+1.0079d0
C
C fbgam=1.0d0/1.0d0
C
C open (unit=101,file='ddata1.dat',status='unknown')
C open (unit=102,file='ddata2.dat',status='unknown')
C open (unit=103,file='ddata3.dat',status='unknown')
C
C DO LOOP (10) TO CHANGE pH OF SOLUTION PHASE
C
C do 10 ph=1,125
C
C DO LOOPS (11,12) TO SET ARRAYS TO INITIAL VALUES

```



```

C EQUAL TO HALF THE IDEAL Na MOLALITY
C
temp=bmc(1)/amc(1)
bmc(1)=temp*1.4d0
call afunc(bmc,amc,bma,ama,bgc,agc,bga,aga,fx,fbgam)

C
if(fx.gt.0.0d0)then
  b=c
  fb=fc
else
  a=c
  fa=fc
endif
if(width.gt.1.0d-11)goto 40
C OUTPUT DATA TO FILE
C
do 50 i=1,ncat
  cubmc(i)=bmc(i)*mmc(i)*1000.0d0
  cuamc(i)=amc(i)*mmc(i)*1000.0d0
  continue
cubma(1)=bma(1)*mma(i)*1000.0d0
cuama(1)=ama(1)*mma(i)*1000.0d0
C
print *, phr,bmc(1)/amc(1),bgc(3)
write (101,*) phr,bgc(1),agc(1)
write (102,*) phr,bgc(3),agc(3)
write (103,*) phr,bgc(4),agc(4)
C
10 continue
C
close(unit=101,status='keep')
close(unit=102,status='keep')
close(unit=103,status='keep')
end
C
*****
* SUBROUTINE TO FIND ROOT TO NON-IDEAL DONNAN EQUILIBRIUM
* FOR USE WITH PROGRAM DON5.FOR
*
subroutine afunc(bmc,amc,bma,ama,bgc,agc,bga,aga,fx,fbgam)
implicit double precision (a-h,m-z)
integer ncat,nani
parameter (ncat=5,nani=2)
common o1a,o1c,o2a,o2b,o2c,v,f,ak,akw,xkb0,xkb1
+,xkb2,xkb3
double precision amc(ncat),ama(nani),bmc(ncat)
+,bma(nani),agc(ncat),aga(nani),bgc(ncat),bga(nani)
*

```

```

* LIST OF VARIABLES:
*
* NCAT: NUMBER OF CATIONS
* NANI: NUMBER OF ANIONS
* AMCO: MOLALITY OF CATIONS IN ALPHA, MOL/KG SOLVENT
* AMAO: MOLALITY OF ANIONS IN ALPHA, MOL/KG SOLVENT
* BMCO: MOLALITY OF CATIONS IN BETA, MOL/KG SOLVENT
* BMAO: MOLALITY OF ANIONS IN BETA, MOL/KG SOLVENT
* INDICES ARE AS FOLLOWS:
* FOR THE CATIONS:
* 1. SODIUM, Na+
* 2. HYDROGEN, H+
* 3. CALCIUM, Ca+2
* 4. MAGNESIUM, Mg+2
* 5. MANGANESE, Mn+2
* FOR THE ANIONS:
* 1. CHLORINE, Cl-1
* 2. hydroxide, OH-1
* AFC: ACTIVITY PARAMETER FOR FIBRE
* RMXB: FIBRE MOLALITY OF IONIZABLE GROUPS, MOL/KG SOLVENT
* FX: FUNCTION TO BE ZEROED
* ALM: DONNAN PARTITIONING ROOT
*
* SET ACTIVITY RATIOS FROM ACTIVITY COEFFICIENTS
*
ac1a=agc(1)/bgc(1)
ac1b=agc(2)/bgc(2)
ac1c=aga(1)/bga(1)
ac1d=aga(2)/bga(2)
ac2a=agc(3)/bgc(3)
ac2b=agc(4)/bgc(4)
ac2c=agc(5)/bgc(5)
c
c
c
Data for three dis. const.
ak1=1.6d-4
ak2=1.1d-8
ak3=1.0d-9
xk1=0.095d0
xk2=0.055d0
xk3=0.0d0
alm=bmc(1)
c
bmc(2)=alm*(ac1b*amc(2))
ama(2)=akw/(agc(2)*aga(2)*amc(2))
bma(2)=akw/(bgc(2)*bga(2)*bmc(2))
c
c
c
Data for three dis. const.
mmx1=ak1*xk1/f/((bmc(2)*bgc(2))+ak1)
mmx2=ak2*xk2/f/((bmc(2)*bgc(2))+ak2)
mmx3=ak3*xk3/f/((bmc(2)*bgc(2))+ak3)
rmxb=rmx1+rmx2+rmx3
c
micromols charge/g od fibre
c
c
phr=-dlog10(bmc(2)*bgc(2))
if (phr.lt.2.7d0) then
xk=0.0d0
c
else
xk=xkb0+xkb1*phr+xkb2*(phr**2.0d0)+xkb3*(phr**3.0d0)
c
xk=xk/1000.0d0
endif
c
rmxb=xk/f
c
bmc(1)=o1a*alm/(f*alm+((v-f)/ac1a))
alm2=alm**2.0d0
bmc(3)=o2a*alm2/(f*alm2+((v-f)/ac2a))
bmc(4)=o2b*alm2/(f*alm2+((v-f)/ac2b))
bmc(5)=o2c*alm2/(f*alm2+((v-f)/ac2c))
c
amc(1)=bmc(1)/(ac1a*alm)
amc(3)=bmc(3)/(ac2a*alm2)
amc(4)=bmc(4)/(ac2b*alm2)
amc(5)=bmc(5)/(ac2c*alm2)
c
ama(1)=amc(1)+amc(2)+2.0d0*(amc(3)+amc(4)+amc(5))-ama(2)
bma(1)=bmc(1)+bmc(2)+2.0d0*(bmc(3)+bmc(4)+bmc(5))-bma(2)-rmxb
fx=alm-ac1d*(ama(1)/bma(1))
c
return
end
*
*****
* SUBROUTINE FOR PITZER'S ACTIVITY COEFFICIENTS
*
subroutine pitz(mc,ma,acc,aca)
implicit double precision (a-h,m-z)
integer ncat,nani
parameter (ncat=5,nani=2)
common o1a,o1c,o2a,o2b,o2c,v,f,ak,xkb0,xkb1

```



```

*
* ris=0.0d0
* z=0.0d0
* do 10 i=1,ncat
*   ris=ris+0.5d0*(zc(i)**2.0d0)*mc(i)
*   z=z+abs(zc(i))*mc(i)
10 continue
* do 15 i=1,nani
*   ris=ris+0.5d0*(za(i)**2.0d0)*ma(i)
*   z=z+abs(za(i))*ma(i)
15 continue
*
* * CALCULATE G FUNCTIONS (G1,G2,G'1,G'2) FROM IONIC STRENGTH
*
*   alpha1=2.0d0
*   alpha2=12.0d0
*   x1=alpha1*dsqrt(ris)
*   x2=alpha2*dsqrt(ris)
*   g1=2.0d0*(1.0d0-(1.0d0+x1)*dexp(-x1))/(x1**2.0d0)
*   g2=2.0d0*(1.0d0-(1.0d0+x2)*dexp(-x2))/(x2**2.0d0)
*   x1sq=x1**2.0d0
*   x2sq=x2**2.0d0
*   gp1=-2.0d0*(1.0d0-(1.0d0+x1+x1sq/2.0d0)*dexp(-x1))/x1sq
*   gp2=-2.0d0*(1.0d0-(1.0d0+x2+x2sq/2.0d0)*dexp(-x2))/x2sq
*
* * CALCULATE B, BP (B') AND C ARRAYS BY USING THE
* * BETA PARAMETERS INPUT PREVIOUSLY
*
* do 20 i=1,ncat
*   do 25 j=1,nani
*     b(i,j)=bt0(i,j)+bt1(i,j)*g1+bt2(i,j)*g2
*     bp(i,j)=bt1(i,j)*gp1+bt2(i,j)*gp2/ris
*     c(i,j)=ch(i,j)/(2.0d0*((abs(zc(i)*za(i))**0.5d0))
25 continue
20 continue
*
* * FILL PSI AND PHI ARRAYS WITH ZEROS (DUE TO THE SYSTEM
* * CONSIDERED, THERE IS NO DATA FOR THE SECOND VIRIAL
* * COEFFICIENTS FOR THE SYSTEM CONSIDERED)
*
* do 30 i=1,ncat
*   do 35 j=1,ncat
*     cphi(i,j)=0.0d0
*     cphilp(i,j)=0.0d0
*     do 40 k=1,nani
*       cpsi(i,j,k)=0.0d0
40 continue

```

```

35 continue
do 45 j=1,nani
do 50 k=1,nani
aphi(j,k)=0.0d0
aphilp(j,k)=0.0d0
apsi(i,j,k)=0.0d0
50 continue
45 continue
30 continue
*
* * SOLVE FOR PF (F) BEFORE SOLVING FOR ALL ACTIVITIES
*
*   bb=1.2d0
*   fl=1.0d0+bb*(ris**0.5d0)
*   fl=-0.3915d0*((ris**0.5d0/(fl)))+(2.0d0/bb)*log(fl)
*
*   sum1=0.0d0
*   do 55 i=1,ncat
*     do 60 j=1,nani
*       sum1=sum1+mc(i)*ma(j)*bp(i,j)
60 continue
55 continue
*
*   sum2=0.0d0
*   do 65 i=1,(ncat-1)
*     do 70 j=i,ncat
*       sum2=sum2+mc(i)*mc(j)*cphilp(i,j)
70 continue
65 continue
*
*   sum3=0.0d0
*   do 75 i=1,(nani-1)
*     do 80 j=i,nani
*       sum3=sum3+ma(i)*ma(j)*aphilp(i,j)
80 continue
75 continue
*
*   pf=fl+sum1+sum2+sum3
*
* ***** SOLVE FOR ACTIVITIES OF ALL CATIONS *****
*
* *
*   do 100 i=1,ncat
* *
* * FIRST SUMMATION FOR CATIONS
* *
*   term1=0.0d0

```



```

do 110 j=1,nani
  term1=term1+ma(i)*(2.0d0*b(i,j)+z*c(i,j))
  continue
110
*
* SECOND SUMMATION FOR CATIONS
*
  term2=0.0d0
  do 120 j=1,ncat
    term2a=0.0d0
    do 130 k=1,nani
      term2a=term2a+ma(k)*cpsi(i,j,k)
    continue
  term2=term2+mc(i)*(2.0d0*cphi(i,j)+term2a)
  continue
120
*
* THIRD SUMMATION FOR CATIONS
*
  term3=0.0d0
  do 140 j=1,(nani-1)
    do 150 k=j+1,nani
      term3=term3+ma(j)*ma(k)*apsi(i,j,k)
    continue
  continue
140
150
*
* FOURTH SUMMATION FOR CATIONS
*
  term4=0.0d0
  do 160 j=1,ncat
    do 170 k=1,nani
      term4=term4+mc(j)*ma(k)*c(j,k)
    continue
  continue
160
170
*
* TOTAL ACTIVITY COEFFICIENT TERMS
*
  rhacc(i)=(zc(i)**2.0d0)*pf+term1+term2+term3+term4
  acc(i)=dexp(rhacc(i))
  continue
100
*
*****
* SOLVE FOR ACTIVITIES OF ALL ANIONS
*
do 200 i=1,nani
  FIRST SUMMATION FOR ANIONS
  term1=0.0d0
  do 210 j=1,ncat
    term1=term1+mc(j)*(2.0d0*b(j,i)+z*c(j,i))
  continue
210
*
* SECOND SUMMATION FOR ANIONS
*
  term2=0.0d0
  do 220 j=1,nani
    term2a=0.0d0
    do 230 k=1,ncat
      term2a=term2a+mc(k)*apsi(k,i,j)
    continue
  term2=term2+ma(j)*(2.0d0*aphi(i,j)+term2a)
  continue
230
220
*
* THIRD SUMMATION FOR ANIONS
*
  term3=0.0d0
  do 240 j=1,(ncat-1)
    do 250 k=j+1,ncat
      term3=term3+mc(j)*mc(k)*cpsi(j,k,i)
    continue
  continue
250
240
*
* FOURTH SUMMATION FOR CATIONS
*
  term4=0.0d0
  do 260 j=1,ncat
    do 270 k=1,nani
      term4=term4+mc(j)*ma(k)*c(j,k)
    continue
  continue
270
260
*
* TOTAL ACTIVITY COEFFICIENT TERMS
*
  rhnaca(i)=(za(i)**2.0d0)*pf+term1+term2+term3+term4
  aca(i)=dexp(rhnaca(i))
  continue
200
*
  return
end

```

Appendix G: FORTRAN code for potentiometric titration interpretation

```

c
c      Volume V of 0.1M NaOH is added to 60g of solution containing
c      10mM HCl and 90mM NaCl with 0.6g of od fibre containing
c      "infinite" charged groups.
c      PURPOSE TO FIT THE MULTI-MODEL MATCHES THE EXPERIMENTAL
c      DATA WHEN IN THE DONNAN FRAMEWORK.
c
c      implicit double precision (a-h,m-z)
c      integer n,vhold,dhold,niso
c      parameter (n=2,imax=300)
c      common akw,xk,cl,nac,mi,mf,tcor,v
c      double precision f(n),x(n),dat(imax,imax),error(imax)
c
c      LOGICAL check
c
c      data kif/102/
c      filein = 'init2'
c      open (102,file='init2',form='formatted')
c      read(kif,*) headline
c      read(kif,*) niso
c      do 115 j=1,niso
c      read(kif,*) dat(1,j),dat(2,j)
c      115 continue
c      close(kif)
c
c      do 116 j=1,niso
c      print*, dat(1,j), dat(2,j)
c      116 continue
c
c      Titration correction factor for NaOH or HCl contents
c
c      tcor=1.025d0
c      akw=1.0d-14
c
c      Acid group content (mol/L)
c
c      Initial guesses
c
c      x(1)=1.05d0
c      x(2)=1.0d-2
c      xk=0.0d0
c      i=1
c      sum=0.0d0
c
c      continue
c
c      v=dat(1,i)
c      x(2)=10.0d0**(-dat(2,i))
c      xk=xk+0.0001d0

```

```

c
c      Background ions
c
c      mi=60.0d0-0.84d0
c      mf=0.84d0
c      cl=((90.0d0+10.0d0)/1000.0d0)*(mi+mf)
c      nac=((90.0d0)/1000.0d0)
c
c      call newt(x,N,check)
c      call funcv(N,x,f)
c
c      if(x(2).gt.10.0d0**(-dat(2,i)))then
c      if (check) then
c      write(*,*) 'Convergence problems.'
c      write(101,*) 'Convergence problems'
c      endif
c
c      error(i)=xk
c      print *,xk,10.0d0**(-dat(2,i)),x(2)
c      write(101,*) xk,10.0d0**(-dat(2,i)),x(2)*x(1)
c      xk=xk-0.0001d0
c      call newt(x,N,check)
c      call funcv(N,x,f)
c
c      print *,xk,10.0d0**(-dat(2,i)),x(2)
c      if(xk.gt.0.031d0)then
c      xk=xk-0.03d0
c      else
c      xk=0.0d0
c      endif
c      i=i+1
c      endif
c      check squared error
c
c      vhold=int(v*1000.0d0)
c      dhold=int(dat(1,i)*1000.0d0)
c      if(vhold.eq.dhold)then
c      error(i)=(-dlog10(x(2))-dat(2,i))*2.0d0
c      print *,i,'v,v',error,error(i)
c      print *, -dlog10(x(2)),dat(2,i)
c      write(101,*) v,error(i)
c      sum=sum+error(i)
c      i=i+1
c      endif
c
c      if(xk.lt.0.5d0)goto 5
c      print *, 'sum of errors',sum
c
c

```



```

11  continue
    if (amax.eq 0.) pause 'singular matrix in ludcmp'
    vv(i)=1./amax

12  continue
    do 19 j=1,n
        do 14 i=1,j-1
            sum=a(i,j)
            do 13 k=1,i-1
                sum=sum-a(i,k)*a(k,j)
            continue
            a(i,j)=sum
        continue
        aamax=0.
        do 16 i=j,n
            sum=a(i,j)
            do 15 k=i,j-1
                sum=sum-a(i,k)*a(k,j)
            continue
            a(i,j)=sum
            dum=vv(i)*abs(sum)
            if (dum.ge.aamax) then
                imax=i
                aamax=dum
            endif
        continue
        if (j.ne.imax) then
            do 17 k=1,n
                dum=a(imax,k)
                a(imax,k)=a(j,k)
                a(j,k)=dum
            continue
            d=-d
            vv(imax)=vv(j)
        endif
        indx(j)=imax
        if (a(j,j).eq 0.) a(j,j)=TINY
        if (j.ne.n) then
            dum=1./a(j,j)
            do 18 i=j+1,n
                a(i,j)=a(i,j)*dum
            continue
        endif
    continue
    return
END
C -----
SUBROUTINE fdjac(n,x,fvec,np,df)
INTEGER n,np,NMAX

```

```

DOUBLE PRECISION df(np,np),fvec(n),x(n),EPS
PARAMETER (NMAX=40,EPS=1.e-4)
CU USES funcv
INTEGER ij
DOUBLE PRECISION h,temp,f(NMAX)
common akw,xk,cl,nac1,mi,mf,tcov,v

do 12 j=1,n
temp=x(j)
h=EPS*abs(temp)
if(h.eq.0.)h=EPS

x(j)=temp+h
h=x(j)-temp

call funcv(n,x,f)

x(j)=temp
do 11 i=1,n
df(i,j)=(f(i)-fvec(i))/h
11 continue
12 continue

return
END

C -----
SUBROUTINE lubksb(a,n,np,indx,b)
INTEGER n,np,indx(n)
DOUBLE PRECISION a(np,np),b(n)
INTEGER i,ii,j,ll
DOUBLE PRECISION sum
common akw,xk,cl,nac1,mi,mf,tcov,v

ii=0
do 12 i=1,n
ll=indx(i)
sum=b(ll)
b(ll)=b(i)
if (ii.ne.0)then
do 11 j=ii,i-1
sum=sum-a(i,j)*b(j)
11 continue
else if (sum.ne.0.) then
ii=i
endif
b(i)=sum
12 continue
do 14 i=n,1,-1
x(i)=xold(i)+alam*p(i)

```

```

sum=b(i)
do 13 j=i+1,n
sum=sum-a(i,j)*b(j)
13 continue
b(i)=sum/a(i,i)
14 continue
return
END

C -----
SUBROUTINE lnsrch(n,xold,fold,g,p,x,f,stpmax,check,func)
INTEGER n
LOGICAL check
DOUBLE PRECISION f,fold,stpmax,g(n),p(n),x(n),xold(n),
*func,ALF,TOLX
PARAMETER (ALF=1.e-4,TOLX=1.e-7)
EXTERNAL func
CU USES func
INTEGER i
DOUBLE PRECISION a,alam,alam2,alamin,b,disc,f2,
*fold2,rhs1,rhs2,slope,sum,temp,test,tmp1am
common akw,xk,cl,nac1,mi,mf,tcov,v

check=.false.
sum=0.
do 11 i=1,n
sum=sum+p(i)*p(i)
11 continue
sum=sqrt(sum)
if(sum.gt.stpmax)then
do 12 i=1,n
p(i)=p(i)*stpmax/sum
12 continue
endif
slope=0.
do 13 i=1,n
slope=slope+g(i)*p(i)
13 continue
test=0.
do 14 i=1,n
temp=abs(p(i))/max(abs(xold(i)),1.)
if(temp.gt.test)test=temp
14 continue
alamin=TOLX/test
alam=1.
1 continue
do 15 i=1,n
x(i)=xold(i)+alam*p(i)

```

```

15      continue
      f=func(x)
      if(alam.lt.alamin)then
        do 16 i=1,n
          x(i)=xold(i)
        continue
16      check=.true.
        return
      else if(f.le.fold+ALF*alam*slope)then
        return
      else
        if(alam.eq.1.)then
          tmplam=-slope/(2.*(f-fold-slope))
        else
          rhs1=f-fold-alam*slope
          rhs2=f2-fold2-alam2*slope
          a=(rhs1/alam**2-rhs2/alam2**2)/(alam-alam2)
          b=(-alam2*rhs1/alam**2+alam*rhs2/alam2**2)/(alam-alam2)
          if(a.eq.0.)then
            tmplam=-slope/(2.*b)
          else
            disc=b*b-3.*a*slope
            if(disc.lt.0.) pause 'roundoff problem in Insrch'
            tmplam=(-b+sqrt(disc))/(3.*a)
          endif
          if(tmplam.gt..5*alam)tmplam=.5*alam
        endif
        alam2=alam
      endif
      f2=f
      fold2=fold
      alam=max(tmplam,.1*alam)
      goto 1
    END
  C
C
-----
  FUNCTION fmin(x)
  INTEGER n,NP
  DOUBLE PRECISION fmin,x(*),fvec
  PARAMETER (NP=40)
  COMMON /newtv/ fvec(NP),n
    common akw,xk,cj,nacl,mi,mf,icor,v
  SAVE /newtv/
  CU  USES funcv
  INTEGER i

```

```

      DOUBLE PRECISION sum
      call funcv(n,x,fvec)
      sum=0.
      do 11 i=1,n
        sum=sum+fvec(i)**2
      11 continue
      fmin=0.5*sum
      return
    END
  C
-----

```